DESIGN OF A NON-AXISYMMETRIC STATOR FOR IMPROVED PROPELLER PERFORMANCE

by

LAWRENCE J. BOWLING

B.S., Ocean Engineering, United States Coast Guard Academy

SUBMITTED TO THE DEPARTMENT OF OCEAN ENGINEERING IN PARTIAL FULFILLMENT OF THE REQUIREMENTS FOR THE DEGREE OF

MASTER OF SCIENCE IN
NAVAL ARCHITECTURE AND MARINE ENGINEERING
AND
MASTER OF SCIENCE IN MECHANICAL ENGINEERING

at the

MASSACHUSETTS INSTITUTE OF TECHNOLOGY

June 1987

Signature of Author _____
Department of Ocean Engineering
June 1, 1987

Certified by _____
Professor Justin E. Kerwin
Thesis Supervisor

Accepted by _____
Professor David E. Wilson
Thesis Reader, Mechanical Engineering

Accepted by _____
A. Douglas Carmichael
Chairman, Departmental Graduate Committee
Department of Ocean Engineering

DESIGN OF A NON-AXISYMMETRIC STATOR FOR IMPROVED PROPELLER PERFORMANCE

by

LAWRENCE J. BOWLING

Submitted to the Department of Ocean Engineering on June 1, 1987
in partial fulfillment of the requirements for the degree of Master of Science in
Naval Architecture and Marine Engineering
and
Master of Science in Mechanical Engineering.

Abstract

The inclination of a propeller shaft relative to the fluid inflow results in a once per revolution tangential velocity fluctuation in the plane of the propeller. A more desireable condition from the view point of efficiency and cavitation considerations is to have a more uniform tangential inflow. A nine bladed non-axisymmetric stator was designed based on a lifting line computer code for multi-component propulsors. The stator, 1.2 feet in diameter, was designed to operate with DTNSRDC (David Taylor Naval Ship Research and Development Center) model propeller 4497, which is one foot in diameter.

Experimentation with the aluminum stator model was conducted to validate the design and the computer program wake predictions. Laser Doppler Anemometry (LDA) was used to measure the velocities at several radial locations in a plane behind the stator where the propeller would operate. Comparisons were made between the measured propeller inflow wake and the computer predicted inflow wake. Non-dimensional circulation measurements about the blades of the stator were also made to provide data for comparison to computer generated predictions. The stator was tested in an axisymmetric and non-axisymmetric blade alignment.

The experimental results validated the computer wake predictions for the tangential wake in the plane of the propeller. The results support a conclusion that the non-axisymmetric stator would induce velocities in the plane of the propeller to counteract an inclined flow. The LDA measurements of the tangential wake indicate that the velocity fluctuation would be reduced by the non-axisymmetric stator.

Open-water tests were conducted with the propeller and the stator/propeller combination. Accounting for increased drag due to the stator, the stator/propeller propulsor was more efficient than the propeller operating by itself.

Thesis Supervisor: Professor Justin E. Kerwin
Title: Professor of Naval Architecture and Marine Engineering

Dedication

I wish to acknowledge and thank several individuals for their assistance in helping me perform this work. Without their effort and advice, this thesis would not be at a stage of completion. Primary thanks go to Professor "Jake" Kerwin for suggesting this experiment and offering me the opportunity to develop it. The construction of the stator model and the performance of the experiment had associated costs which were not inexpensive. In this financial regard, thanks are extended to the U.S. Navy for their portion of the funding of this effort. The author hereby grants full permission to the U.S. Government and its agencies to reproduce and distribute this thesis document.

The computer analysis required before and after the experiment was made possible by the programs developed primarily by Bill Coney and Ching-Yeh Hsin. The design of the stator and the performance of the experiment were greatly facilitated by Mr. Dean Lewis. Lastly, sincere thanks to my wife, Michelle, and my daughter, Amberly, for tolerating my lifestyle and moods of the past two years.

Table of Contents

List of Figures

List of Tables

Chapter 1

INTRODUCTION

The propulsion plant design and installation on ships of all sizes leads to the condition were the propeller shaft often penetrates the hull at a slight downward angle as measured from horizontal. A reason for this shaft inclination is to allow for adequate clearance between the hull form and the tips of the rotating propeller blades, without requiring an excessively long shaft. The shaft angle produces inclined flow which yields a once per revolution tangential velocity fluctuation in the plane in which the propeller blades are rotating [3]. This condition detracts from the operating efficiency of the propeller. Specifically, it can lead to the inception of cavitation at lower speeds when compared to propellers operating under the same conditions but in a more uniform inflow. Cavitation increases the drag on the propeller blades which results in an increased torque and reduced propulsive efficiency. Cavitation can eventually lead to physical damage to the blade surface. Improved propeller performance in terms of propeller efficiency, η, and increased operating speed before the inception of cavitation are the rewards for the development of a device which can minimize or reduce the effects of inclined flow due to shaft inclination.

The design of a pre-swirl stator, to be used in conjunction with a model propeller, DTNSRDC propeller 4497, is the focus of this experimental thesis effort. The design was developed with the use of existing MIT Marine Hydrodynamics Laboratory (MHL) propeller lifting line codes. While unable to exactly model inclined flow in the laboratory, an experiment was designed to test the stator and provide results to validate the design and the computer lifting line code. The

experiment was designed to demonstrate the propulsive efficiency of the stator/propeller combination and to map the inflow wake to the propeller for comparison with computer predictions. By achieving the desired flow field mapping in the plane of the propeller, it would be demonstrated that the stator was modifying the flow to counteract inclined flow.

Chapter 2

PROBLEM STATEMENT

As mentioned in Chapter 1, the flow resulting from a propeller shaft angle exhibits a once per revolution velocity fluctuation. The harmonic is in the tangential direction as considered in the propeller blade frame of reference. The flow situation can be better visualized by referring to Figure 2-1.

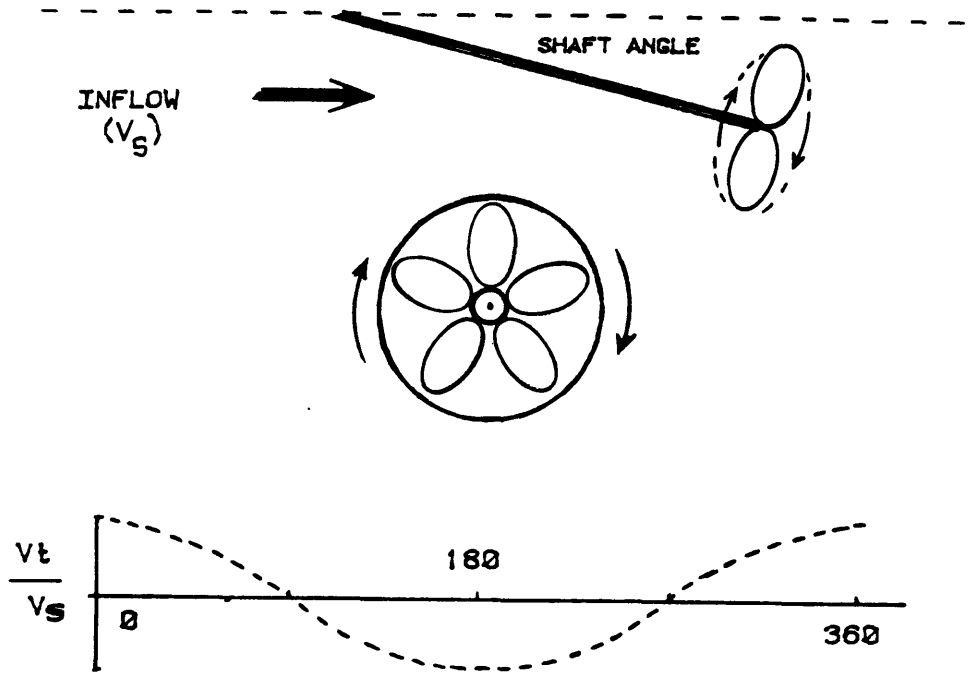

Figure 2-1: Tangential Wake Variation.

The amplitude of the fluctuation is a function of the shaft angle and the ship speed. The goal of this experimental effort was to design a non-axisymmetric stator with a prescribed radial circulation distribution which would induce tangential velocities in the plane of the propeller to minimize those velocity variations experienced due to shaft angle. A shaft angle of seven degrees was assumed for

purposes of the experiment. The desired result would be to achieve a deflected flow to counteract the shaft angle inclination. Additionally, it was desired to achieve this inflow modification and increase the efficiency of the propulsor combination after taking into account the increase in drag due to the stator.

A model propeller, DTNSRDC propeller 4497, was selected for use in the experiment. This propeller was available for use in the MIT MHL. The propeller, by virtue of its existing physical geometry and pitch angles, has a design circulation distribution. This distribution was established by Boswell [2]. The characteristics of DTNSRDC propeller 4497 are presented in Table 2-I.

Table 2-I: Characteristics of DTNSRDC Propeller 4497 [5]

Number of Blades:	5
Expanded Area Ratio:	0.725
Hub-Diameter Ratio:	0.2
Section Meanline:	NACA a = 0.8
Section Thickness Distr:	NACA 66 (Modified)
Design Advance Coefficient:	0.889

r/R	c/D	tan Bi	P/D	Skew	t/D	f/c
0.20	0.174	1.8256	1.455	0.0	0.0434	0.0430
0.25	0.202	-	1.444	2.33	0.0396	0.0395
0.30	0.229	1.3094	1.433	4.65	0.0358	0.0370
0.40	0.275	1.0075	1.412	9.36	0.0294	0.0344
0.50	0.312	0.8034	1.361	13.95	0.0240	0.0305
0.60	0.337	0.6483	1.285	18.38	0.0191	0.0247
0.70	0.347	0.5300	1.200	22.75	0.0146	0.0199
0.80	0.334	0.4390	1.112	27.14	0.0105	0.0161
0.90	0.280	0.3681	1.027	31.57	0.0067	0.0134
0.95	0.210	-	0.985	33.79	0.0048	0.0140
1.00	0.000	-	0.942	36.00	0.0029	-

The first task in approaching the stator design problem was to determine the required radial distribution of circulation for each of the stator blades which would modify the inflow to improve the propeller's performance in inclined flow. To

establish these circulation distributions for the stator blades, extensive use was made of the MIT MHL propeller lifting line computer code called, appropriately, Propeller Lifting Line (PLL) [8]. The PLL code, which can accomodate multiple component propulsors, uses an optimization procedure which results in the radial circulation distributions for the individual propulsive components. Additionally, a program option allows the required non-axisymmetric analysis to be studied. More about the use of PLL will be discussed in Chapter 3.

The anticipated modification to the propeller inflow as predicted by PLL is also shown in Figure 2-2. A comparison of the tangential inflow wakes with the stator and without the stator shows that there are more fluctuations per revolution in the tangential inflow wake with the stator. However, the more significant observation is that the predicted amplitudes of these variations with the stator in place are much less. This is the desired modification to the inflow for which the stator is to be designed. As mentioned earlier, a further consideration in the design of the stator/propeller propulsor was to achieve a propulsive efficiency greater than or equal to the propeller operating by itself. By designing a stator which introduces circulation into the flow which is opposite to the circulation provided by the propeller, there is less rotational energy left in the wake. The result should be an increase in propulsive efficiency. The performance of the propeller and the stator/propeller open-water tests would provide the necessary data for propulsive efficiency analysis.

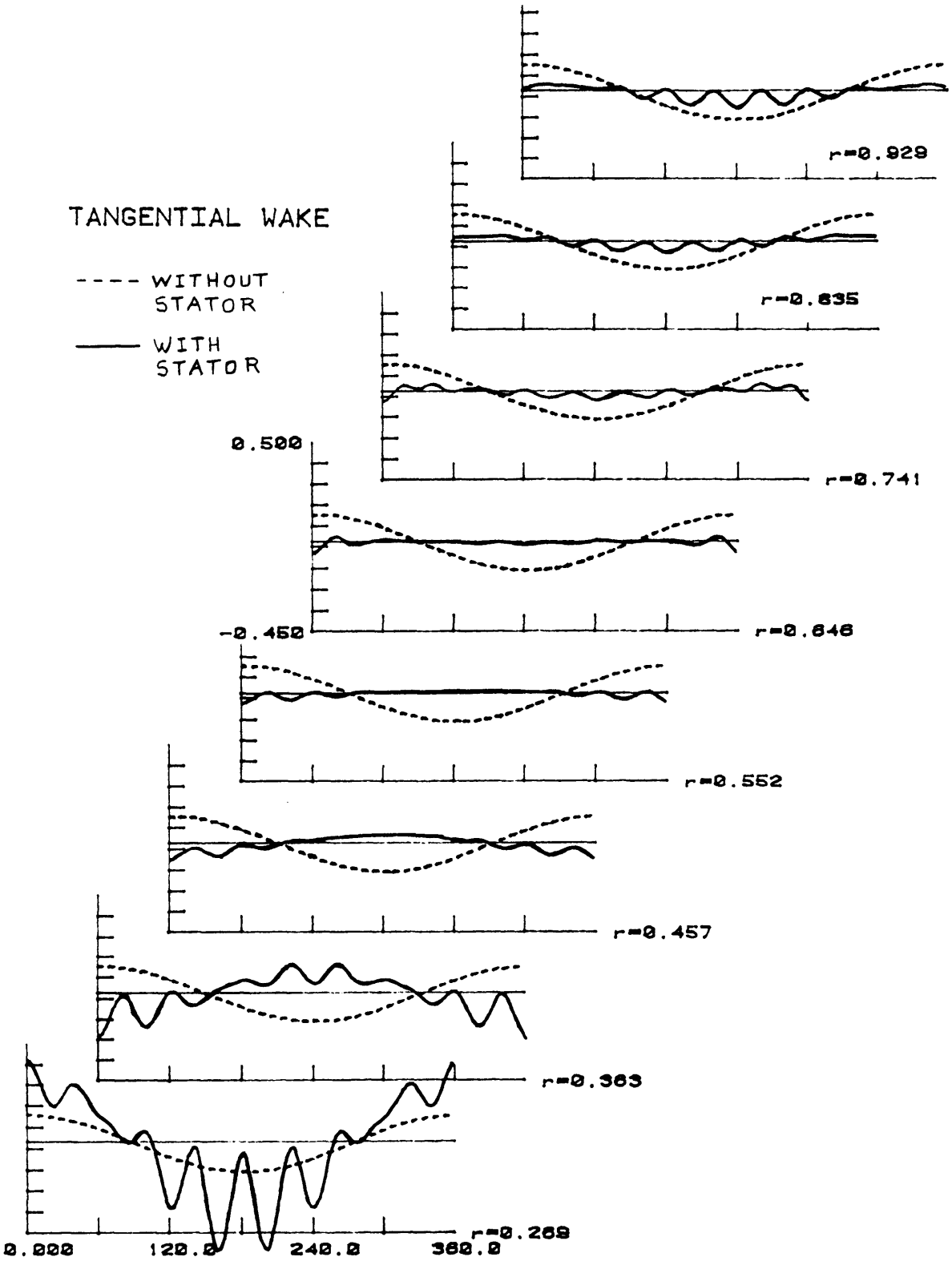

Figure 2-2: PLL Wake Predictions at Various Radii.

Chapter 3

STATOR DESIGN

3.1 MIT MHL Computer Programs

This experimental thesis effort would not have been possible without the availability of the MIT MHL computer codes. With the design problem clearly defined, numerous computer runs were made with PLL to determine the radial circulation distribution required on each stator blade.

Prior to being able to obtain the "optimum" stator circulation distribution from PLL, it was necessary to prepare appropriate file inputs for the computer program for both the stator and the propeller. The design circulation on the model propeller was determined using another MIT propeller code, LLL-2. With this information, an appropriate input file for PLL was prepared. One difficulty experienced in using the circulation optimization procedure for this experiment, was that PLL optimizes circulation for both components, the stator and the propeller. The desired result was to obtain the stator's optimum circulation, given a prescribed circulation on the existing propeller. To overcome this situation, PLL was first run optimizing circulation for both components. The optimized propeller circulation from PLL was compared to the input design circulation. There were differences, but not significant as to invalidate the PLL output. The next run of PLL was performed without selecting circulation optimization. The previously determined stator optimum circulation and the design circulation for the propeller were prescribed as inputs. The results of this run were not significantly different from the previous one. This iterative technique deviates from the ideal design

situation which would be to design both a stator and a propeller for use as one propulsive unit.

The first stage of use of PLL results in optimum circulation distributions for the stator in an axisymmetric blade arrangement with a propeller. In the axisymmetric case, all blades of the stator have the same circulation distribution. A sample output from PLL for the axisymmetric case can be found in Appendix 1. At this point in the program, PLL allows for the non-axisymmetric analysis necessary to study the stator effects on inflow to the propeller considering inclined flow. Beginning with a mean circulation distribution obtained from the axisymmetric case, the program allows the user to vary this distribution until the desired modification to the inflow is obtained. The program outputs include the local circulation distributions at various radii for every blade on the stator. Appendix 1 also contains a sample output for the non-axisymmetric analysis.

To obtain this axisymmetric circulation distribution on a stator blade, 2-dimensional wing theory was used ar a rough estimate to determine the angle of attack required at each local radii. The non-dimensional circulation from the PLL axisymmetric case resulted in a varying angle of attack from hub to tip in the stator blade. The varying angle of attack translated to a twist in the stator blade. It was later determined with a stator analysis program, SSF-1, what angles of attack would be required in 3-dimensional flow to produce the required circulation distributions. This program and its analysis had not been developed at the time that the physical geometry of the stator was being determined..

After construction of the model, the program SSF-1 was available to determine the actual radial circulation distributions on the stator blades accounting for 3-dimensional effects. The effects of the 3-dimensional analysis of SSF-1 were significant and dominated the earlier 2-dimensional estimation. The

axisymmetric circulation distribution from SSF-1 was shifted further from the hub than the distribution obtained from PLL. See Figure 3-1. Additionally, for the axisymmetric case, SSF-1 was used to determine an angle of attack of thirteen degrees to obtain a circulation distribution similar to PLL. Thickness effects were taken into account. Anticipating adjustments to the required angle of attack, the hub assembly which holds the stator blades was designed to allow each blade to be independently set at any desired angle.

For the non-axisymmetric case, SSF-1 was used in a trial and error fashion, varying the angles at which each blade were set. The goal was to duplicate the PLL non-axisymmetric circulations which produced the desired inflow. The initial thought concerning the non-axisymmetric circulation distributions was that their shape on all blades would be very similar. It was felt that by adjusting the angle of attack of the entire blade the desired distribution could be approximately obtained. An exact match was not able to be obtained for all blades due to 3-dimensional effects. However, an excellent match was achieved on three blades, a very good match was achieved on two blades, and an acceptable match was obtained on the remaining four. These four were the most lightly loaded blades. An attempt was made to match the magnitude of the maximum circulation for these blades, despite the different shape of the distribution. Due to the fact that these blades were very lightly loaded, a possible alternative would have been to remove these blades completely during the experiment. This was not done. Figure 3-2 shows this comparison. Only five blade circulations are shown as, due to symmetry, the remaining four are identical to those plotted. In effect, the real "designing" of the stator blade circulation distributions was performed with the SSF-1 computer program in determining the right angle of attack. This trial and error procedure was performed after the physical construction of the model.

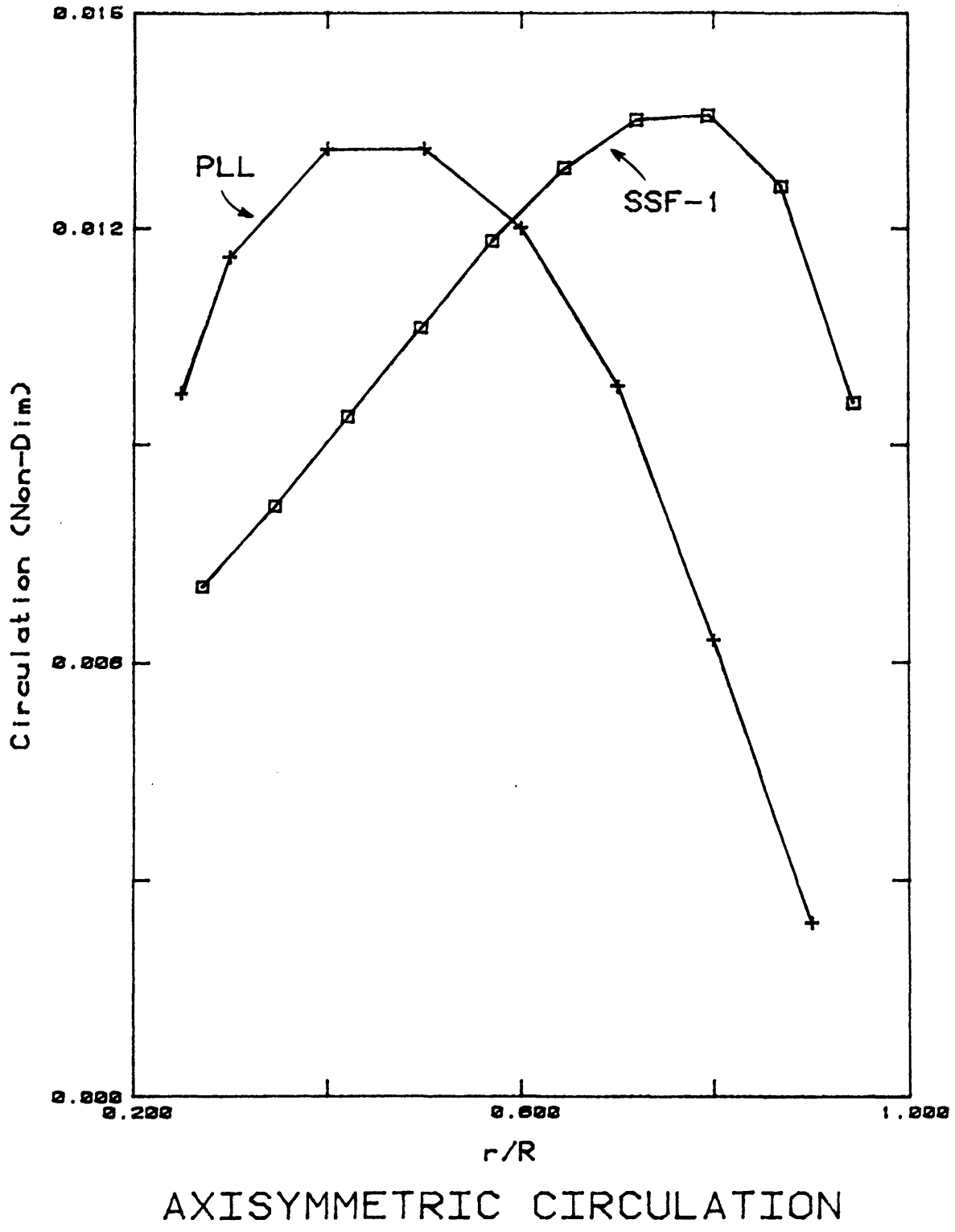

Figure 3-1: PLL and SSF-1 Circulations

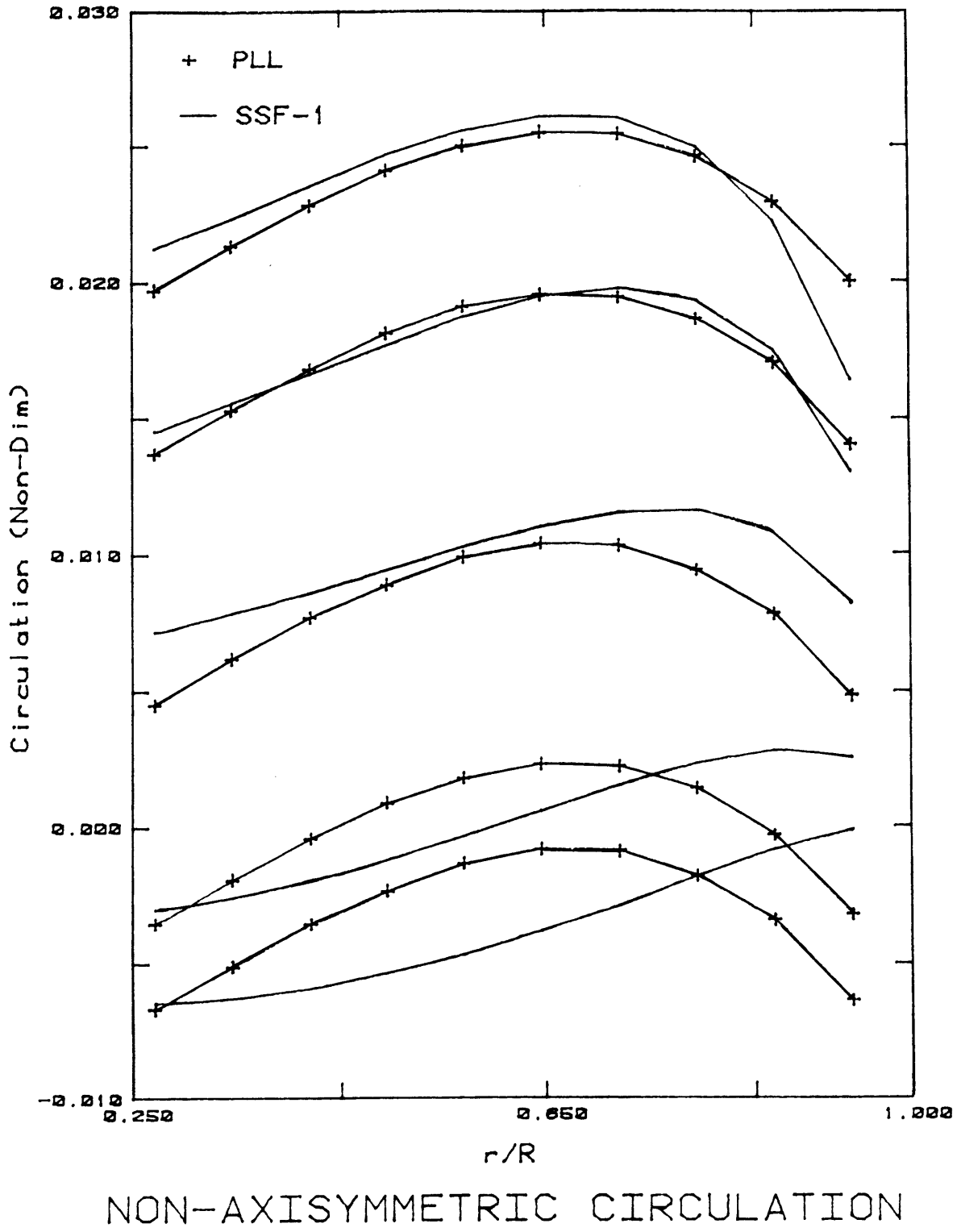

Figure 3-2: PLL and SSF-1 Circulations

Besides the pure hydrodynamic considerations of circulation, PLL was also used to conduct a parametric study to establish some of the features of the physical geometry of the stator. The number of stator blades, the diameter, the chord lengths, the blade thickness, the blade airfoil shape, and the axial position of the stator from the propeller all needed to be determined. Decisions concerning these aspects of the design were influenced by the practical limitations of machining capabilities. The design selection of the stator geometry, as well as the considerations of machine fabrication, will now be addressed.

3.2 Design Considerations

3.2.1 Stator Blade Number and Planform

The decision to establish the number of stator blades was made early in the design process. The primary consideration in this selection was to choose a number of blades which was not a multiple of five. The 4497 propeller has five blades. Therefore, by not selecting multiples of five, the design avoids exciting a harmonic mode of propeller induced vibration. The choice of a high number of blades has the advantage of minimizing the amplitudes of the velocity variations in the plane of the propeller. However, an excessively large number of blades would not only create flow blockage, but would not physically be able to be mounted around a hub assembly of practical dimensions. Guided by these considerations, it was decided that the stator would have nine blades, equally spaced around the hub. This number represented a compromise to the above mentioned selection criteria.

The diameter of the stator was originally input in PLL as 1.08 feet. This choice was initially based on general guidance obtained from Takekuma's paper [17]. The diameter was subsequently increased to 1.2 feet. This was done after

studying PLL output which predicted relatively large amplitudes of tangential wake variation at the propeller disk's outer radii. As anticipated, the modest increase in stator diameter of approximately 1.5 inches, improved the inflow wake prediction.

The determination of chord lengths was not as straight forward as the diameter selection. The sensitivity of the success of the stator design to the chord lengths was noted to be high. The goal of maximizing efficiency and equalling the thrust of the lone propeller with the thrust of the stator/propeller combination, obviously dictated that minimum drag on the stator was essential. This meant that chord lengths on the stator needed to be as short as possible. A trade-off exists between minimizing drag and loading on the blades. As shorter chord lengths were proposed in the PLL input files, the local radial lift coefficients (loading) increased, as would be expected. Therefore, as chord lengths were shortened to minimize drag, the required angle of attack, to provide the necessary circulation, increased. This raised some concern about possible stator blade stall at the low Reynold's Number of operation. The Reynold's Number for the stator was calculated to be 4.38×10^5 at the test condition. The low Reynold's Number data available in reference [10] was consulted for NACA 0012 thickness forms, which are very similar to the stator blade shapes. It was determined that stall could be avoided using reasonable chord lengths.

A further consideration for establishing the chord lengths was that the computer design tool, PLL, is a lifting line code. In lifting line theory, the blade is replaced by a straight line. It was felt that a blade of constant chord length would simplify the design. Numerous iterations with PLL, varying chord, eventually resulted in a constant chord length of 2.75 inches. This chord length in the final design resulted in a prediction of 13 pounds of stator drag. Brockett's report [4] was consulted to ensure that at the operating condition cavitation would not be

a concern. The cavitation number for the stator blade was sufficiently high such that cavitation was not a problem.

The final stator design features uncambered or symmetric blades. The primary motivation for using uncambered foils shapes was to facilitate fabrication. A very realistic constraint on any experiment is the project budget. The final blade design had a slight linear taper in thickness from the hub to the tip and had a twist which varied the angle of attack at different radii. The complexity of machining a cambered foil, as well as one with taper and twist, would have resulted in a prohibitively expensive construction cost. Another reason for not using camber was that the angle of attack at which the blades needed to be set at had not been determined at the time of the model construction. For stall considerations, it was decided to construct blades of symmetric foil shape with a 2.75 inch chord length.

In determining the thickness of the stator blades, several factors needed to be addressed. These included adequate strength for minimizing tip deflections under load, cavitation, and form drag. For adequate strength, it was decided to construct the stator model from high tensile strength, heat treated aluminum (6061, T6). The resulting blade design had a one-half inch diameter circular shaft extending into the hub for attachment by clamping action. Beam theory was used to estimate the minimum shaft dimensions to withstand the anticipated forces during experimentation. This calculation eliminated the possible use of blades with thickness ratios less than ten percent at the hub. Thin blades minimize form drag, but thickness helps make the foil less sensitive to cavitation at increasing angles of attack. The result was a foil shape with a tapering thickness from hub to tip. The blade, 5.5 inches in span, was designed to be thirteen percent thick at the hub, and ten percent thick at the tip, with linear tapering in between. In fabricating the stator model, a constraint on the cutting tool capabilities resulted in a slight

thickening of the blade at the hub. From a hydrodynamic viewpoint, this was deemed insignificant due to the fact that the inflow would already disturbed by the stator hub assembly at this location.

3.2.2 Axial Separation Distance of Components

The axial separation of the stator and propeller as input into PLL required some interpretation. This was due to the fact that PLL is based on lifting line representations of the stator and the propeller. The logical reference point from which to assume a lifting line and measure this separation was the quarter-chord location for both components. The quarter-chord location is the point at which the lift force acts. The selection of a 4.5 inch separation distance was the result of numerous program runs of PLL and information contained in Hecker's report [6]. The water tunnel arrangement for mounting the stator ahead of the propeller on the propeller drive housing also placed a lower limit on this separation distance. As the separation distance between the components increased, the local radial coefficients of lift, required to produce the necessary circulation, also increased.

To summarize, the resulting stator design was machined from high tensile strength aluminum. It had nine blades and was 1.2 feet in diameter. The chord lengths were constant at 2.75 inches with a smooth rounded tip. The blade foil was uncambered. The thickness tapered linerly from a thickness ratio of thirteen percent at the hub to ten percent at the tip. The axial separation of the stator from the propeller was set at 4.5 inches. Each stator blade was clamped about a circular shaft into the hub assembly. This allowed for the adjustment of individual blades to any angle of attack. See Figure 3-3 for details on the hub assembly and Figure 3-4 for details on the stator blades. A photograph of the stator mounted on the drive shaft housing is included in Appendix 2.

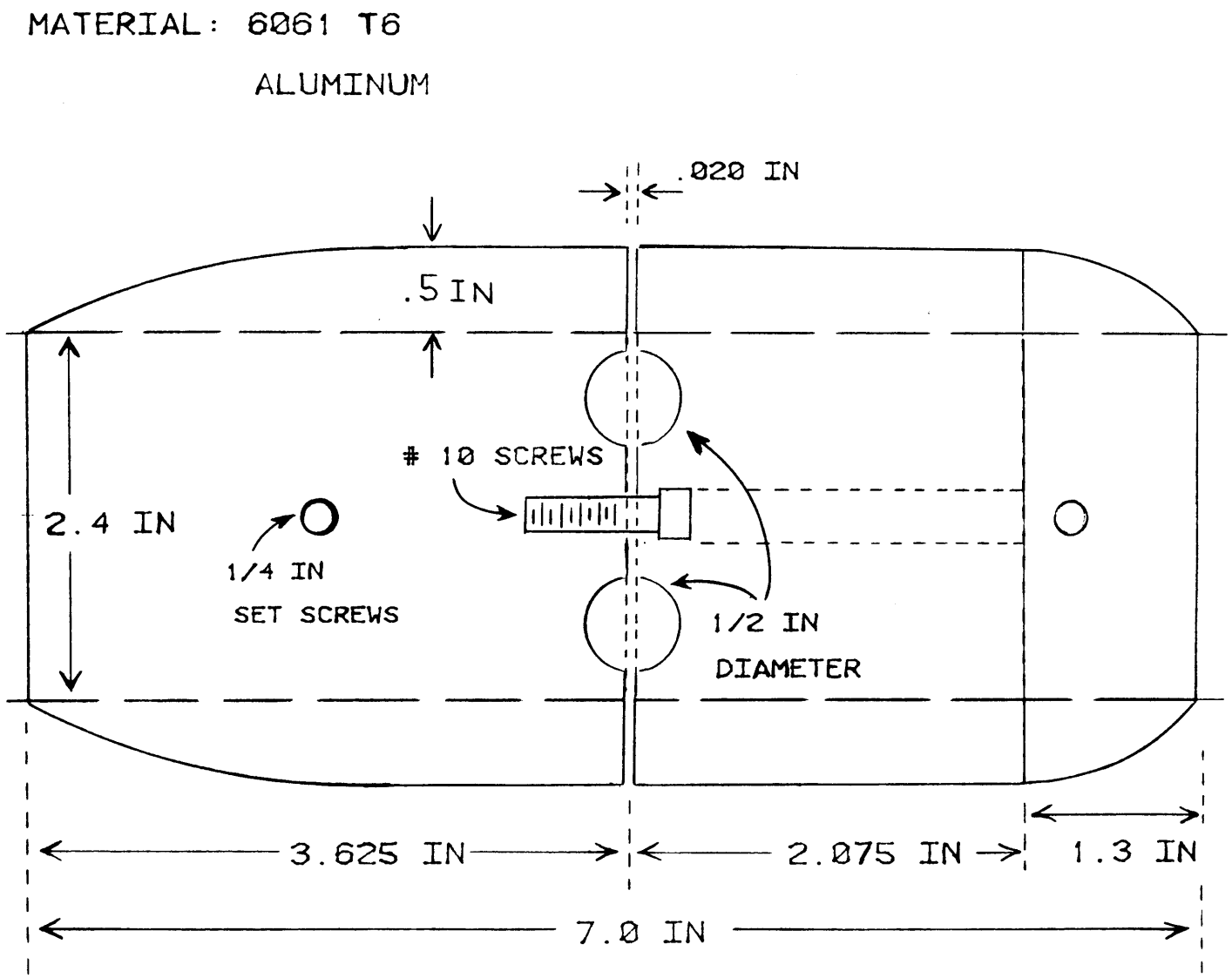

Figure 3-3: Hub Assembly

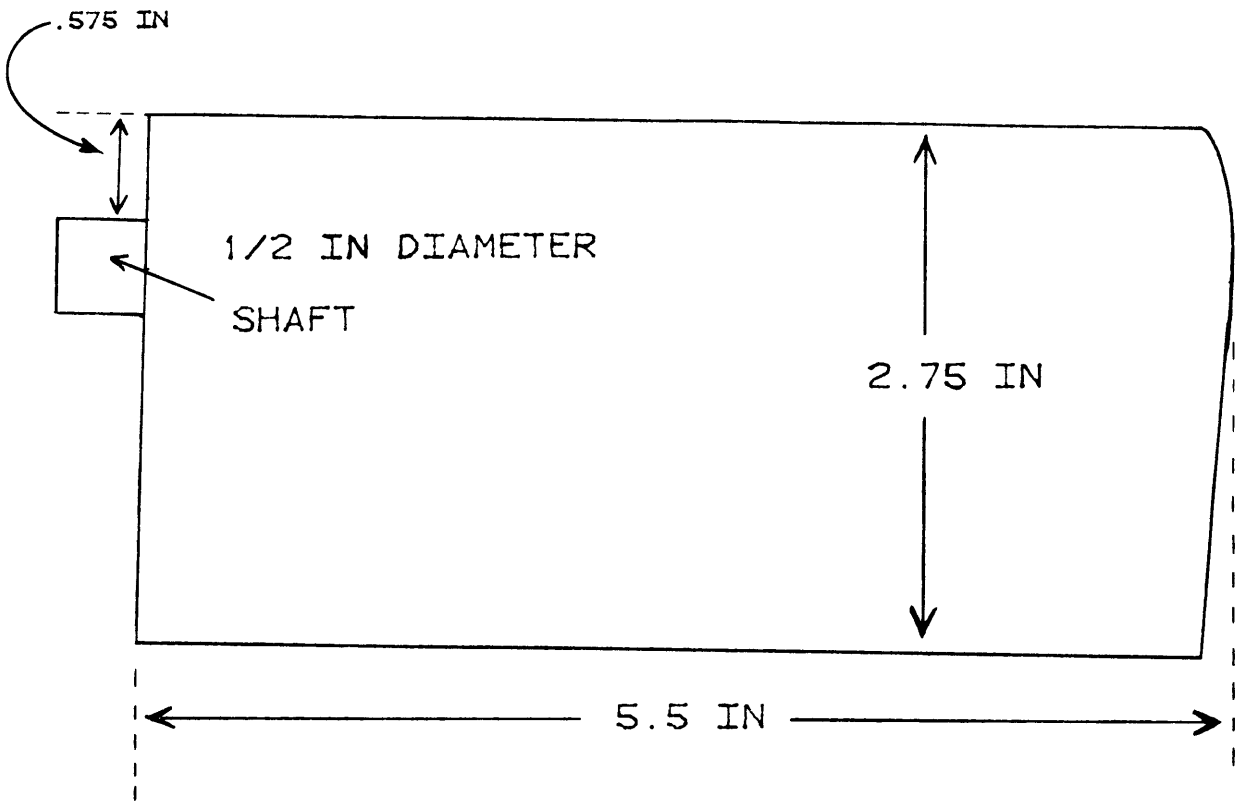

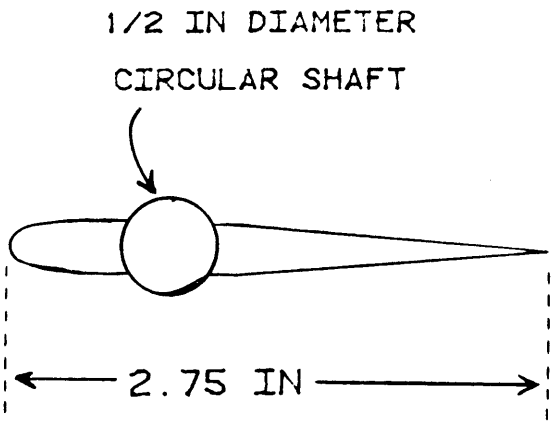

Figure 3-4: Stator Blade

Chapter 4

DESCRIPTION OF EXPERIMENTAL FACILITY

The experiment was conducted at the MIT Marine Hydrodynamics Laboratory (MHL). The lab features a variable pressure water tunnel. Water velocities of up to thirty feet per second can be generated. There are plexiglass windows in the tunnel test section which is 20 inches square by 55 inches long. A removable propeller drive shaft extends from upstream into the test section. The outside housing of the shaft does not rotate. Fluid flow is symmetric about the shaft.

Along side the tunnel, a two component laser doppler anemometer (LDA) system is in place. The LDA system is used for measuring local vertical and horizontal velocities in the test section. The laser is a Lexel, model 95, argon ion laser rated at 2 watts of power. The laser operates in conjunction with a photodector, a signal tracker, and a signal processor which ultimately convert particle velocities in the fluid to a proportional voltage signal. Further operational theory of LDA system functions will not be discussed, but clarification of how such systems operate can be found in Reference [19].

The laser is mounted on a motordriven transverse table system with digital position readout. Repeatability of positioning of the laser table is 0.0001 inches. Minimum movement of the table is also 0.0001 inches. The laser can be positioned by either a handheld remote control or by computer. A minicomputer system is used for data acquisition and reduction.

Chapter 5

DESIGN OF THE EXPERIMENT

5.1 Scope of the Experiment

The scope of the experiment was defined to study several of the theoretical models upon which the MIT MHL computer codes are based. The primary goal was to validate the computer predicted wake of the stator in the non-axisymmetric alignment by comparison with experimental velocity measurements.

The hub vortex generated by a propeller is of a Rankine vortex structure [18]. The stator, when operating in the tunnel by itself, generates a highly visible hub vortex cavity. These two vortices should tend to counteract each other when the stator is mounted ahead of the propeller. The effect should manifest itself in some cancellation of the strength of the hub vortex. This phenomena was studied and the results are discussed in Chapter 6.

Also performed in the course of the experiment were open-water tests for the 4497 propeller and for the stator/propeller combination. These tests provided the data necessary for the comparison of the propulsive efficiencies of the propulsors. The method of comparison requires some interpretation as there can be some justification for analysis at numerous operating points. It was decided that the fairest comparison would be at a point where an equal amount of thrust was provided.

The LDA system was used to collect velocity measurements to verify the non-dimensional circulation distributions for the stator blades for comparison with the numerical SSF-1 solutions. This was done in both the axisymmetric and non-

axisymmetric blade alignments. This check would ensure that the stator circulation input into PLL was actually the distribution on the blade. Additionally, the LDA system was used to map the flow field velocities in the plane of the propeller at several radii. Tangential and axial velocities were obtained for both the axisymmetric and non-axisymmetric blade alignments. This information was required for comparison with the PLL wake inflow predictions at the plane of the propeller.

5.2 Modeling Inclined Flow

As proposed in Chapter 1, the basis of the experiment is to design a stator which will favorably alter inflow to a propeller operating in an inclined flow. In formulating the approach to this experiment, it was recognized that the situation being addressed by this thesis could not be exactly modeled with the facilities in the lab. It is not possible to conduct an experiment with the propeller shaft inclined to the fluid flow in the MIT MHL water tunnel. Only axial flow can be obtained about the stationary shaft to which the stator was to be mounted. It was determined that a valid experiment could still be conducted.

By ***not*** inclining the flow, a predictable effect in the anticipated inflow wake can be taken into account. The once per revolution tangential velocity fluctuation is not actually present in the axial flow. Therefore, validation of the design and the code is accomplished by obtaining results which, when superimposed with the ***absent*** tangential periodic variation, yield the PLL wake prediction for the actual condition of inclined flow. Refer to Figure 5-1 to observe the anticipated experimental results for tangential wake in the plane of the propeller. Testing was done in both an axisymmetric and non-axisymmetric stator blade alignment. Discussion of the results is contained in Chapter 6.

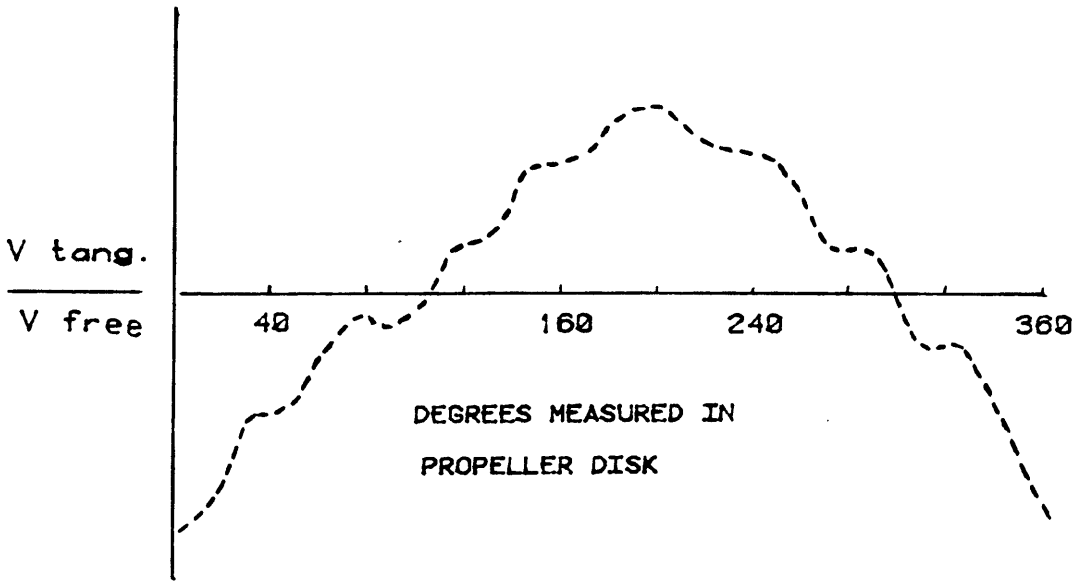

Figure 5-1: Desired Test Results

5.3 The Stator Model

The resulting stator design is shown in photographs in Appendix 2 and the figures of Chapter 3. A diagram of the stator mounted in the tunnel is also shown in Figure 5-2. Also indicated in this figure are the approximate radii in the plane of the propeller where the velocity measurements were obtained. where the velocity measurements were obtained. The nine identical stator blades each had a one-half inch diameter circular shaft at the hub. Once set to the desired angle, the blade was clamped in the hub assembly about the circular shaft. This controllable pitch feature allowed the angle of attack of each blade to be set individually as required for the non-axisymmetric analysis. The entire stator, blades and hub assembly,

were black anodized. Set screws were used to fix the hub assembly at the desired location on the shaft.

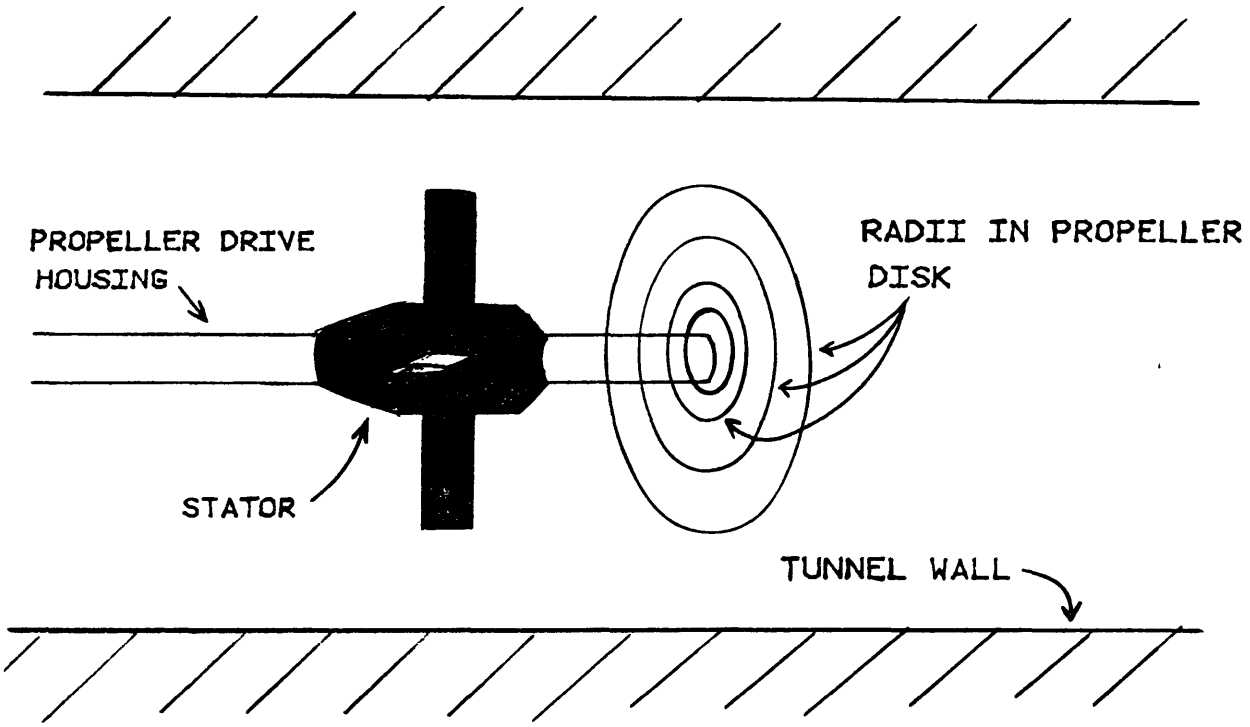

Figure 5-2: Stator Mounted in Water Tunnel

In order to measure the tangential velocities in the plane of the propeller for all stator blades, it was necessary to rotate the stator nine times during the course of the experiment. This repositioning was necessary to point the tip of the blade being measured directly at the laser. Tangential velocity measurements were made at selected radii in a forty degree sector on each stator blade, twenty degrees on either side of the blade's tip.

5.4 Operating Conditions

It was logically assumed to design the stator for use with the propeller at its design operating condition. This lead to the immediate establishment of some operating variables. The design advance coefficient, J , of the 4497 propeller is 0.889, which at a selected 1200 rpm establishes the water tunnel velocity at 17.72 feet per second. The thrust coefficient, K_T, is nearly 0.23 at design J, which provides a thrust of approximately 180 pounds. The water tunnel velocity and the required thrust were also inputs to PLL in earlier computer runs.

Chapter 6

EXPERIMENTAL RESULTS

6.1 Hub Vortex Strength

As mentioned in Chapter 5, there were several objectives of the experiment. These were to be accomplished in addition to the primary task of designing a stator which would modify the inflow in the plane of the propeller to counteract a shaft angle.

The first portion of the experiment dealt with the stator in an axisymmetric configuration, all nine blades set at the same angle of attack. As shown in the graph of Figure 3-1, the circulation distribution from SSF-1 was approximately equal to the PLL circulation when the angle of attack was thirteen degrees. With the stator model mounted in the water tunnel by itself at the operating speed of 17.72 feet per second, a significant hub vortex cavity was visible. See Appendix 2, still photograph No. 2 to note its appearance. The LDA system was used to collect tangential velocity measurements for the hub vortex at a distance one inch downstream from the apex of the tip of the hub. This location was selected for study as it was observed that the vortex position was very stable at this point. Velocity measurements were obtained beginning at a position three inches horizontally from centerline of the axis of the shaft inward to the point at which the laser signal was lost due to the hub vortex cavity. This data is presented in the graph of Figure 6-1. The sign of these velocity measurements was changed and plotted a second time to provide for easier comparison with the magnitude of other velocity measurements. Similar measurements at the same location were made for

the 4497 propeller operating by itself. The propeller hub vortex was similar in visual appearance to the stator hub vortex, and, as it should be, its direction of rotation was reversed. See Appendix 2, still photograph No.3 to note its appearance.

Lastly, the hub vortex velocity measurements for the stator and propeller combination were obtained. Its direction of rotation was the same as that of the propeller's hub vortex. In this configuration, at a water tunnel speed of 17.72 feet per second and the propeller at 1200 rpm, the hub vortex was not visible. These curves are also plotted and labelled in Figure 6-1. The peak value of tangential velocity was definitely obtained for the stator operating alone and for the stator/propeller combination. This statement is made based on the data points which shape these curves just inward from the peak. These points attest to the Rankine vortex nature of the hub vortex. The Rankine vortex is discussed further in Wang's doctoral thesis [18]. It is strongly suspected that the peak value of the curve for the 4497 propeller hub vortex was not obtained due to the loss of the LDA signal when the measuring volume was moved just adjacent to the hub vortex cavity. Referencing Wang's thesis, an approximation was made for the the magnitude of the peak tangential velocity and for the radius of the hub vortex. It is recognized that Wang experimented with a slightly different propeller at a lower advance coefficient, however, extrapolation of his data does provide a reasonable analytical approximation. It was estimated that the peak tangential velocity, if able to be measured, would be nearly 28 feet per second and its radius would be approximately 0.28 inches. Further justification for this value is derived from the fact that it was visually observed that the laser signal was lost at a location adjacent to the hub vortex cavity. This was at a radius greater than 0.6 inches. In view of Wang's experimentation, this radius seems too large to be the actual hub

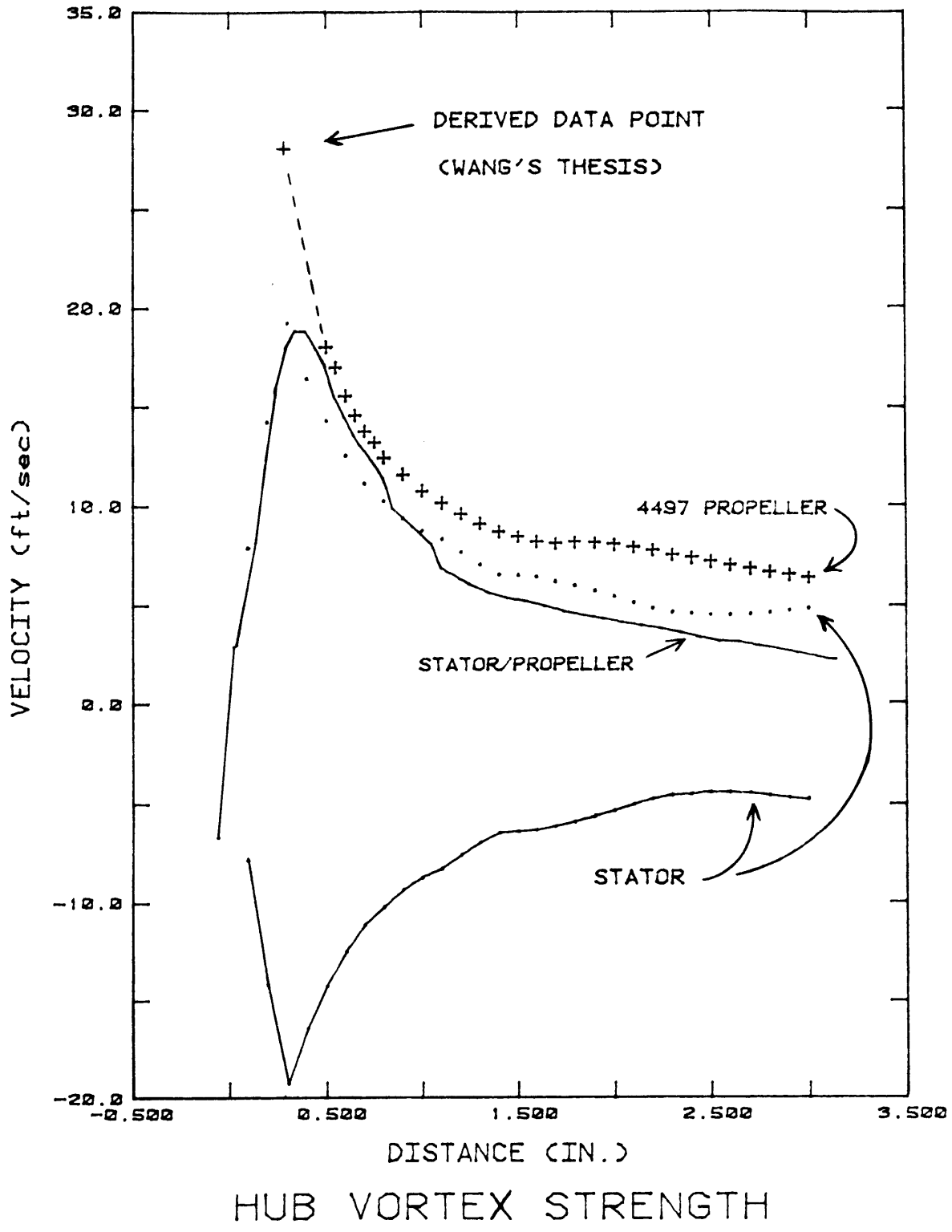

Figure 6-1: Hub Vortex Comparisons

vortex radius. It is highly probable that the cavity was enlarged due to entrained air. The conclusion is that the peak tangential velocity must be greater than the last measurement obtained and must be located closer to the centerline. This derived data point was later plotted and labelled on the graph of Figure 6-1.

The data shows a partial cancellation of the strength of the peak value of the hub vortex for the stator and the propeller operating together. This result was anticipated based on theoretical considerations, and on the absence of any visible vortex cavity during this phase of the experiment. See Appendix 2, still photograph No.4 which documents this phenomena.

6.2 Axisymmetric Testing

6.2.1 Non-Dimensional Circulation Measurements

The angle of attack which provided the desired circulation distribution for the stator blades in the axisymmetric case was determined to be +13 degrees relative to the inflow. To ensure that the circulation distribution on the stator blades was as predicted by the SSF-1 analysis program, velocity measurements were made around a stator blade a several radii. These measurements were made around rectangular closed contours at numerous discrete location. These velocities were converted to a non-dimensional circulation consistent with the manner used in the computer programs to allow for comparison. The distribution of the experimental non-dimensional circulation is graphed and presented in Figure 6-2 with the SSF-1 predicted distribution. Thickness effects were accounted for in the SSF-1 distribution. The comparison is excellent with respect to the shape of the distribution, but is in disagreement by approximately 7 percent in magnitude. The experimental data was greater. One possible explanation for the experimental

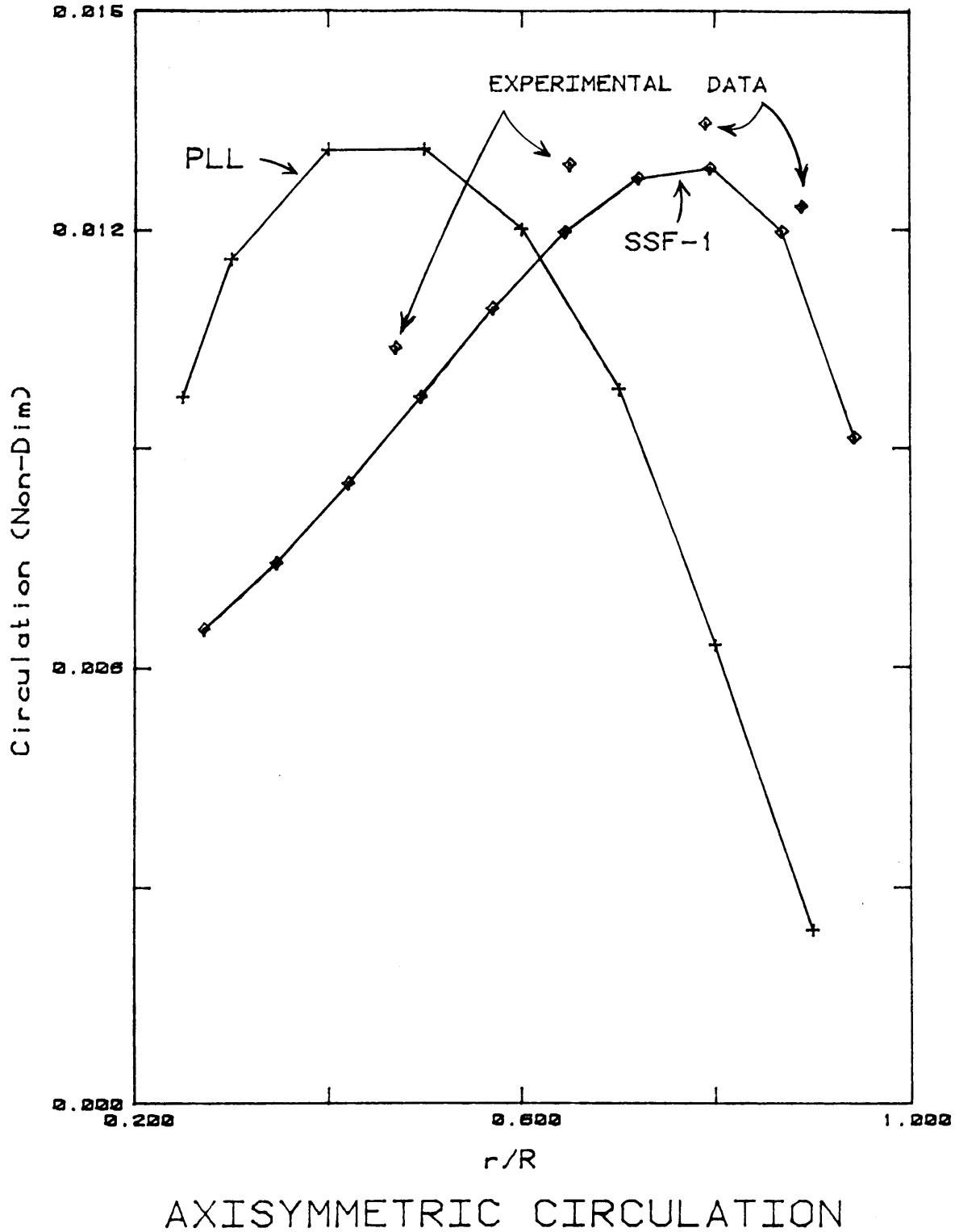

Figure 6-2: Experimental & Axisymmetric Circulation

circulation being greater is the tunnel wall effect experienced in the test section. The presence of the tunnel wall restricts the flow in the test section and could thereby result in more circulation on the blade than would otherwise be present in an unrestricted flow. Additional deviation could be introduced by not setting the stator blade angles accurately. It is estimated that the bench technique for setting blade angles is accurate to within one-half degree. A circulation distribution from the SSF-1 program for an angle setting of +13.5 degrees was obtained. This was done to better establish the magnitude of error which could be introduced by inaccurate setting of the blade's angle of attack. The results of this program run are plotted in Figure 6-3 along with experimental data and the circulation distribution for the +13 degree angle of attack. Assuming that the angle of attack was set one-half degree greater than desired, the graph shows the experimental data to be in much closer agreement with the computer prediction.

It can therefore be concluded that the SSF-1 program is a reliable tool for predicting circulation distributions. This would again be demonstrated in the non-axisymmetric stator testing.

6.2.2 Flow Field Measurements

With the stator blades in an axisymmetric alignment, axial and tangential velocity measurements were made at several radii in the plane of the propeller. Figure 6-4 displays the tangential velocities at five different radii, 4.5 inches downstream from the quarter-chord location of the stator blades. The shape of these curves was as anticipated and can be logically explained. Referring to Figure 6-5 assists in visualizing the flow situation. At the smallest radius, the major fluctuation is due to the hub vortex effects. At the outer radii, the large fluctuation is due to the proximity of the tip vortex. This is also true for r/R = 0.8. At the

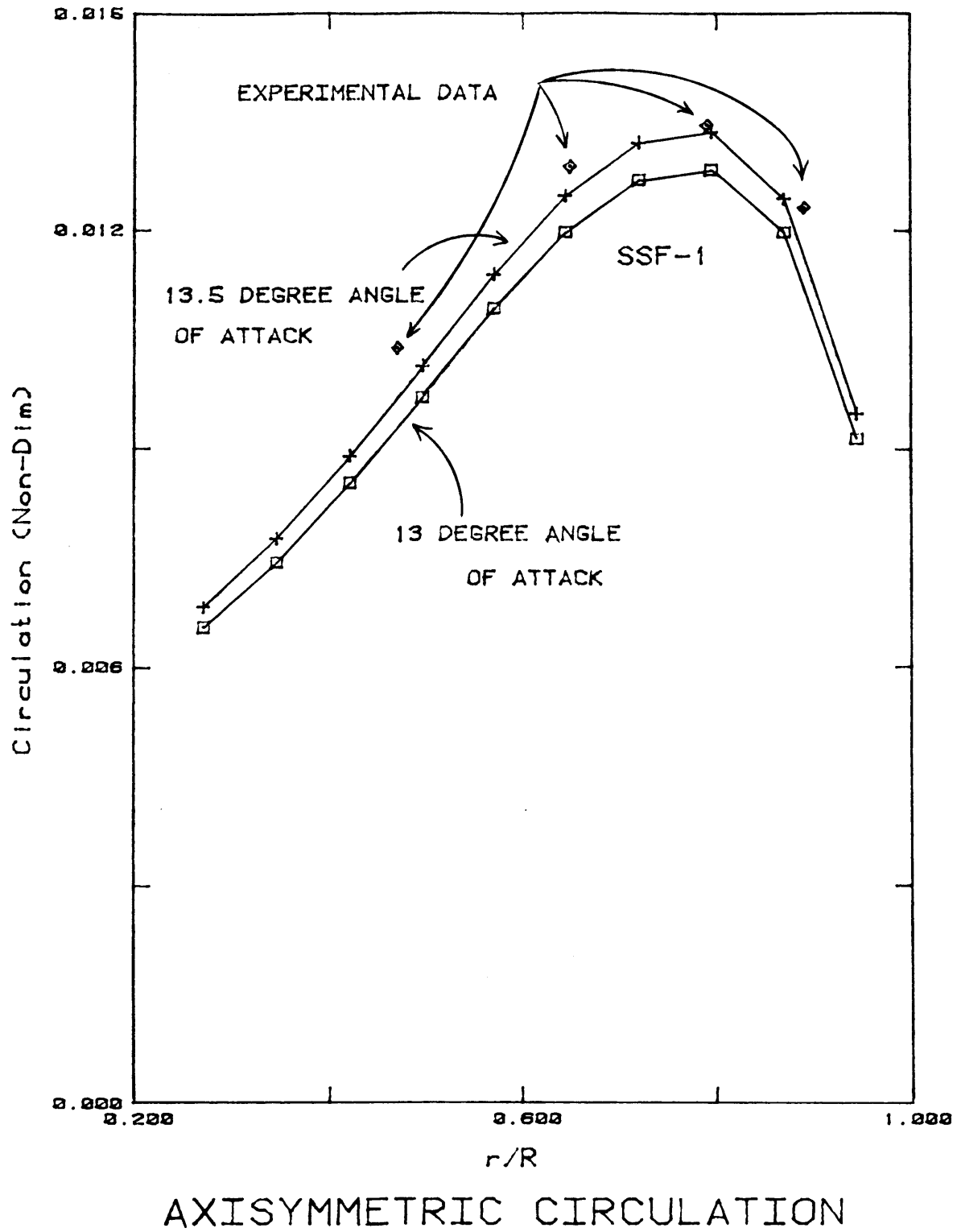

Figure 6-3: Circulation Distribution Comparison

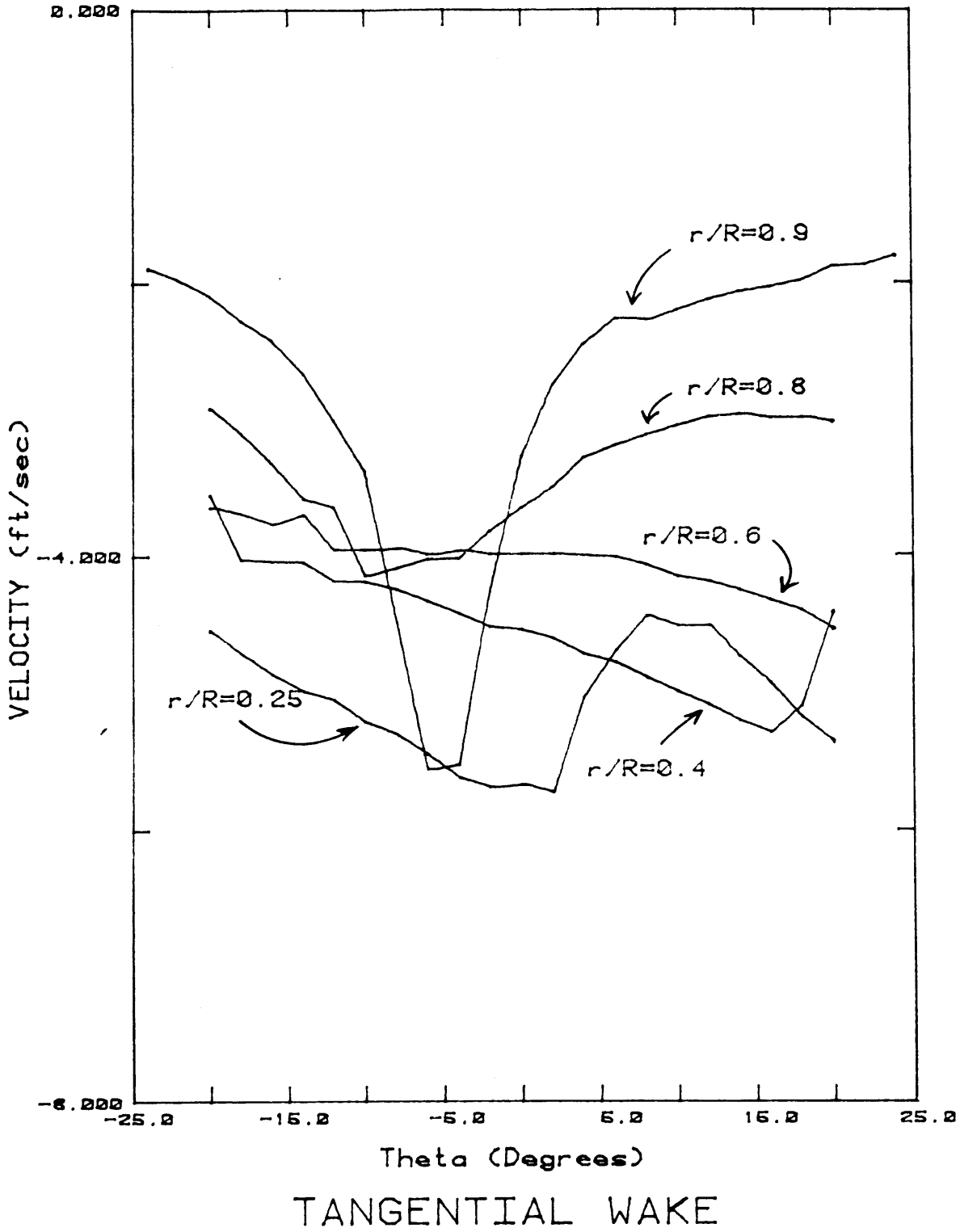

Figure 6-4: Tangential Wake - Axisymmetric Stator

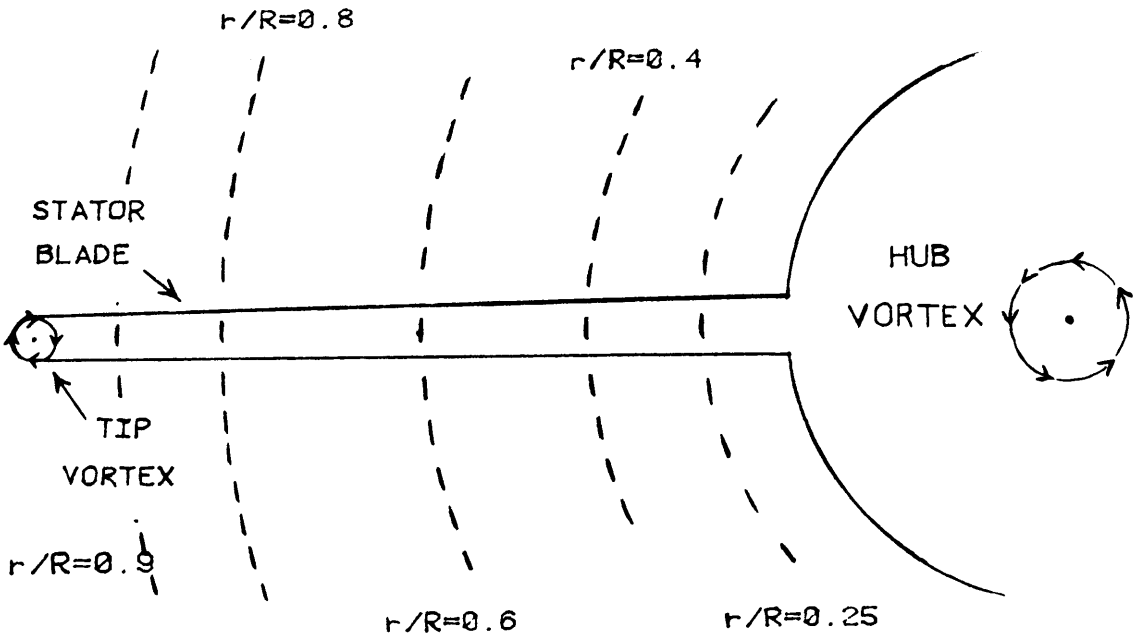

Figure 6-5: Radial Locations for Velocity Measurements

radii near mid-span, the tangential velocity fluctuation is not as pronounced due to the distance from both the tip vortex and the hub vortex. The modest negative (downward) velocity at these radii is due to the flow being inclined by the thirteen degree angle of attack of the blades.

6.3 Non-Axisymmetric Testing

6.3.1 Non-Dimensional Circulation Measurements

In the non-axisymmetric testing of the stator, the nine blades were set at angles of attack determined from the SSF-1 program. Numbering the nine blades consecutively around the stator, the angles were as follows: 19.0 degrees for blade 1, 16.1 degrees for blades 2 and 9, 11.0 degrees for blades 3 and 8, 7.0 degrees for blades 4 and 7, and 5.5 degrees for blades 5 and 6. As shown in Figure 3-2, these

angles gave the best match to the PLL circulation distributions which produced the desired predicted tangential velocities. As was done in the axisymmetric case, non-dimensional circulation measurements were obtained. Based on the reliability of the SSF-1 program established in earlier testing, only three radii on two blades were selected for circulation measurements. The most heavily and lightly loaded blades were sampled at radii about the location the maximum circulation was anticipated to occur. This experimental data is plotted for comparison with the SSF-1 program distribution in Figure 6-6.

Only five blade circulation distributions are shown in the graph because blades 6,7,8, and 9 are symmetric with blades 5,4,3, and 2 respectively. The circulation distributions for the symmetric blades are essentially the same. For the most heavily loaded blade, a similar experimental result to the axisymmetric circulation measurement is noted. With only three data points to compare, it would be suspect to generalize about the shape of the entire distribution. However, with the previous axisymmetric results as a basis, it is claimed that the shape of the distribution matches very well to the SSF-1 program prediction. The magnitude is in disagreement by approximately 8 percent. The same justifications stated for the axisymmetric discrepancies between experimental and computer predicted circulation apply here as well. For blade 5, the most lightly loaded blade, the experimental results are nearly identical for two of the three radii sampled. The shape of the circulation distribution for the lightly loaded blades, which are set at small angles of attack, is more heavily influenced by the blade twist.

Based on these experimental results, it is claimed that the circulation distributions predicted by the SSF-1 program are very nearly the actual distributions on the stator blades. This validation was necessary prior to proceeding to the flow field measurements in the plane of the propeller for the non-

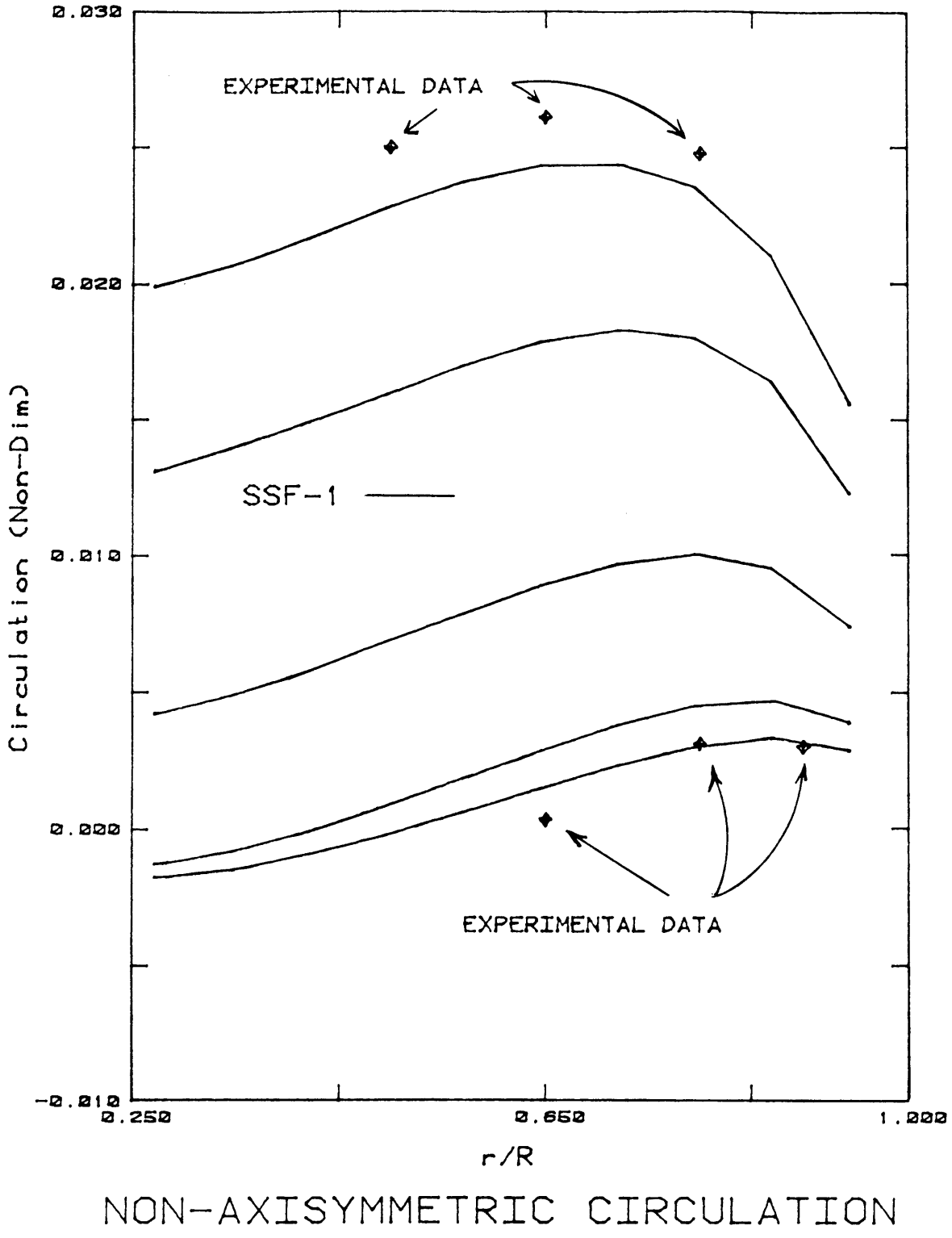

Figure 6-6: Experimental & Non-Axisymmetric Circulation

axisymmetric stator. The mapping of these tangential velocities is the key indicator for comparison to PLL wake predictions and the basis for judging the success of the design. The induced tangential velocities represent solid evidence that the stator is providing the desired modification to the inflow.

The non-axisymmetric circulation distributions provided by the SSF-1 program were used to supply inputs back into PLL for revised wake predictions. This was done to allow for the fact that the circulation distributions on the stator blades in the non-axisymmetric alignment were not exactly those originally used by the PLL program. The matching procedure between the PLL and SSF-1 programs discussed in Chapter 3 resulted in some differences in circulation when the 3-dimensional effects were considered. In order to perform a more accurate comparison between the computer wake prediction and the experimentally obtained data, this iteration was performed. Figure 6-10 presents this revised wake prediction.

6.3.2 Non-Axisymmetric Flow Field Measurements

The mapping of the velocity measurements in the plane of the propeller for the non-axisymmetric case was done at three different radii. The experimental results for the tangential velocity measurements are presented in Figure 6-7, Figure 6-8, and Figure 6-9.

As shown in Figure 5-1, the overall desired experimental result for the shape of the tangential wake is periodic for one revolution about the disk of the propeller. This is due to the absence of inclined flow in the tunnel. The superposition of a once per revolution tangential velocity fluctuation due to inclined flow upon the experimental tangential flow mapping should produce the wake predicted by PLL. These wake predictions from PLL were presented in Figure 2-2 and the revised wake

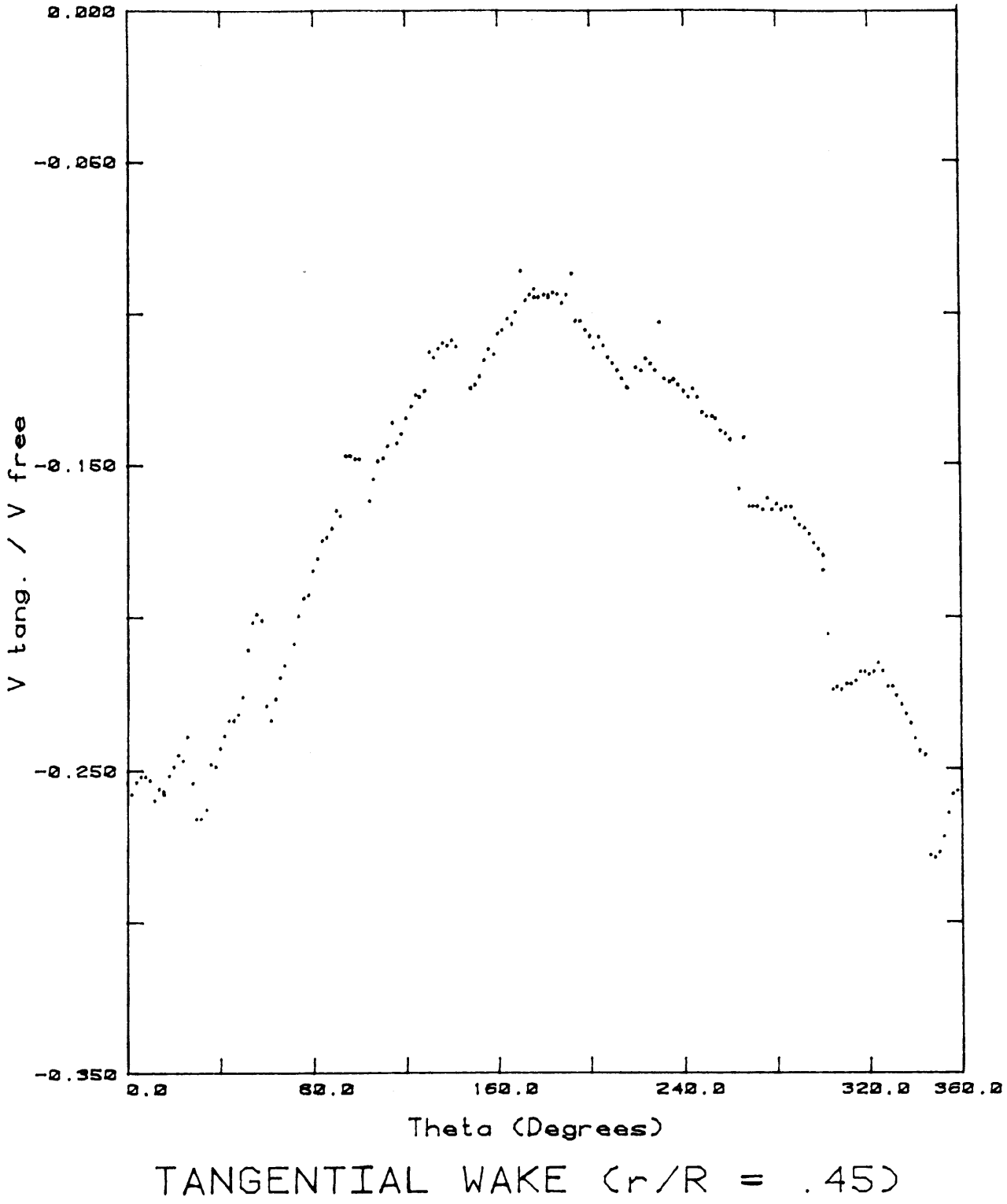

Figure 6-7: Tangential Wake, r/R = .45

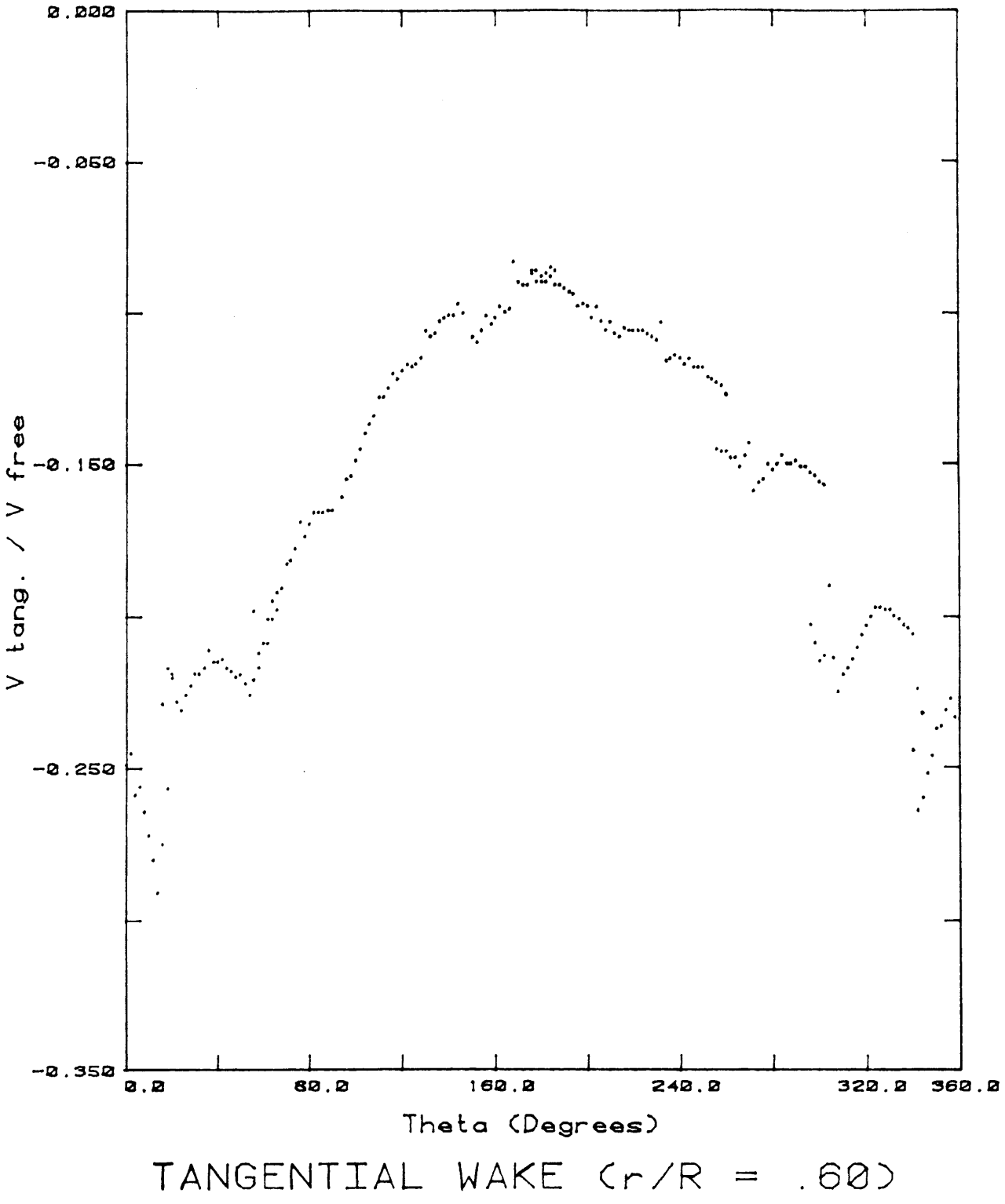

Figure 6-8: Tangential Wake, r/R = .60

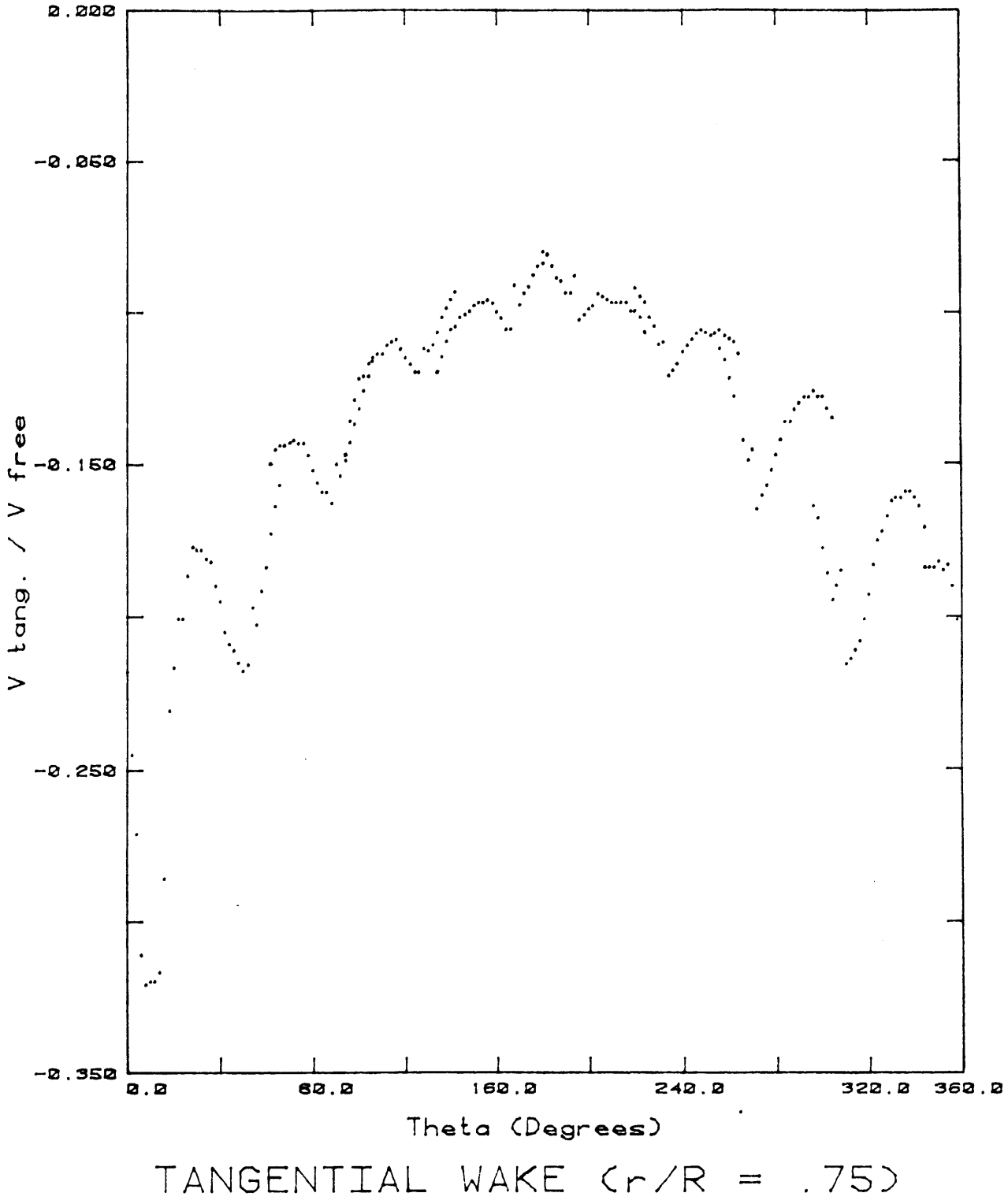

Figure 6-9: Tangential Wake, r/R = .75

is shown in Figure 6-10. Some overlap of the data points exists on the graphs due to sampling about 24 degrees on either side of each stator blade. This was done intentionally to assist in bringing the nine data files together on one graph. It should be noted that some measurement error due to positioning was undoubtedly introduced each time one of the nine blade tips was directed at the laser by rotating the entire stator assembly on the shaft housing.

From the graphs, the amplitude of the ratio of the tangential velocity to the free stream velocity about its mean is approximately 0.10. The assumed shaft angle for producing the inclined flow was seven degrees for purposes of this experiment. The amplitude of the tangential velocity fluctuation due to a seven degree shaft angle is 0.12. This represents a favorable comparison. Figure 6-10 shows the PLL wake prediction when the SSF-1 program results for non-axisymmetric analysis are used to supply input back to the PLL program. This would be the wake pattern if the experimental results were superimposed upon the inclined flow harmonic fluctuation in tangential velocity. Note that the data for tangential wake inflow does roughly capture the nine smaller amplitude periodic oscillations which represent the influence of the nine stator blades. This effect is best seen in Figure 6-9. This effect was part of the PLL wake prediction, especially at the outer radii. The general observation, which is supported by graphical presentations of experimental data, is that the non-axisymmetric stator does induce tangential velocities to counter the inclined flow. It can be concluded that the stator in this non-axisymmetric alignment, when placed in 7 degree inclined flow, would have a tangential wake as predicted by PLL in Figure 6-10.

During the non-axisymmetric testing, axial and tangential velocity measurements were taken at various radii in the plane of the propeller. These measurements indicate that the flow was indeed inclined by the non-axisymmetric

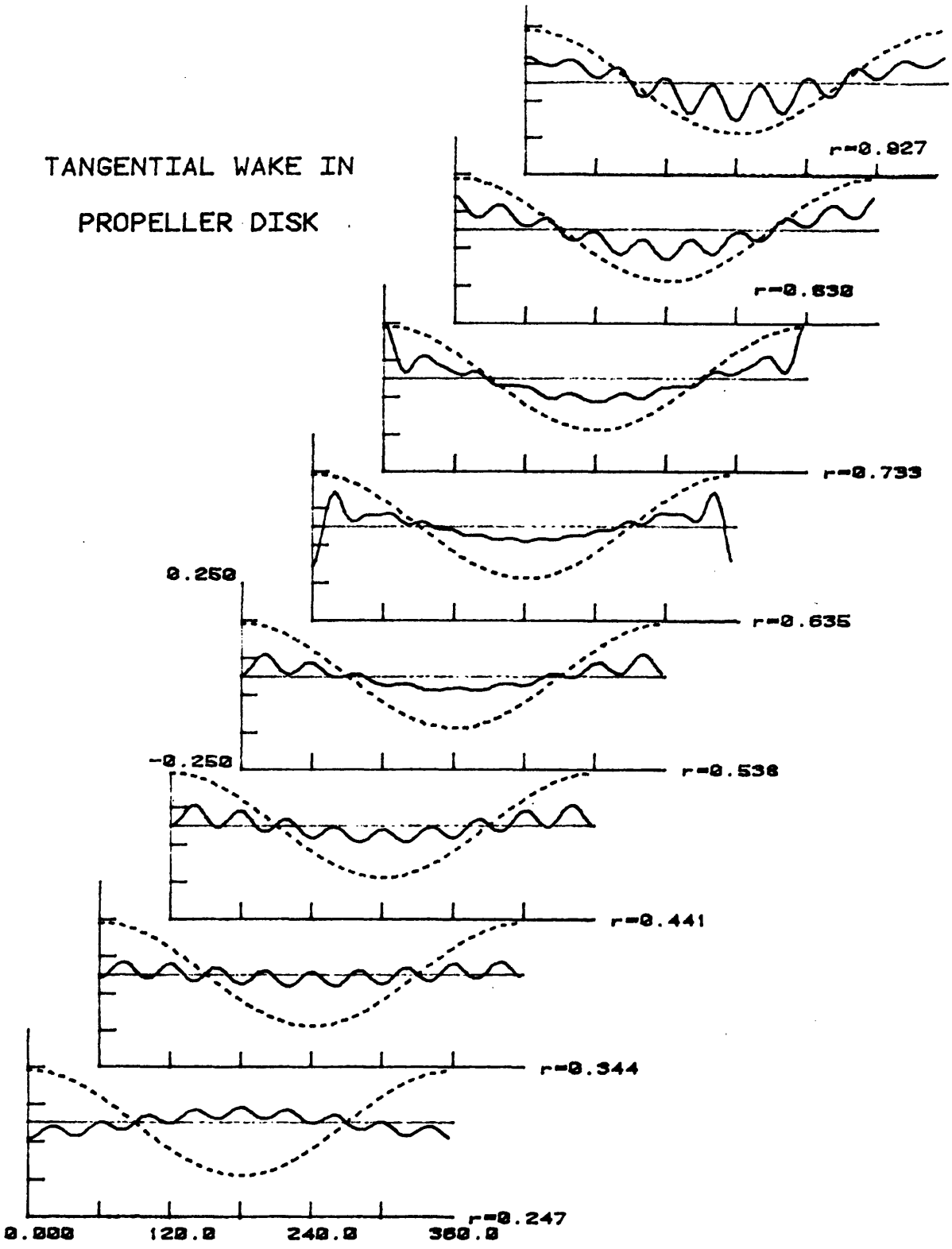

Figure 6-10: Revised PLL Tangential Wake

stator. The angle of inclination did vary with radius. The flow inclination is easily observed by referring to Appendix 2, photographs No.5 and No.6.

6.4 Propulsive Efficiency

In order to compare the efficiency of the propeller to the stator/propeller combination, standard open-water tests were performed in the water tunnel. Programs were available in the MIT MHL for conducting these tests. The 4497 propeller was tested several times to ensure that a reliable test result was obtained. The representative output from one of these open-water tests in included in Appendix 3. At the design advance coefficient, J, of .889, the thrust coefficient, K_T was .233. At 1200 RPM the thrust provided is 180.0 pounds. Its propulsive efficiency, η, was 0.65 at design J. Figure 6-11 graphically displays the results of this open-water test. Appendix 1 contains a PLL output for the propeller operating by itself. The η value numerically predicted was by PLL was 0.67. The slight discrepancy is most likely accounted for by some difference between the propeller circulation distribution input to PLL and the actual distribution on the blades.

After mounting the stator model on the propeller drive housing just forward of the 4497 propeller, more open-water tests were conducted. The stator was positioned on the housing such that the quarter chord location of the stator was 4.5 inches forward of the quarter chord location of the propeller. A representative result from one of these tests is included in Appendix 3. Figure 6-12 graphically displays the results of this test. Before comparing these results with the results for the propeller alone, the increased drag on the propulsor combination due to the stator must be taken into account.. More water tunnel tests were conducted to determine the drag on the stator. A testing sequence was devised whereby the drag on the stator, minus any hub vortex effects, was estimated over a range of

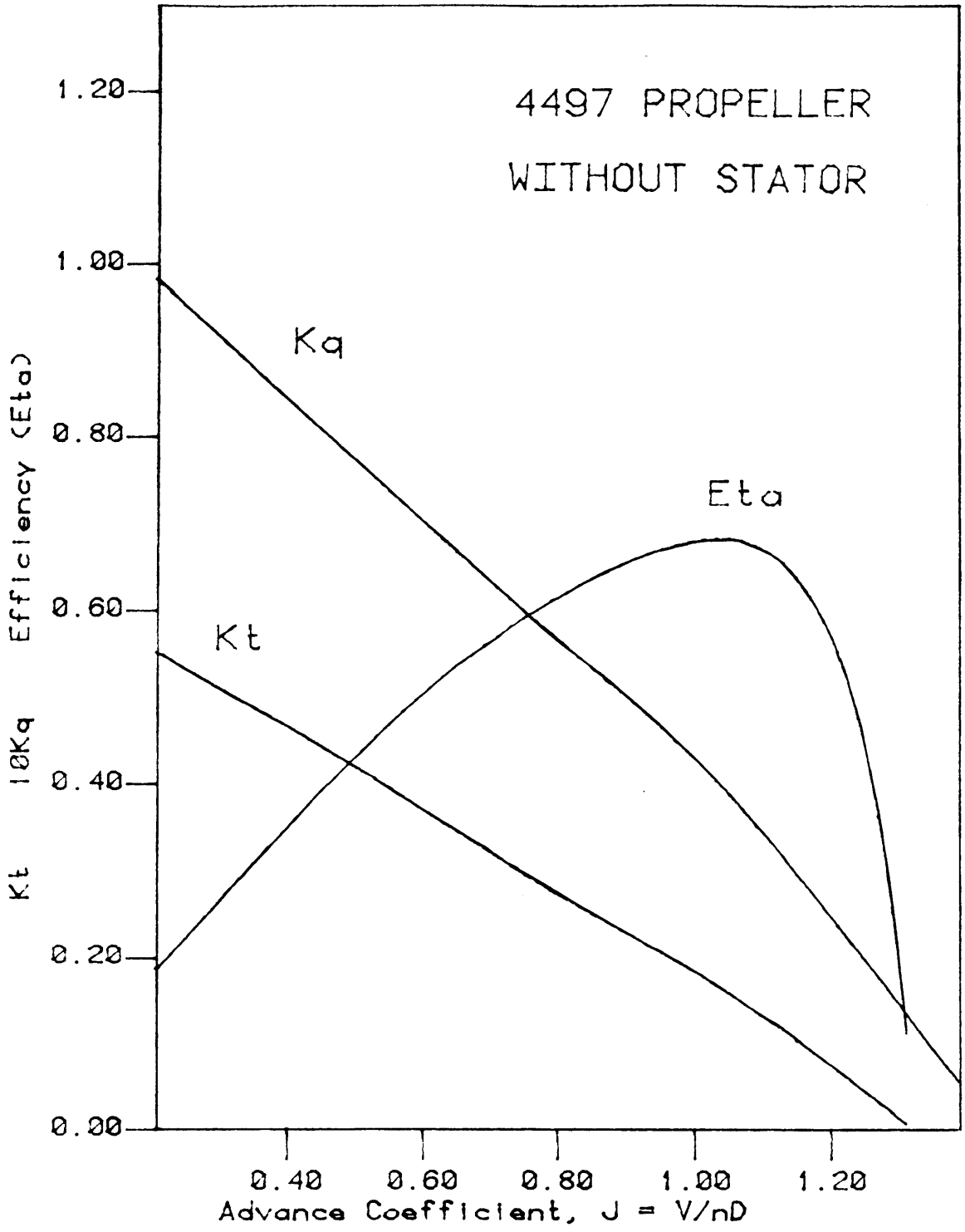

Figure 6-11: Propeller 4497 Open-Water Test

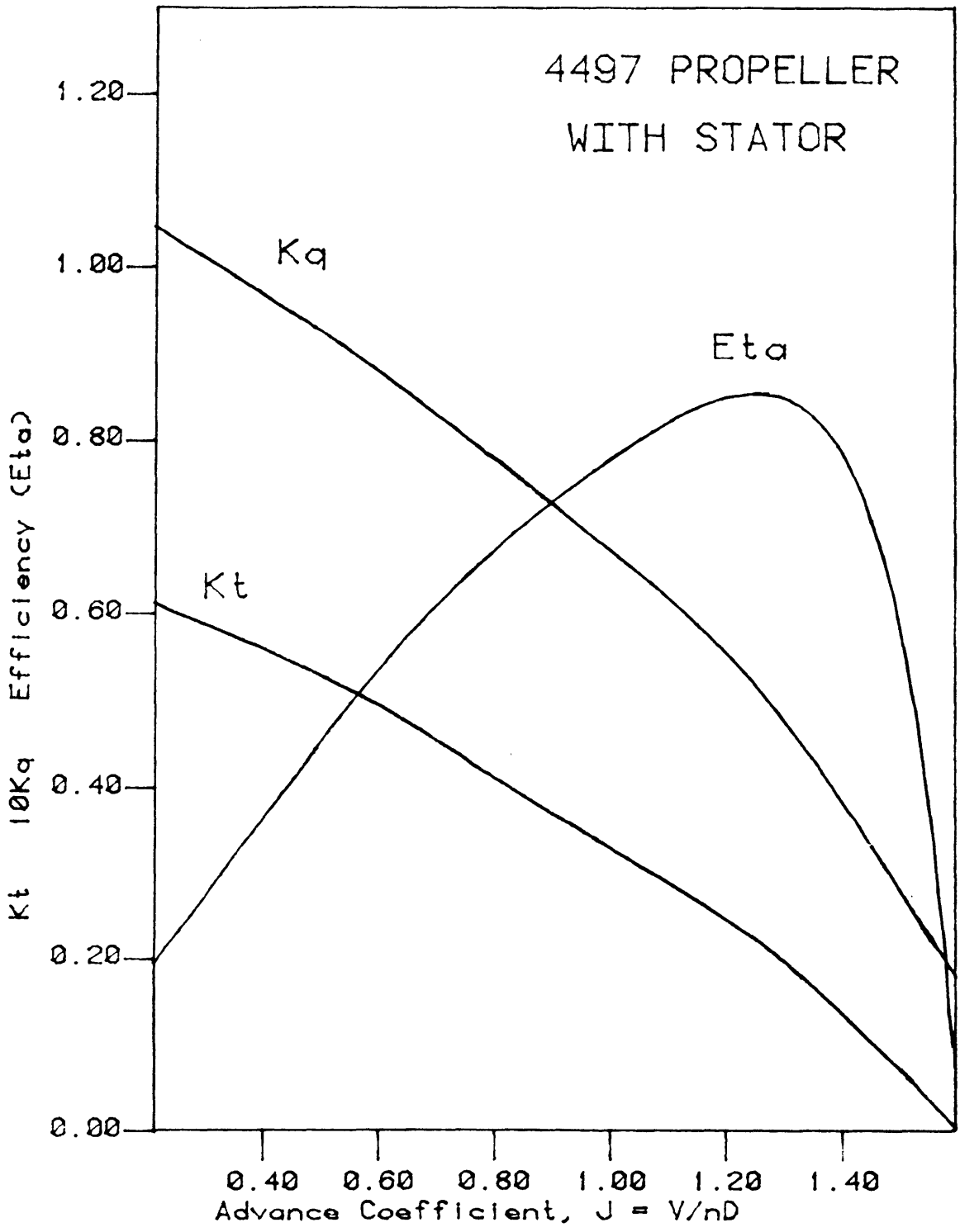

Figure 6-12: Stator/Propeller Open-Water Test

operating speeds. The influence of the hub vortex was experimentally estimated at 2.2 pounds at the operating speed of 17.72 feet per second. This correction was applied to the experimentally derived value of 15.3 pounds of drag on the stator with hub vortex. Therefore, the drag due to the stator alone was estimated at 13.1 pounds. This value compares remarkably well with the PLL prediction of 11 pounds of drag. The experimental value is substantially verified by the computer result.

Having established a reliable estimate for the stator drag, the propulsive efficiencies of the propeller and the stator/propeller can now be compared. To perform a fair comparison, it was decided to select operating points where both propulsors were providing an equal amount of thrust. At the J value of 0.89, the 4497 propeller provided 180 pounds of thrust. The K_T at this point was 0.233. The propulsive efficiency, η, was 0.65. This information is also graphically presented in Figure 6-13, which presents the open-water test results for the propeller operating with and without the stator. Also plotted for the propeller is the curve of constant K_T/J^2, a ratio which relates to the thrust loading coefficient, C_T. Basically, the K_T/J^2 curve represents the operating points where an equal amount of thrust is provided.

To locate the appropriate stator/propeller operating point for comparison of efficiency, it was first necessary to account for the reduced thrust due to drag on the stator. The operating point selected would have to represent approximately 193 pounds of thrust to offset the estimated 13.1 pounds of stator drag at the water speed of 17.72 feet per second. Through a trial and error procedure, numerous operating points were selected and analyzed. This lead to the determination of a comparison operating point at J equal to 1.01. At this J, the thrust loading coefficient, C_T, was .636 and when corrected for stator drag, a thrust of 180.1

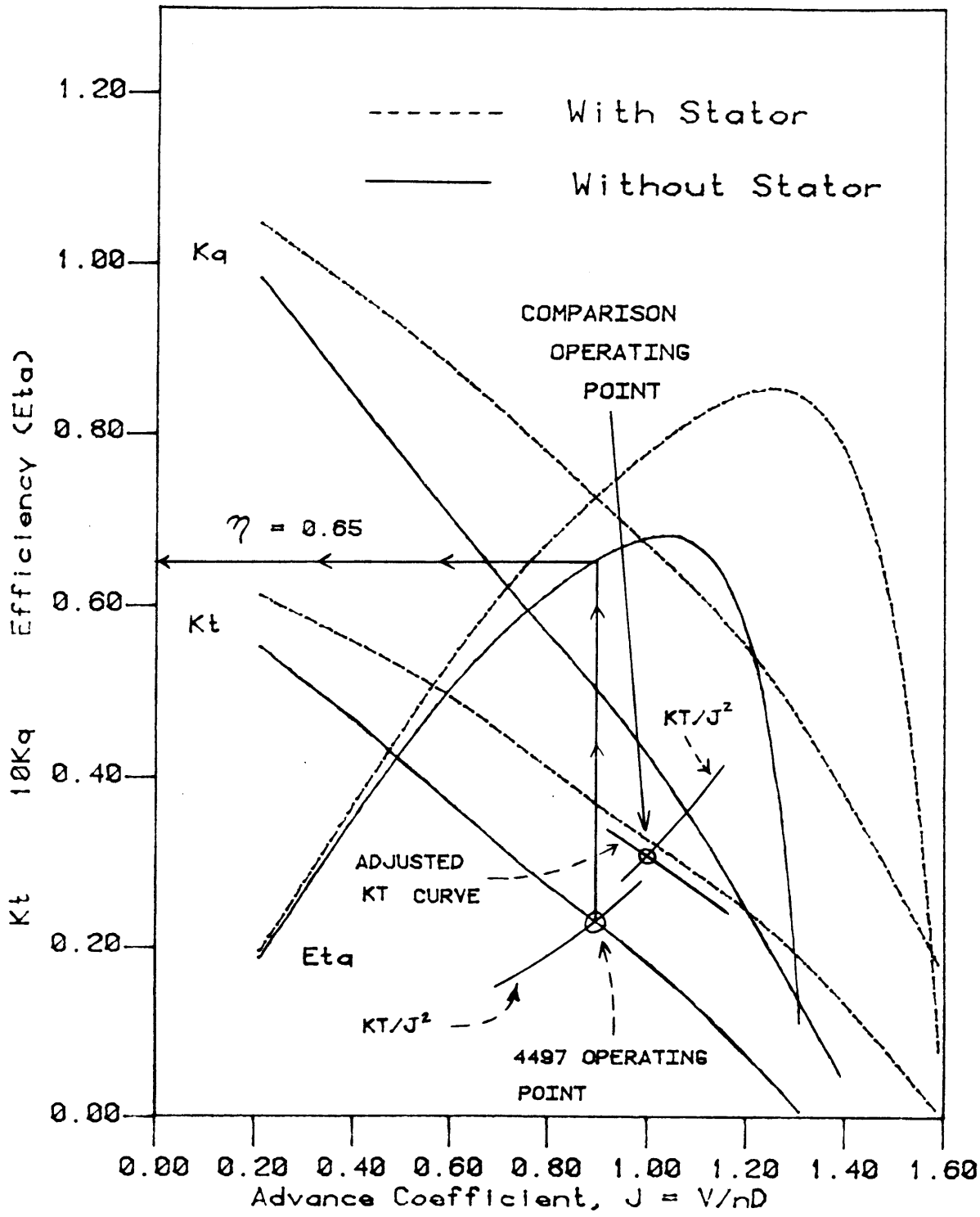

Figure 6-13: 4497 Propeller Tests

pounds is anticipated. The K_T/J^2 ratio was equal to 0.31795 and K_T was 0.324. Therefore, assuming that the operating speed is fixed at 17.72 feet per second, the thrust provided at this operating point would be 192.9 pounds. Correcting for stator drag results in a net thrust of approximately 180 pounds. The calculated propulsive efficiency, $\eta = K_T J/2\pi K_Q$, at this point is 0.73. This indicates an 8 percent increase in η even after accounting for stator drag.

The curves of Figure 6-13 for the stator/propeller are not corrected for drag due to the stator. The K_T curve would be shifted downward to adjust for the reduced thrust. A portion of the corrected K_T, in the vicinity of the comparison operating point is plotted on Figure 6-13. Also, the propulsive efficiency curve would be slightly reduced in amplitude to reflect this correction.

Chapter 7

CONCLUSIONS

7.1 Experimental Summary

This experimental thesis effort was designed to address a propulsive problem associated with a propeller operating on an inclined shaft. This is the case for a large majority of surface ships of all sizes. The objective was to design a stator model which would minimize the once per revolution tangential wake harmonic associated with inclined flow. The primary benefit of achieving this modified inflow would be an increase in propulsive efficiency. A validation of the PLL computer wake predictions was performed by a comparison with experimental flow field measurements.

The results of the experiment support the claim that the stator improves the propeller's performance. When the two component propulsor was tested with the stator in an axisymmetric blade alignment, there was a significant increase in the propulsive efficiency when compared to the propeller operating alone. This was indicated by the results of the open-water tests. This increase was approximately 8 percent at an operating point where an equal amount of thrust was provided.

The focus of the non-axisymmetric testing was to incline the flow and to map the flow field velocities in the plane of the propeller. The results validate the computer generated wake predictions of the PLL program. The non-axisymmetric stator induced tangential velocities which tended to minimize the once per revolution harmonic due to shaft angle. While unable to model inclined flow, superposition of this harmonic fluctuation on the flow field mapping obtained did

produce the desired result. It is reasonable to conclude that the propulsive efficiency of the non-axisymmetric stator and propeller in an inclined flow would be greater than that of the propeller alone.

During the course of the experiment, the experimentally obtained non-dimensional circulation distributions were used to check the accuracy of the output of the recently developed MIT MHL SSF-1 program. The experimental data collected in this portion of the testing generally exceeded the computer prediction by 7 to 8 percent. However, there appeared to be excellent agreement with regard to the shape of the distribution.

The additional testing performed with reference to the hub vortex strength supports the following statements. The cancellation effect concerning the hub vortices of the stator and the propeller does not represent a significant gain in terms of thrust and efficiency. It was observed that the cancellation effect is not complete at operating points where a reasonable amount of thrust is provided. The negative thrust caused by the hub vortex is not significant in comparison to the net thrust. The results of velocity measurements of hub vortex strength for the stator, the propeller, and the combination support the concept of the Rankine vortex as a model for the hub vortex.

7.2 Discussion

Upon reflection of the results obtained from this experiment, some logical extensions for further testing of the stator can be identified. It was noted that the combination of the stator/propeller was more efficient than the propeller alone. A testing scheme could be devised whereby open-water tests with the axisymmetric stator and propeller would be performed. Successive tests could be conducted

varying the angle at which the stator blades are set. The objective would be to determine the optimum angle in terms of achieving the highest propulsive efficiency while providing an equal amount of thrust as the propeller operating alone. The existing computer programs could be exercised to conduct the same experiment to arrive at the analytical answer. A favorable comparison between the determined angles should result.

The number of non-dimensional circulation data points obtained in the non-axisymmetric testing was limited. This was felt to be justified in this experiment by the reliability established during more extensive axisymmetric sampling. However, the collection of more data would provide greater confidence to the output provide by the SSF-1 analysis program.

The general conclusion which can be drawn from this effort is that the non-axisymmetric stator can be used to favorably modify propeller inflow to counteract the effects of shaft angle. Increased propulsive efficiency can be achieved by a stator by reducing the energy left in the propeller's wake. It is recognized that these results were produced in the laboratory, and that extension of this concept to operating ships presents a greater challenge.

Bibliography

[1] Abbott, Ira H. and Von Doenhoff, Albert E.
Theory of Wing Sections.
Dover Publications, 1959.

[2] Boswell, R.J.
Design, Cavitation Performance, and Open-Water Performance of a Series of Research Skewed Propellers.
Technical Report 3339, DTNSRDC, March, 1971.

[3] Boswell,R.J.; Jessup, S.D. and Kim, K.
Periodic Single-Blade Loads on Propellers in Tangential and Longitudinal Wakes.
SNAME Propellers '81 Symposium , May, 1981.

[4] Brockett, T.
Minimum Pressure Envelopes for Modified NACA - 66 Sections with NACA a=0.8 Camber and Buships Type I and Type II Sections.
Technical Report 1780, DTNSRDC, February, 1966.

[5] Greely, D.S. and Kerwin, J.E.
Numerical Methods for Propeller Design and Analysis in Steady Flow.
Transactions SNAME, Vol. 90 , 1982.

[6] Hecker, R. and McDonald, N.A.
The Effect of Axial Spacing and Diameter on the Powering.
Technical Report 1342, DTNSRDC, February, 1960.

[7] Kerwin, J.E.
Hydrodynamic Theory for Propeller Design and Analysis.
MIT, Department of Ocean Engineering, 1986.

[8] Kerwin, J.E.; Coney, W.B. and Hsin, C.
Optimum Circulation Distributions for Single and Multiple-Component Propulsors.
Proceedings, 21st American Tow Tank Conference, Wash, D.C. , August, 1986.

[9] Larimer,G.; Gearhart, W.; Van Liew, D.; Shields, C.
Reaction Fin Applications in Marine Propulsion.
SNAME, Hampton Roads Section , March, 1987.

[10] Miley, S.J.
A Catalog of Low Reynolds Number Airfoil Data for Wind Turbine Applications.
Dept. of Aerospace Engineering, Texas A & M University, 1982.

[11] Nelka, J.J.
Experimental Evaluation of a Series of Skewed Propellers with Forward Rake: Open-Water Performance, Cavitation Performance, Field-point Pressures, and Unsteady Propeller Loading.
Technical Report 4113, DTNSRDC, July, 1974.

[12] Newman, J.N.
Marine Hydrodynamics.
The MIT Press, Cambridge, MA., 1977.

[13] Okamura, N.
Experimental Analysis of the Flow Field Around a Screw Propeller.
IHI Engineering Review , October, 1983.

[14] Sabersky, R.H.; Acosta, A.J. and Hauptmann,E.G.
Fluid Flow: A First Course in Fluid Mechanics.
Macmillan Publishing Co, Inc., 1971.

[15] Sayre, C.H.
Laser Doppler Anemometry and the Measurement of Loading Characteristics of Lifting Sections.
June, 1980.
Master's Thesis, MIT.

[16] Schoenberger, R.B.,
Experimental Determination of Propeller Field Point Velocities Using Laser Doppler Anemometry.
June, 1983.
Master's Thesis, MIT.

[17] Takekuma, K.
Evaluation of Various Types of Nozzle Propellers and Reaction Fins as the Device for Improvement of the Propulsive Performance of High Block Coefficient Ships.
Proceedings, Shipboard Energy Conservation Symposium , Sept, 1980.

[18] Wang, M.
Hub Effects in Propeller Design and Analysis.
June, 1985.
Ph.D. Thesis, MIT.

[19] Watrasiewicz and Rudd.
Laser Doppler Measurements.
Butterworths, 1976.

Appendix A
PLL OUTPUT

PROPELLER LIFTING LINE RUN: 17:23:44
stator/propeller axisymmetric

PLL SUMMARY OUTPUT

SHIP SPEED (FT/SEC):	17.72	FLUID DENSITY:	1.9350
SHAFT DEPTH (FT):	2.00	NUMBER OF DEVICES:	2
TOTAL THRUST (LBS):	180	TORQUE (FT-LBS):	0
HORSEPOWER:	8	EFFICIENCY:	0.699
IMAGE HUB USED:	T	IMAGE DUCT USED:	F
HUB DRAG (lbs):	0	(HUB VORTEX)/(RHUB):	0.4000

****

SUMMARY OUTPUT FOR COMPONENT NUMBER: 1

AXIAL LOCATION(FT) :	0.00	DIAMETER (FT):	1.00
NUMBER OF BLADES:	5	HUB DIAMETER (FT):	0.20
NUMBER OF CONTROL POINTS:	8	REVS. PER MINUTE:	1200.00
BLADE FILE:	blade11121.out	WAKE DIAMETER (FT):	1.00
WAKE FILE:	blawake1112.out	THRUST (LBS):	191
TORQUE (FT-LBS):	36	HORSEPOWER:	8
ADVANCE COEFFICIENT:	0.886	EX. AREA RATIO:	0.720
BLADE VOLUME (CU FT):	0.00	MOM. OF INERTIA (FT**5):	0.00
NUMBER OF PANELS:	8		

CT: 0.8035 CQ: 0.1522 CP: 1.0790 KT: 0.2477 KQ: 0.0469

SUMMARY OUTPUT FOR COMPONENT NUMBER: 2

AXIAL LOCATION(FT) :	-0.38	DIAMETER (FT):	1.20
NUMBER OF BLADES:	9	HUB DIAMETER (FT):	0.28
NUMBER OF CONTROL POINTS:	10	REVS. PER MINUTE:	0.00
BLADE FILE:	sta1124.dat;6	WAKE DIAMETER (FT):	1.20
WAKE FILE:	stawake1112.out	THRUST (LBS):	-11
TORQUE (FT-LBS):	-35	HORSEPOWER:	0
ADVANCE COEFFICIENT:	999.000	EX. AREA RATIO:	0.978
BLADE VOLUME (CU FT):	0.00	MOM. OF INERTIA (FT**5):	0.00
NUMBER OF PANELS:	10		

CT: -0.0340 CQ: -0.0872 CP: 0.0000 KT:999.0000 KQ:999.0000

COMPUTATION TOOK: 31.31 SECONDS

****

PROPELLER LIFTING LINE RUN: 17:23:44

DETAILED OUTPUT FOR COMPONENT NUMBER: 1

R/R0	Cin/D	T/D	CDRAG	Gin	UA/VS nominal	UA/VS effective	UT/VS	BETA
0.2000	0.1740	0.0434	0.0085	0.0000	1.0000	1.0000	0.0000	54.66
0.2500	0.2020	0.0396	0.0085	0.0149	1.0000	1.0000	0.0000	48.44
0.3000	0.2290	0.0358	0.0085	0.0213	1.0000	1.0000	0.0000	43.23
0.4000	0.2750	0.0294	0.0085	0.0308	1.0000	1.0000	0.0000	35.19
0.5000	0.3120	0.0240	0.0085	0.0361	1.0000	1.0000	0.0000	29.42
0.6000	0.3370	0.0191	0.0085	0.0369	0.0000	1.0000	0.0000	25.18
0.7000	0.3470	0.0146	0.0085	0.0337	0.0000	1.0000	0.0000	21.94
0.8000	0.3340	0.0105	0.0085	0.0277	0.0000	1.0000	0.0000	19.42
0.9000	0.2800	0.0067	0.0085	0.0189	0.0000	1.0000	0.0000	17.40
0.9500	0.2100	0.0048	0.0085	0.0132	0.0000	1.0000	0.0000	16.53
1.0000	0.0000	0.0029	0.0085	0.0000	0.0000	1.0000	0.0000	15.75

****

R/R0	C/D	BETAI	G	UA*/VS	UT*/VS	CL	DCT	DCQ	SIGMA
0.2000	0.1740	44.22	0.0124	-0.0248	0.2929	0.2594	0.2581	0.0331	3.7814
0.2500	0.2020	44.24	0.0125	0.0529	0.1949	0.2602	0.2613	0.0337	3.2263
0.3000	0.2290	43.49	0.0168	0.1238	0.1208	0.2894	0.3861	0.0577	2.7535
0.4000	0.2750	40.29	0.0279	0.2321	0.0352	0.3334	0.7925	0.1415	2.0207
0.5000	0.3120	35.52	0.0325	0.2773	0.0167	0.2986	1.1408	0.2160	1.5146
0.6000	0.3370	30.66	0.0331	0.2792	0.0304	0.2461	1.4011	0.2692	1.1625
0.7000	0.3470	26.41	0.0304	0.2577	0.0509	0.1947	1.5049	0.2909	0.9131
0.8000	0.3340	22.69	0.0249	0.2168	0.0729	0.1480	1.4131	0.2755	0.7333
0.9000	0.2800	19.52	0.0171	0.1629	0.0893	0.1117	1.0924	0.2178	0.6013
0.9500	0.2100	18.12	0.0117	0.1323	0.0922	0.0921	0.7846	0.1603	0.5488
1.0000	0.0000	16.83	0.0000	0.0997	0.0897	0.0000	0.0000	0.0000	0.5031

PROPELLER LIFTING LINE RUN: 17:23:44

SERIES CIRCULATION COEFFICIENTS FOR COMPONENT 1

NUMBER	COEFFICIENT	NORMALIZED COEFFICIENT
1	0.01092	0.00052
2	0.44689	0.02132
3	-3.27240	-0.15609
4	11.92451	0.56878
5	-18.90395	-0.90168
6	3.22106	0.15364
7	20.96522	1.00000
8	-14.98079	-0.71455

****

OUTPUT AT THE CONTROL POINTS FOR COMPONENT NUMBER: 1

R/R0	G	VA/VS	VT/VS	UA*/VS	UT*/VS	UA*SELF	UA*OTHR	UT*SELF	UT*OTHR
0.2466	0.0124	1.0000	0.0000	0.0478	0.2007	0.0462	0.0017	-0.0743	0.2750
0.3438	0.0224	1.0000	0.0000	0.1777	0.0737	0.1791	-0.0014	-0.1554	0.2291
0.4410	0.0304	1.0000	0.0000	0.2589	0.0209	0.2634	-0.0045	-0.1893	0.2102
0.5382	0.0331	1.0000	0.0000	0.2807	0.0204	0.2871	-0.0064	-0.1727	0.1931
0.6355	0.0326	1.0000	0.0000	0.2744	0.0373	0.2823	-0.0079	-0.1427	0.1800
0.7327	0.0288	1.0000	0.0000	0.2460	0.0581	0.2551	-0.0091	-0.1104	0.1686
0.8299	0.0228	1.0000	0.0000	0.2019	0.0789	0.2118	-0.0099	-0.0787	0.1576
0.9271	0.0144	1.0000	0.0000	0.1466	0.0914	0.1567	-0.0101	-0.0504	0.1418

PROPELLER LIFTING LINE RUN: 17:23:44

DETAILED OUTPUT FOR COMPONENT NUMBER: 2

R/R0	Cin/D	T/D	CDRAG	Gin	UA/VS nominal	UA/VS effective	UT/VS	BETA
0.1666	0.2290	0.0298	0.0085	-0.0070	1.0000	1.0000	0.0000	90.00
0.2721	0.2290	0.0298	0.0085	-0.0070	1.0000	1.0000	0.0000	90.00
0.3460	0.2290	0.0294	0.0085	-0.0081	1.0000	1.0000	0.0000	90.00
0.4266	0.2290	0.0289	0.0085	-0.0097	1.0000	1.0000	0.0000	90.00
0.4930	0.2290	0.0281	0.0085	-0.0106	1.0000	1.0000	0.0000	90.00
0.5744	0.2290	0.0272	0.0085	-0.0119	0.0000	1.0000	0.0000	90.00
0.6483	0.2290	0.0264	0.0085	-0.0127	0.0000	1.0000	0.0000	90.00
0.7222	0.2290	0.0255	0.0085	-0.0135	0.0000	1.0000	0.0000	90.00
0.7961	0.2290	0.0246	0.0085	-0.0135	0.0000	1.0000	0.0000	90.00
0.8633	0.2290	0.0238	0.0085	-0.0127	0.0000	1.0000	0.0000	90.00
0.9440	0.2200	0.0234	0.0085	-0.0095	0.0000	1.0000	0.0000	90.00
1.0000	0.0000	0.0229	0.0085	0.0000	0.0000	1.0000	0.0000	90.00

****

R/R0	C/D	BETAI	G	UA*/VS	UT*/VS	CL	DCT	DCQ	SIGMA
0.1666	0.2290	81.76	-0.0063	0.0728	0.1554	-0.1603	-0.0343	-0.0327	6.2817
0.2721	0.2290	84.97	-0.0063	0.0726	0.0945	-0.1605	-0.0344	-0.0329	6.3325
0.3460	0.2290	85.21	-0.0073	0.0688	0.0896	-0.1864	-0.0363	-0.0483	6.3751
0.4266	0.2290	85.08	-0.0087	0.0636	0.0916	-0.2243	-0.0415	-0.0710	6.4266
0.4930	0.2290	85.30	-0.0095	0.0596	0.0870	-0.2461	-0.0424	-0.0894	6.4720
0.5744	0.2290	85.36	-0.0107	0.0540	0.0855	-0.2778	-0.0454	-0.1164	6.5328
0.6483	0.2290	85.30	-0.0114	0.0483	0.0862	-0.2981	-0.0478	-0.1395	6.5947
0.7222	0.2290	84.99	-0.0121	0.0420	0.0913	-0.3186	-0.0521	-0.1641	6.6602
0.7961	0.2290	84.66	-0.0121	0.0356	0.0968	-0.3204	-0.0544	-0.1798	6.7279
0.8633	0.2290	84.31	-0.0114	0.0297	0.1026	-0.3027	-0.0541	-0.1823	6.7887
0.9440	0.2200	84.05	-0.0085	0.0241	0.1068	-0.2371	-0.0441	-0.1482	6.8476
1.0000	0.0000	84.16	0.0000	0.0221	0.1046	0.0000	0.0000	0.0000	6.8702

PROPELLER LIFTING LINE RUN: 17:23:44

SERIES CIRCULATION COEFFICIENTS FOR COMPONENT 2

NUMBER	COEFFICIENT	NORMALIZED COEFFICIENT
1	-0.00625	-0.00467
2	-0.05462	-0.04087
3	0.24780	0.18541
4	-0.81656	-0.61097
5	1.33650	1.00000
6	-0.93138	-0.69688
7	0.04283	0.03205
8	0.16173	0.12101

****

OUTPUT AT THE CONTROL POINTS FOR COMPONENT NUMBER: 2
(Quantities are nondimensionalized with the diameter of component 1)

R/R0	G	VA/VS	VT/VS	UA*/VS	UT*/VS	UA*SELF	UA*OTHR	UT*SELF	UT*OTHR
0.3249	-0.0075	1.0000	0.0000	0.0727	0.0948	-0.0001	0.0727	0.0948	0.0000
0.4146	-0.0087	1.0000	0.0000	0.0688	0.0896	-0.0017	0.0705	0.0896	0.0000
0.5044	-0.0104	1.0000	0.0000	0.0639	0.0918	-0.0035	0.0674	0.0918	0.0000
0.5941	-0.0115	1.0000	0.0000	0.0594	0.0869	-0.0043	0.0637	0.0869	0.0000
0.6839	-0.0128	1.0000	0.0000	0.0543	0.0855	-0.0051	0.0594	0.0855	0.0000
0.7737	-0.0137	1.0000	0.0000	0.0486	0.0860	-0.0059	0.0545	0.0860	0.0000
0.8634	-0.0146	1.0000	0.0000	0.0422	0.0911	-0.0070	0.0492	0.0911	0.0000
0.9532	-0.0146	1.0000	0.0000	0.0357	0.0967	-0.0082	0.0439	0.0967	0.0000
1.0429	-0.0136	1.0000	0.0000	0.0292	0.1031	-0.0094	0.0387	0.1031	0.0000
1.1327	-0.0103	1.0000	0.0000	0.0241	0.1068	-0.0096	0.0337	0.1068	0.0000

PROPELLER LIFTING LINE RUN:

CIRCULATION ON EACH BLADE OF PRESWIRL STATOR

RADIUS	ANGLE AND CIRCULATION								
	0.00	40.00	80.00	120.00	160.00	200.00	240.00	280.00	320.00
0.2889	0.0009	-0.0020	-0.0092	-0.0174	-0.0228	-0.0228	-0.0174	-0.0092	-0.0020
0.3618	-0.0005	-0.0033	-0.0106	-0.0188	-0.0242	-0.0242	-0.0188	-0.0106	-0.0033
0.4347	-0.0010	-0.0039	-0.0111	-0.0194	-0.0247	-0.0247	-0.0194	-0.0111	-0.0039
0.5077	-0.0008	-0.0037	-0.0109	-0.0192	-0.0245	-0.0245	-0.0192	-0.0109	-0.0037
0.5806	-0.0001	-0.0029	-0.0102	-0.0184	-0.0238	-0.0238	-0.0184	-0.0102	-0.0029
0.6536	0.0013	-0.0016	-0.0088	-0.0171	-0.0225	-0.0225	-0.0171	-0.0088	-0.0016
0.7265	0.0032	0.0004	-0.0069	-0.0151	-0.0205	-0.0205	-0.0151	-0.0069	0.0004
0.7994	0.0059	0.0030	-0.0042	-0.0124	-0.0178	-0.0178	-0.0124	-0.0042	0.0030
0.8724	0.0090	0.0061	-0.0011	-0.0093	-0.0147	-0.0147	-0.0093	-0.0011	0.0061
0.9453	0.0105	0.0077	0.0004	-0.0078	-0.0132	-0.0132	-0.0078	0.0004	0.0077

PROPELLER LIFTING LINE RUN: 0501.1 1-MAY-87 15:32:26
4497 alone

PLL SUMMARY OUTPUT

SHIP SPEED (FT/SEC):	17.72	FLUID DENSITY:	1.9500
SHAFT DEPTH (FT):	2.00	NUMBER OF DEVICES:	1
TOTAL THRUST (LBS):	180	TORQUE (FT-LBS):	37
HORSEPOWER:	8	EFFICIENCY:	0.677
IMAGE HUB USED:	T	IMAGE DUCT USED:	F
HUB DRAG (lbs):	1	(HUB VORTEX)/(RHUB):	0.4000

****

SUMMARY OUTPUT FOR COMPONENT NUMBER: 1

AXIAL LOCATION(FT) :	0.00	DIAMETER (FT):	1.00
NUMBER OF BLADES:	5	HUB DIAMETER (FT):	0.20
NUMBER OF CONTROL POINTS:	10	REVS. PER MINUTE:	1200.00
BLADE FILE: blade11121.out		WAKE DIAMETER (FT):	1.00
WAKE FILE: blawake1112.out		THRUST (LBS):	181
TORQUE (FT-LBS):	37	HORSEPOWER:	8
ADVANCE COEFFICIENT:	0.886	EX. AREA RATIO:	0.721
BLADE VOLUME (CU FT):	0.00	MOM. OF INERTIA (FT**5):	0.00
NUMBER OF PANELS:	10		

CT: 0.7532 CQ: 0.1559 CP: 1.1056 KT: 0.2322 KQ: 0.0481

COMPUTATION TOOK: 7.04 SECONDS

****

PROPELLER LIFTING LINE RUN: 0501.1 1-MAY-87 15:32:26

DETAILED OUTPUT FOR COMPONENT NUMBER: 1

R/R0	Cin/D	T/D	CDRAG	Gin	UA/VS nominal	UA/VS effective	UT/VS	BETA
0.2000	0.1740	0.0434	0.0085	0.0000	1.0000	1.0000	0.0000	54.66
0.2500	0.2020	0.0396	0.0085	0.0149	1.0000	1.0000	0.0000	48.44
0.3000	0.2290	0.0358	0.0085	0.0213	1.0000	1.0000	0.0000	43.23
0.4000	0.2750	0.0294	0.0085	0.0308	1.0000	1.0000	0.0000	35.19
0.5000	0.3120	0.0240	0.0085	0.0361	1.0000	1.0000	0.0000	29.42
0.6000	0.3370	0.0191	0.0085	0.0369	0.0000	1.0000	0.0000	25.18
0.7000	0.3470	0.0146	0.0085	0.0337	0.0000	1.0000	0.0000	21.94
0.8000	0.3340	0.0105	0.0085	0.0277	0.0000	1.0000	0.0000	19.42
0.9000	0.2800	0.0067	0.0085	0.0189	0.0000	1.0000	0.0000	17.40
0.9500	0.2100	0.0048	0.0085	0.0132	0.0000	1.0000	0.0000	16.53
1.0000	0.0000	0.0029	0.0085	0.0000	0.0000	1.0000	0.0000	15.75

****

R/R0	C/D	BETAI	G	UA*/VS	UT*/VS	CL	DCT	DCQ	SIGMA
0.2000	0.1740	46.26	0.0095	-0.1006	0.1515	0.2314	0.1515	0.0238	4.7412
0.2500	0.2020	51.58	0.0104	0.0602	-0.0454	0.2434	0.1686	0.0278	3.9852
0.3000	0.2290	51.58	0.0182	0.1546	-0.1479	0.3379	0.3244	0.0645	3.3589
0.4000	0.2750	45.30	0.0285	0.2349	-0.1963	0.3742	0.6809	0.1440	2.4126
0.5000	0.3120	38.88	0.0337	0.2757	-0.1909	0.3348	1.0439	0.2216	1.7601
0.6000	0.3370	33.14	0.0343	0.2826	-0.1626	0.2719	1.3193	0.2763	1.3188
0.7000	0.3470	28.19	0.0313	0.2623	-0.1271	0.2124	1.4443	0.2976	1.0156
0.8000	0.3340	24.02	0.0258	0.2234	-0.0919	0.1611	1.3803	0.2819	0.8018
0.9000	0.2800	20.54	0.0176	0.1729	-0.0614	0.1195	1.0744	0.2216	0.6473
0.9500	0.2100	19.01	0.0122	0.1442	-0.0475	0.1028	0.7897	0.1646	0.5855
1.0000	0.0000	17.60	0.0000	0.1138	-0.0343	0.0000	0.0000	0.0000	0.5305

PROPELLER LIFTING LINE RUN: 0501.1 1-MAY-87 15:32:26

SERIES CIRCULATION COEFFICIENTS FOR COMPONENT 1

NUMBER	COEFFICIENT	NORMALIZED COEFFICIENT
1	0.00955	0.00019
2	0.49592	0.00962
3	-3.18467	-0.06177
4	7.98490	0.15487
5	0.10413	0.00202
6	-33.43883	-0.64854
7	51.56028	1.00000
8	-23.88635	-0.46327

****

OUTPUT AT THE CONTROL POINTS FOR COMPONENT NUMBER: 1

R/R0	C/D	G	VA/VS	VT/VS	UA*/VS	UT*/VS
0.2371	0.1948	0.0095	1.0000	0.0000	0.0261	-0.0049
0.3154	0.2368	0.0207	1.0000	0.0000	0.1738	-0.1654
0.3936	0.2723	0.0281	1.0000	0.0000	0.2315	-0.1958
0.4719	0.3026	0.0328	1.0000	0.0000	0.2677	-0.1953
0.5501	0.3262	0.0344	1.0000	0.0000	0.2828	-0.1785
0.6283	0.3416	0.0338	1.0000	0.0000	0.2794	-0.1528
0.7066	0.3470	0.0310	1.0000	0.0000	0.2602	-0.1247
0.7848	0.3378	0.0268	1.0000	0.0000	0.2301	-0.0970
0.8631	0.3081	0.0209	1.0000	0.0000	0.1926	-0.0721
0.9413	0.2259	0.0133	1.0000	0.0000	0.1493	-0.0499

Appendix B
PHOTOGRAPHIC PLATES

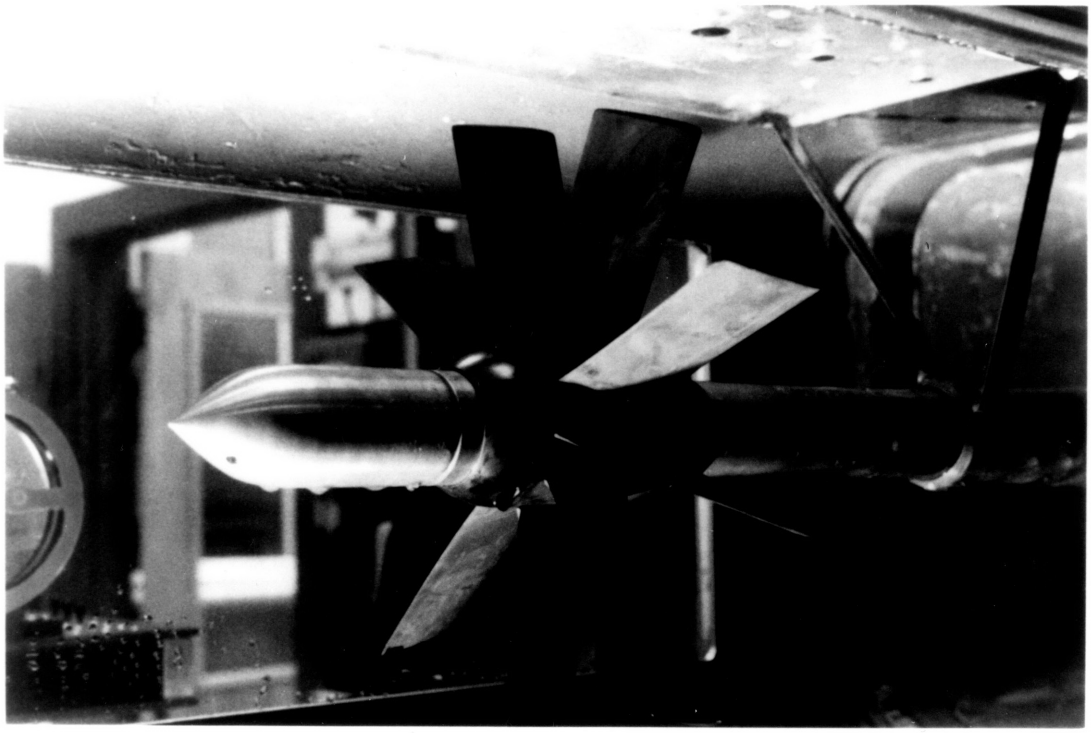

Photograph #1 : Stator Mounted in the Water Tunnel.

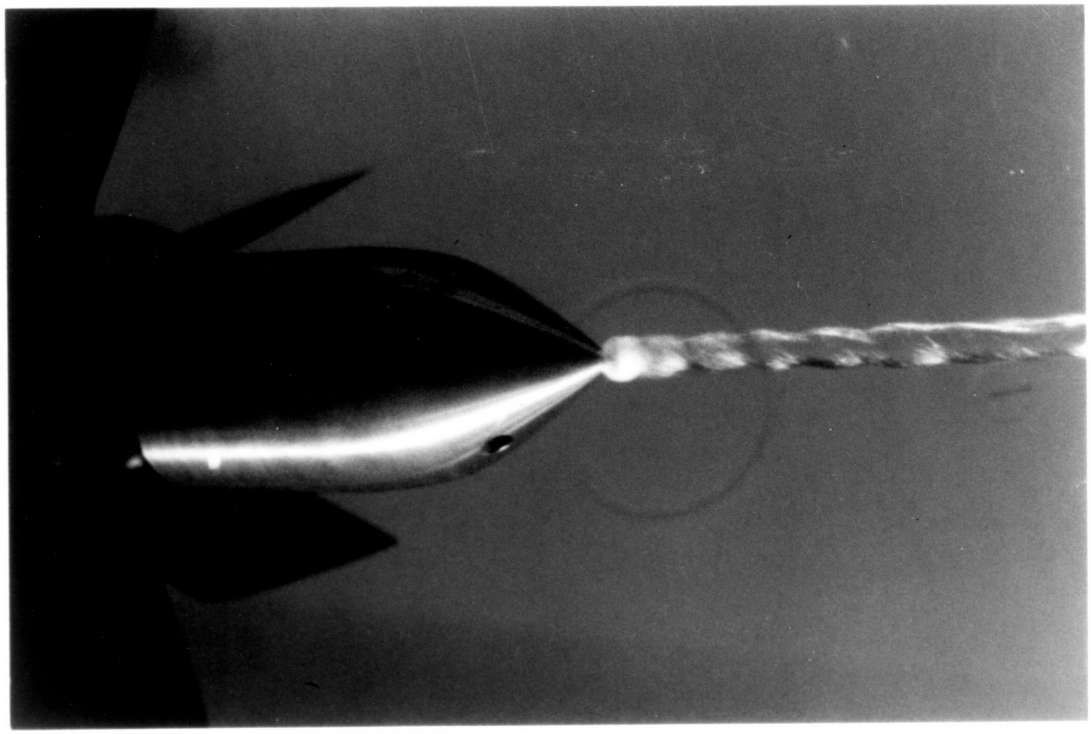

Photograph #2 : Hub Vortex from Stator Operating Alone.

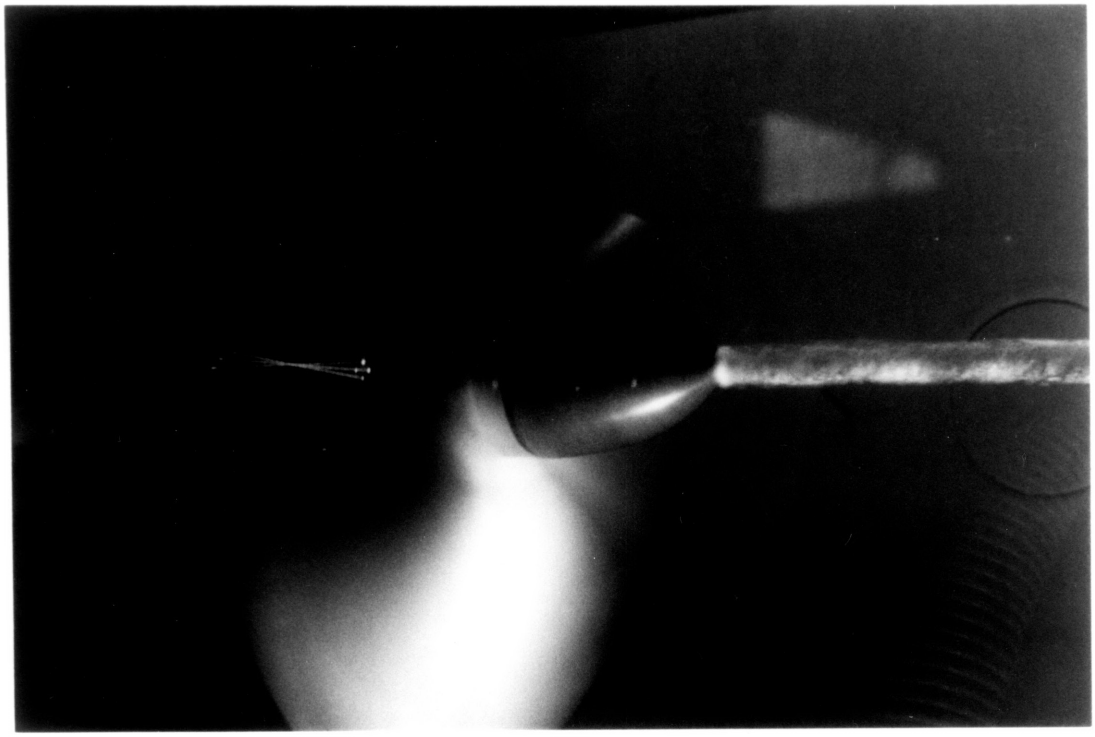

Photograph #3 : Hub Vortex from Propeller Operating Alone.

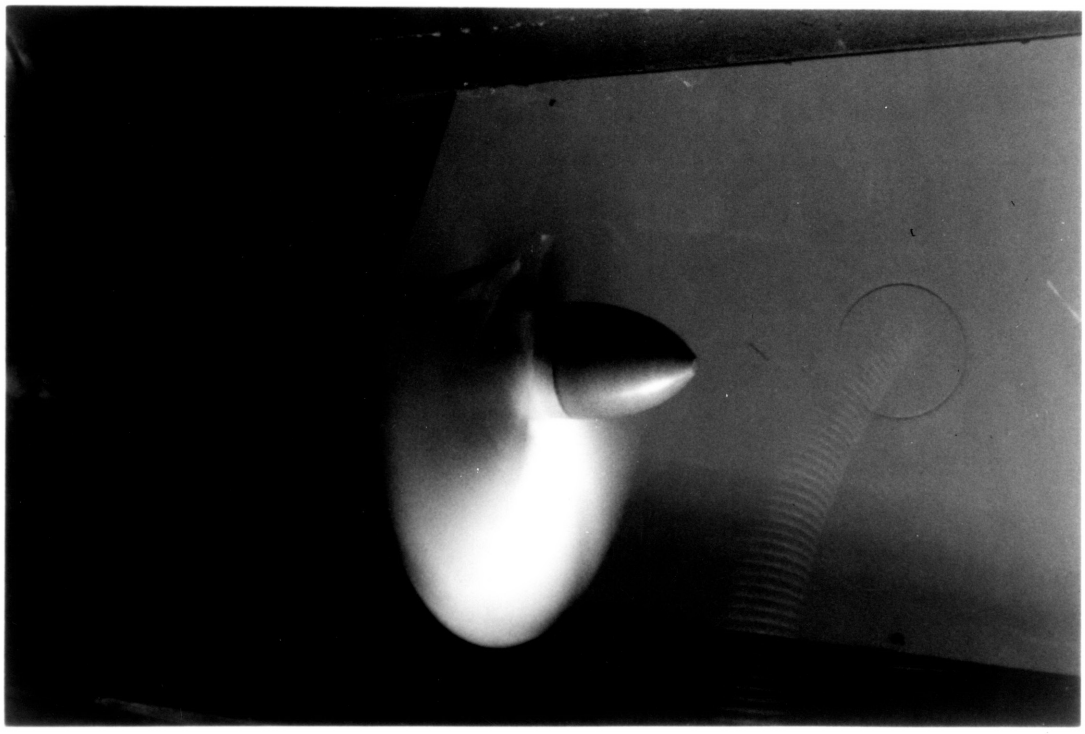

Photograph #4 : Propeller and Stator Operating Together.
No Visible Hub Vortex.

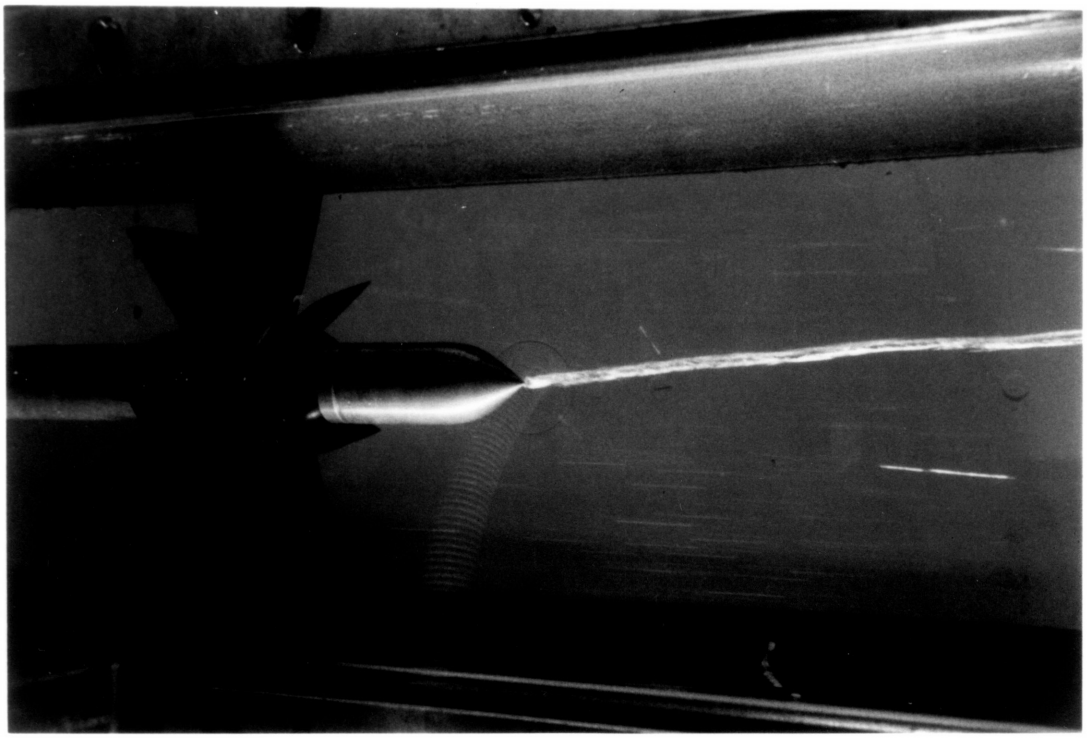

Photograph #5 : Non-Axisymmetric Stator Operating Alone.
Note Flow Inclination.

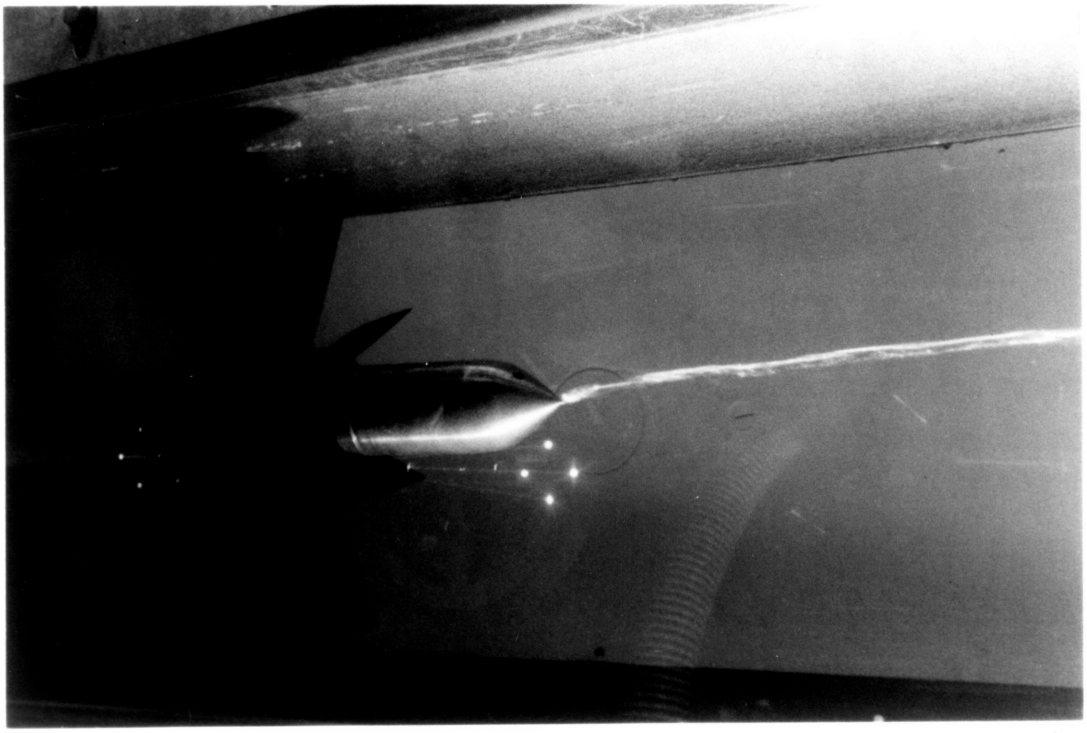

Photograph #6 : Non-Axisymmetric Stator.

Appendix C
OPEN-WATER TESTS

DATA FILE: 449704
OWPP1 PROGRAM RELEASED: 21 AUG 84
PROP 4497 OPEN WATER TEST

DIA (INCHES)	0.7R CHORD (INCHES)	HUB COR	VELINC	WATER TEMP (DEGREE F)	BAROMETER (MMHG)	ROOM TEMP (DEGREE F)
12.0000	4.0000	-0.0010	0.0000	82.0000	758.4728	75.00

TUNNEL VEL (FT/SEC)	STAT PRESS (MMHG)	RPM	T (LBS)	Q (INCH-LBS)	J CORR	WTEMP (F)	IMP RPM
4.794	814.526	784.100	171.883	369.718	0.279	82.0	0.
6.193	814.642	845.705	185.852	402.221	0.357	82.0	1.
7.760	815.778	893.052	191.013	417.299	0.449	82.0	77.
8.994	813.533	938.248	197.290	436.469	0.504	82.0	102.
9.889	811.270	991.391	213.754	476.665	0.529	82.0	116.
10.527	810.658	1007.800	212.860	477.744	0.559	82.0	130.
11.211	807.273	1026.865	212.214	481.579	0.590	82.0	142.
12.250	803.069	1043.912	203.617	470.665	0.648	82.0	162.
13.480	795.654	1069.292	196.596	465.433	0.702	82.0	185.
14.375	791.369	1101.880	199.819	479.682	0.730	82.0	199.
15.724	782.168	1119.906	185.510	460.193	0.796	82.0	223.
18.182	764.014	1147.570	155.465	414.087	0.919	82.0	265.
20.418	745.550	1174.312	127.607	367.035	1.016	82.0	303.
22.159	728.233	1179.294	95.031	303.175	1.107	82.0	332.
24.226	708.423	1181.308	46.596	206.306	1.222	82.0	366.
25.285	696.886	1184.753	19.658	153.432	1.277	82.0	384.
25.798	691.872	1187.464	6.352	127.363	1.302	82.0	393.
0.000	0.000	0.000	0.000	0.000	0.000	0.0	0.

OUTPUT LIST DATA FILE: 44974F
TEST DATA FILE: 449704 TEST DATE:
PROP 4497 OPEN WATER TEST

J-TUN	J-CORR	KT	KQ	ETA	V	RPM	RN*10E-6
0.367	0.279	0.5204	0.09326	0.248	4.79	784.1	1.071
0.439	0.357	0.4837	0.08722	0.315	6.19	845.7	1.161
0.521	0.449	0.4459	0.08114	0.393	7.76	893.1	1.236
0.575	0.504	0.4173	0.07689	0.435	8.99	938.2	1.306
0.598	0.529	0.4050	0.07521	0.453	9.89	991.4	1.384
0.627	0.559	0.3903	0.07295	0.476	10.53	1007.8	1.411
0.655	0.590	0.3749	0.07083	0.497	11.21	1026.9	1.443
0.704	0.648	0.3481	0.06698	0.536	12.25	1043.9	1.476
0.756	0.702	0.3205	0.06313	0.567	13.48	1069.3	1.523
0.783	0.730	0.3068	0.06127	0.582	14.38	1101.9	1.575
0.842	0.796	0.2759	0.05690	0.614	15.72	1119.9	1.615
0.951	0.919	0.2205	0.04876	0.661	18.18	1147.6	1.684
1.043	1.016	0.1732	0.04128	0.679	20.42	1174.3	1.750
1.127	1.107	0.1284	0.03381	0.669	22.16	1179.3	1.785
1.230	1.222	0.0636	0.02293	0.540	24.23	1181.3	1.823
1.281	1.277	0.0277	0.01695	0.332	25.28	1184.8	1.846
1.304	1.302	0.0101	0.01401	0.149	25.80	1187.5	1.859

J-CORR	DKT	DKQ	SIGN	SIGB	SIGV
0.279	0.0003	0.00012	13.250	11.679	98.462
0.357	-0.0014	-0.00028	11.392	9.549	59.010
0.449	0.0026	0.00027	10.231	8.044	37.639
0.504	-0.0002	-0.00006	9.242	6.945	27.939
0.529	-0.0006	0.00004	8.254	6.077	23.044
0.559	-0.0008	-0.00011	7.981	5.730	20.320
0.590	-0.0010	-0.00006	7.654	5.356	17.838
0.648	0.0010	0.00012	7.367	4.925	14.860
0.702	0.0001	-0.00004	6.954	4.423	12.154
0.730	0.0001	-0.00000	6.512	4.038	10.628
0.796	0.0004	0.00003	6.228	3.643	8.776
0.919	0.0002	0.00008	5.789	3.041	6.405
1.016	-0.0021	-0.00029	5.389	2.581	4.952
1.107	0.0006	0.00004	5.215	2.296	4.103
1.222	0.0027	0.00038	5.050	2.009	3.335
1.277	0.0002	0.00006	4.935	1.870	3.010
1.302	-0.0020	-0.00029	4.876	1.806	2.870

OUTPUT LIST DATA FILE: 44974F
TEST DATA FILE: 449704 TEST DATE:
PROP 4497 OPEN WATER TEST

J-COR	KT	KQ	ETA	KT/J**2	J'	KT'	KQ'
0.200	0.555	0.0989	0.179	13.884068	0.196	0.534	0.0951
0.210	0.551	0.0981	0.188	12.491432	0.206	0.528	0.0940
0.220	0.546	0.0974	0.196	11.289039	0.215	0.521	0.0929
0.230	0.542	0.0967	0.205	10.244104	0.224	0.515	0.0918
0.240	0.537	0.0960	0.214	9.330596	0.233	0.508	0.0907
0.250	0.533	0.0952	0.223	8.527615	0.243	0.502	0.0896
0.260	0.529	0.0945	0.231	7.818235	0.252	0.495	0.0885
0.270	0.524	0.0938	0.240	7.188635	0.261	0.488	0.0874
0.280	0.520	0.0931	0.249	6.627441	0.270	0.482	0.0863
0.290	0.515	0.0923	0.257	6.125223	0.279	0.475	0.0852
0.300	0.511	0.0916	0.266	5.674108	0.287	0.469	0.0841
0.310	0.506	0.0909	0.275	5.267492	0.296	0.462	0.0829
0.320	0.502	0.0902	0.283	4.899792	0.305	0.455	0.0818
0.330	0.497	0.0895	0.292	4.566271	0.313	0.448	0.0807
0.340	0.493	0.0887	0.301	4.262884	0.322	0.442	0.0795
0.350	0.488	0.0880	0.309	3.986165	0.330	0.435	0.0784
0.360	0.484	0.0873	0.318	3.733125	0.339	0.428	0.0773
0.370	0.479	0.0866	0.326	3.501183	0.347	0.422	0.0761
0.380	0.475	0.0858	0.335	3.288093	0.355	0.415	0.0750
0.390	0.470	0.0851	0.343	3.091901	0.363	0.408	0.0739
0.400	0.466	0.0844	0.351	2.910896	0.371	0.402	0.0728
0.410	0.461	0.0837	0.360	2.743576	0.379	0.395	0.0716
0.420	0.457	0.0830	0.368	2.588618	0.387	0.388	0.0705
0.430	0.452	0.0822	0.376	2.444855	0.395	0.382	0.0694
0.440	0.447	0.0815	0.384	2.311252	0.403	0.375	0.0683

0.450	0.443	0.0808	0.393	2.186890	0.410	0.368	0.0672
0.460	0.438	0.0801	0.401	2.070950	0.418	0.362	0.0661
0.470	0.434	0.0794	0.409	1.962701	0.425	0.355	0.0650
0.480	0.429	0.0787	0.417	1.861489	0.433	0.349	0.0639
0.490	0.424	0.0779	0.424	1.766727	0.440	0.342	0.0629
0.500	0.419	0.0772	0.432	1.677887	0.447	0.336	0.0618
0.510	0.415	0.0765	0.440	1.594494	0.454	0.329	0.0607
0.520	0.410	0.0758	0.448	1.516118	0.461	0.323	0.0597
0.530	0.405	0.0751	0.455	1.442371	0.468	0.316	0.0586
0.540	0.400	0.0744	0.462	1.372900	0.475	0.310	0.0576
0.550	0.395	0.0737	0.470	1.307394	0.482	0.304	0.0566
0.560	0.391	0.0730	0.477	1.245572	0.489	0.297	0.0556
0.570	0.386	0.0723	0.484	1.187180	0.495	0.291	0.0546
0.580	0.381	0.0716	0.491	1.131985	0.502	0.285	0.0536
0.590	0.376	0.0709	0.498	1.079772	0.508	0.279	0.0526
0.600	0.371	0.0702	0.505	1.030347	0.514	0.273	0.0516
0.610	0.366	0.0695	0.511	0.983529	0.521	0.267	0.0506
0.620	0.361	0.0688	0.518	0.939151	0.527	0.261	0.0497
0.630	0.356	0.0681	0.524	0.897062	0.533	0.255	0.0488
0.640	0.351	0.0674	0.530	0.857120	0.539	0.249	0.0478
0.650	0.346	0.0667	0.537	0.819195	0.545	0.243	0.0469
0.660	0.341	0.0660	0.543	0.783167	0.551	0.238	0.0460
0.670	0.336	0.0653	0.549	0.748923	0.557	0.232	0.0451
0.680	0.331	0.0647	0.554	0.716361	0.562	0.227	0.0442
0.690	0.326	0.0640	0.560	0.685384	0.568	0.221	0.0433
0.700	0.321	0.0633	0.566	0.655903	0.573	0.216	0.0425

OUTPUT LIST DATA FILE: 44974F
TEST DATA FILE: 449704 TEST DATE:
PROP 4497 OPEN WATER TEST

J-COR	KT	KQ	ETA	KT/J**2	J'	KT'	KQ'
0.700	0.321	0.0633	0.566	0.655903	0.573	0.216	0.0425
0.710	0.316	0.0626	0.571	0.627835	0.579	0.210	0.0416
0.720	0.312	0.0619	0.576	0.601102	0.584	0.205	0.0408
0.730	0.307	0.0613	0.582	0.575633	0.590	0.200	0.0400
0.740	0.302	0.0606	0.587	0.551359	0.595	0.195	0.0392
0.750	0.297	0.0599	0.592	0.528219	0.600	0.190	0.0384
0.760	0.292	0.0593	0.597	0.506153	0.605	0.185	0.0376
0.770	0.288	0.0586	0.602	0.485106	0.610	0.181	0.0368
0.780	0.283	0.0579	0.606	0.465027	0.615	0.176	0.0360
0.790	0.278	0.0573	0.611	0.445867	0.620	0.171	0.0353
0.800	0.274	0.0566	0.616	0.427580	0.625	0.167	0.0345
0.810	0.269	0.0560	0.620	0.410114	0.629	0.162	0.0338
0.820	0.265	0.0553	0.624	0.393417	0.634	0.158	0.0331
0.830	0.260	0.0546	0.629	0.377443	0.639	0.154	0.0324
0.840	0.256	0.0540	0.633	0.362149	0.643	0.150	0.0316
0.850	0.251	0.0533	0.637	0.347492	0.648	0.146	0.0310
0.860	0.247	0.0527	0.641	0.333434	0.652	0.142	0.0303
0.870	0.242	0.0520	0.645	0.319941	0.656	0.138	0.0296
0.880	0.238	0.0513	0.649	0.306977	0.661	0.134	0.0289

0.890	0.233	0.0507	0.652	0.294512	0.665	0.130	0.0283
0.900	0.229	0.0500	0.656	0.282516	0.669	0.126	0.0276
0.910	0.224	0.0493	0.659	0.270962	0.673	0.123	0.0270
0.920	0.220	0.0486	0.662	0.259823	0.677	0.119	0.0263
0.930	0.215	0.0479	0.665	0.249077	0.681	0.116	0.0257
0.940	0.211	0.0472	0.668	0.238699	0.685	0.112	0.0251
0.950	0.206	0.0465	0.671	0.228668	0.689	0.108	0.0244
0.960	0.202	0.0458	0.673	0.218965	0.693	0.105	0.0238
0.970	0.197	0.0451	0.676	0.209570	0.696	0.102	0.0232
0.980	0.193	0.0443	0.678	0.200465	0.700	0.098	0.0226
0.990	0.188	0.0436	0.679	0.191635	0.704	0.095	0.0220
1.000	0.183	0.0428	0.681	0.183063	0.707	0.092	0.0214
1.010	0.178	0.0420	0.682	0.174734	0.711	0.088	0.0208
1.020	0.173	0.0412	0.682	0.166635	0.714	0.085	0.0202
1.030	0.168	0.0404	0.683	0.158752	0.717	0.082	0.0196
1.040	0.163	0.0396	0.683	0.151073	0.721	0.078	0.0190
1.050	0.158	0.0388	0.682	0.143587	0.724	0.075	0.0185
1.060	0.153	0.0379	0.681	0.136284	0.727	0.072	0.0179
1.070	0.148	0.0371	0.679	0.129162	0.731	0.069	0.0173
1.080	0.143	0.0362	0.677	0.122217	0.734	0.066	0.0167
1.090	0.137	0.0353	0.674	0.115445	0.737	0.063	0.0161
1.100	0.132	0.0344	0.670	0.108842	0.740	0.060	0.0156
1.110	0.126	0.0335	0.666	0.102407	0.743	0.057	0.0150
1.120	0.121	0.0326	0.660	0.096135	0.746	0.053	0.0144
1.130	0.115	0.0316	0.654	0.090023	0.749	0.050	0.0139
1.140	0.109	0.0307	0.646	0.084068	0.752	0.048	0.0133
1.150	0.104	0.0297	0.638	0.078267	0.755	0.045	0.0128
1.160	0.098	0.0287	0.628	0.072618	0.757	0.042	0.0123
1.170	0.092	0.0278	0.616	0.067117	0.760	0.039	0.0117
1.180	0.086	0.0268	0.603	0.061761	0.763	0.036	0.0112
1.190	0.080	0.0258	0.588	0.056548	0.766	0.033	0.0107
1.200	0.074	0.0248	0.571	0.051475	0.768	0.030	0.0102

OUTPUT LIST DATA FILE: 44974F
TEST DATA FILE: 449704 TEST DATE:
PROP 4497 OPEN WATER TEST

J-COR	KT	KQ	ETA	KT/J**2	J'	KT'	KQ'
1.200	0.074	0.0248	0.571	0.051475	0.768	0.030	0.0102
1.210	0.068	0.0238	0.552	0.046540	0.771	0.028	0.0096
1.220	0.062	0.0228	0.530	0.041739	0.773	0.025	0.0091
1.230	0.056	0.0217	0.505	0.037071	0.776	0.022	0.0086
1.240	0.050	0.0207	0.477	0.032532	0.778	0.020	0.0082
1.250	0.044	0.0197	0.444	0.028121	0.781	0.017	0.0077
1.260	0.038	0.0187	0.407	0.023835	0.783	0.015	0.0072
1.270	0.032	0.0176	0.364	0.019672	0.786	0.012	0.0067
1.280	0.026	0.0166	0.315	0.015630	0.788	0.010	0.0063
1.290	0.019	0.0155	0.257	0.011705	0.790	0.007	0.0058
1.300	0.013	0.0145	0.190	0.007897	0.793	0.005	0.0054
1.310	0.007	0.0135	0.112	0.004203	0.795	0.003	0.0050
1.320	0.001	0.0124	0.018	0.000622	0.797	0.000	0.0045

1.330	-0.005	0.0114	-0.094	-0.002850	0.799	-0.002	0.0041
1.340	-0.011	0.0104	-0.230	-0.006214	0.801	-0.004	0.0037
1.350	-0.017	0.0093	-0.397	-0.009472	0.804	-0.006	0.0033
1.360	-0.023	0.0083	-0.609	-0.012625	0.806	-0.008	0.0029
1.370	-0.029	0.0073	-0.881	-0.015676	0.808	-0.010	0.0025
1.380	-0.035	0.0063	-1.245	-0.018626	0.810	-0.012	0.0022
1.390	-0.041	0.0052	-1.752	-0.021477	0.812	-0.014	0.0018
1.400	-0.047	0.0042	-2.502	-0.024232	0.814	-0.016	0.0014

TYPE STAT.DAT

DATA FILE: STAT
OWPP1 PROGRAM RELEASED: 21 AUG 84
STAT0R & 4497, 3/22/87

DIA (INCHES)	0.7R CHORD (INCHES)	HUB COR	VELINC	WATER TEMP (DEGREE F)	BAROMETER (MMHG)	ROOM TEMP (DEGREE F)
12.0000	4.0000	-0.0010	0.0000	78.0000	762.3428	70.00

TUNNEL VEL (FT/SEC)	STAT PRESS (MMHG)	RPM	T (LBS)	Q (INCH-LBS)	J CORR	WTEMP (F)	IMP RPM
4.814	820.543	759.271	182.785	377.904	0.288	78.0	0.
6.555	821.326	829.586	207.100	430.134	0.385	78.0	51.
7.941	824.942	865.362	216.736	453.030	0.474	78.0	81.
9.827	820.582	900.215	217.962	463.934	0.576	78.0	120.
10.807	816.420	915.909	215.925	465.813	0.634	78.0	140.
12.243	809.270	936.101	209.522	462.438	0.723	78.0	166.
13.073	804.618	945.233	204.140	457.492	0.766	78.0	181.
14.182	797.966	947.979	190.696	438.870	0.838	78.0	200.
15.466	789.907	956.834	178.201	422.649	0.917	78.0	224.
16.739	780.565	991.823	180.850	437.814	0.963	78.0	244.
18.129	770.214	996.930	163.707	411.348	1.055	78.0	267.
19.303	761.256	999.230	147.988	385.657	1.121	78.0	288.
21.023	745.366	999.723	121.957	339.668	1.232	78.0	315.
22.716	728.342	996.330	89.158	278.848	1.347	78.0	343.
23.901	716.678	993.483	62.003	228.273	1.429	78.0	363.
25.950	696.281	985.883	4.963	120.429	1.577	78.0	397.
0.000	0.000	0.000	0.000	0.000	0.000	0.0	0.

OUTPUT LIST DATA FILE: FSTAT
TEST DATA FILE: STAT TEST DATE:
STATOR & 4497, 3/22/87

J-TUN	J-CORR	KT	KQ	ETA	V	RPM	RN*10E-6
0.380	0.288	0.5898	0.10160	0.266	4.81	759.3	0.995
0.474	0.385	0.5598	0.09687	0.354	6.55	829.6	1.096
0.551	0.474	0.5385	0.09377	0.433	7.94	865.4	1.152
0.655	0.576	0.5006	0.08873	0.517	9.83	900.2	1.213
0.708	0.634	0.4791	0.08606	0.562	10.81	915.9	1.242
0.785	0.723	0.4452	0.08179	0.626	12.24	936.1	1.283
0.830	0.766	0.4255	0.07936	0.654	13.07	945.2	1.304
0.898	0.838	0.3954	0.07569	0.697	14.18	948.0	1.322
0.970	0.917	0.3629	0.07155	0.740	15.47	956.8	1.350
1.013	0.963	0.3429	0.06898	0.762	16.74	991.8	1.410
1.091	1.055	0.3075	0.06415	0.805	18.13	996.9	1.437
1.159	1.121	0.2769	0.05987	0.825	19.30	999.2	1.458
1.262	1.232	0.2285	0.05268	0.850	21.02	999.7	1.488
1.368	1.347	0.1689	0.04354	0.831	22.72	996.3	1.515
1.443	1.429	0.1189	0.03585	0.754	23.90	993.5	1.534
1.579	1.577	0.0120	0.01920	0.157	25.95	985.9	1.567

J-CORR	DKT	DKQ	SIGN	SIGB	SIGV
0.288	0.0007	0.00025	14.293	12.486	98.766
0.385	-0.0022	-0.00045	11.985	9.785	53.321
0.474	0.0029	0.00025	11.064	8.490	36.498
0.576	-0.0014	-0.00018	10.168	7.116	23.703
0.634	-0.0013	-0.00007	9.772	6.509	19.496
0.723	0.0010	0.00018	9.270	5.737	15.054
0.766	-0.0003	-0.00001	9.038	5.352	13.125
0.838	0.0006	0.00013	8.909	4.934	11.057
0.917	0.0015	0.00017	8.654	4.459	9.201
0.963	0.0001	-0.00000	7.955	3.928	7.758
1.055	0.0007	0.00003	7.766	3.545	6.524
1.121	-0.0034	-0.00049	7.638	3.259	5.685
1.232	-0.0021	-0.00029	7.466	2.880	4.690
1.347	0.0018	0.00027	7.339	2.556	3.922
1.429	0.0037	0.00059	7.259	2.354	3.484
1.577	-0.0023	-0.00037	7.154	2.047	2.868

LIST DATA FILE: FSTAT
TEST DATA FILE: STAT TEST DATE:
STATOR & 4497, 3/22/87

J-COR	KT	KQ	ETA	KT/J**2	J'	KT'	KQ'
0.200	0.614	0.1050	0.186	15.342723	0.196	0.590	0.1010
0.210	0.611	0.1046	0.195	13.852078	0.206	0.585	0.1002
0.220	0.608	0.1042	0.204	12.563206	0.215	0.580	0.0994
0.230	0.605	0.1038	0.214	11.441481	0.224	0.575	0.0985
0.240	0.602	0.1033	0.223	10.459381	0.233	0.570	0.0977
0.250	0.600	0.1029	0.232	9.594806	0.243	0.564	0.0969
0.260	0.597	0.1025	0.241	8.829845	0.252	0.559	0.0960
0.270	0.594	0.1021	0.250	8.149861	0.261	0.554	0.0952

0.280	0.591	0.1017	0.259	7.542803	0.270	0.548	0.0943
0.290	0.589	0.1013	0.268	6.998670	0.279	0.543	0.0934
0.300	0.586	0.1009	0.277	6.509111	0.287	0.537	0.0925
0.310	0.583	0.1004	0.286	6.067114	0.296	0.532	0.0916
0.320	0.580	0.1000	0.295	5.666750	0.305	0.526	0.0907
0.330	0.577	0.0996	0.304	5.302983	0.313	0.521	0.0898
0.340	0.575	0.0992	0.313	4.971509	0.322	0.515	0.0889
0.350	0.572	0.0988	0.322	4.668640	0.330	0.509	0.0880
0.360	0.569	0.0984	0.331	4.391193	0.339	0.504	0.0871
0.370	0.566	0.0980	0.340	4.136416	0.347	0.498	0.0862
0.380	0.563	0.0975	0.349	3.901917	0.355	0.492	0.0852
0.390	0.561	0.0971	0.358	3.685608	0.363	0.487	0.0843
0.400	0.558	0.0967	0.367	3.485662	0.371	0.481	0.0834
0.410	0.555	0.0963	0.376	3.300475	0.379	0.475	0.0824
0.420	0.552	0.0958	0.385	3.128633	0.387	0.469	0.0815
0.430	0.549	0.0954	0.394	2.968888	0.395	0.463	0.0805
0.440	0.546	0.0950	0.402	2.820129	0.403	0.457	0.0796
0.450	0.543	0.0946	0.411	2.681373	0.410	0.452	0.0786
0.460	0.540	0.0941	0.420	2.551744	0.418	0.446	0.0777
0.470	0.537	0.0937	0.429	2.430454	0.425	0.440	0.0767
0.480	0.534	0.0933	0.437	2.316805	0.433	0.434	0.0758
0.490	0.531	0.0928	0.446	2.210163	0.440	0.428	0.0748
0.500	0.527	0.0924	0.454	2.109962	0.447	0.422	0.0739
0.510	0.524	0.0919	0.463	2.015691	0.454	0.416	0.0730
0.520	0.521	0.0915	0.471	1.926887	0.461	0.410	0.0720
0.530	0.518	0.0910	0.480	1.843132	0.468	0.404	0.0711
0.540	0.514	0.0906	0.488	1.764046	0.475	0.398	0.0701
0.550	0.511	0.0901	0.496	1.689285	0.482	0.392	0.0692
0.560	0.508	0.0897	0.505	1.618534	0.489	0.386	0.0683
0.570	0.504	0.0892	0.513	1.551508	0.495	0.380	0.0673
0.580	0.501	0.0887	0.521	1.487945	0.502	0.375	0.0664
0.590	0.497	0.0883	0.529	1.427606	0.508	0.369	0.0655
0.600	0.493	0.0878	0.537	1.370272	0.514	0.363	0.0645
0.610	0.490	0.0873	0.544	1.315742	0.521	0.357	0.0636
0.620	0.486	0.0868	0.552	1.263834	0.527	0.351	0.0627
0.630	0.482	0.0863	0.560	1.214387	0.533	0.345	0.0618
0.640	0.478	0.0858	0.567	1.167258	0.539	0.339	0.0609
0.650	0.474	0.0853	0.575	1.122310	0.545	0.333	0.0600
0.660	0.470	0.0848	0.582	1.079420	0.551	0.328	0.0591
0.670	0.466	0.0843	0.589	1.038471	0.557	0.322	0.0582
0.680	0.462	0.0838	0.597	0.999356	0.562	0.316	0.0573
0.690	0.458	0.0833	0.604	0.961975	0.568	0.310	0.0564
0.700	0.454	0.0828	0.611	0.926234	0.573	0.305	0.0556

OUTPUT LIST DATA FILE: FSTAT
TEST DATA FILE: STAT TEST DATE:
STATOR & 4497, 3/22/87

J-COR	KT	KQ	ETA	KT/J**2	J'	KT'	KQ'
0.700	0.454	0.0828	0.611	0.926234	0.573	0.305	0.0556
0.710	0.450	0.0823	0.617	0.892047	0.579	0.299	0.0547
0.720	0.445	0.0818	0.624	0.859332	0.584	0.293	0.0539
0.730	0.441	0.0813	0.631	0.828014	0.590	0.288	0.0530

0.740	0.437	0.0807	0.637	0.798021	0.595	0.282	0.0522
0.750	0.433	0.0802	0.644	0.769288	0.600	0.277	0.0513
0.760	0.428	0.0797	0.650	0.741752	0.605	0.272	0.0505
0.770	0.424	0.0792	0.657	0.715354	0.610	0.266	0.0497
0.780	0.420	0.0786	0.663	0.690041	0.615	0.261	0.0489
0.790	0.416	0.0781	0.669	0.665760	0.620	0.256	0.0481
0.800	0.411	0.0776	0.675	0.642463	0.625	0.251	0.0473
0.810	0.407	0.0770	0.681	0.620106	0.629	0.246	0.0465
0.820	0.403	0.0765	0.687	0.598644	0.634	0.241	0.0458
0.830	0.398	0.0760	0.692	0.578037	0.639	0.236	0.0450
0.840	0.394	0.0755	0.698	0.558249	0.643	0.231	0.0442
0.850	0.390	0.0749	0.703	0.539242	0.648	0.226	0.0435
0.860	0.385	0.0744	0.709	0.520982	0.652	0.221	0.0428
0.870	0.381	0.0739	0.714	0.503439	0.656	0.217	0.0420
0.880	0.377	0.0733	0.720	0.486580	0.661	0.212	0.0413
0.890	0.373	0.0728	0.725	0.470378	0.665	0.208	0.0406
0.900	0.368	0.0723	0.730	0.454806	0.669	0.204	0.0399
0.910	0.364	0.0717	0.735	0.439837	0.673	0.199	0.0392
0.920	0.360	0.0712	0.740	0.425447	0.677	0.195	0.0386
0.930	0.356	0.0707	0.745	0.411614	0.681	0.191	0.0379
0.940	0.352	0.0702	0.750	0.398314	0.685	0.187	0.0373
0.950	0.348	0.0697	0.755	0.385520	0.689	0.183	0.0366
0.960	0.344	0.0691	0.760	0.373206	0.693	0.179	0.0360
0.970	0.340	0.0686	0.765	0.361344	0.696	0.175	0.0354
0.980	0.336	0.0681	0.770	0.349910	0.700	0.171	0.0347
0.990	0.332	0.0676	0.774	0.338881	0.704	0.168	0.0341
1.000	0.328	0.0671	0.779	0.328234	0.707	0.164	0.0335
1.010	0.324	0.0665	0.784	0.317950	0.711	0.161	0.0329
1.020	0.320	0.0660	0.788	0.308007	0.714	0.157	0.0323
1.030	0.317	0.0655	0.793	0.298389	0.717	0.154	0.0318
1.040	0.313	0.0649	0.797	0.289077	0.721	0.150	0.0312
1.050	0.309	0.0644	0.801	0.280056	0.724	0.147	0.0306
1.060	0.305	0.0638	0.805	0.271309	0.727	0.144	0.0301
1.070	0.301	0.0633	0.810	0.262822	0.731	0.140	0.0295
1.080	0.297	0.0627	0.814	0.254582	0.734	0.137	0.0290
1.090	0.293	0.0622	0.817	0.246574	0.737	0.134	0.0284
1.100	0.289	0.0616	0.821	0.238787	0.740	0.131	0.0279
1.110	0.285	0.0610	0.825	0.231209	0.743	0.128	0.0273
1.120	0.281	0.0604	0.828	0.223829	0.746	0.125	0.0268
1.130	0.277	0.0598	0.832	0.216636	0.749	0.121	0.0263
1.140	0.272	0.0592	0.835	0.209620	0.752	0.118	0.0257
1.150	0.268	0.0586	0.838	0.202772	0.755	0.115	0.0252
1.160	0.264	0.0579	0.841	0.196083	0.757	0.112	0.0247
1.170	0.259	0.0573	0.843	0.189544	0.760	0.110	0.0242
1.180	0.255	0.0566	0.846	0.183147	0.763	0.107	0.0237
1.190	0.250	0.0560	0.848	0.176885	0.766	0.104	0.0232
1.200	0.246	0.0553	0.850	0.170750	0.768	0.101	0.0227

OUTPUT LIST DATA FILE: FSTAT
TEST DATA FILE: STAT TEST DATE:
STATOR & 4497, 3/22/87

J-COR	KT	KQ	ETA	KT/J**2	J'	KT'	KQ'

1.200	0.246	0.0553	0.850	0.170750	0.768	0.101	0.0227
1.210	0.241	0.0546	0.851	0.164735	0.771	0.098	0.0221
1.220	0.236	0.0539	0.852	0.158835	0.773	0.095	0.0216
1.230	0.232	0.0531	0.853	0.153042	0.776	0.092	0.0211
1.240	0.227	0.0524	0.854	0.147350	0.778	0.089	0.0206
1.250	0.221	0.0516	0.854	0.141755	0.781	0.086	0.0201
1.260	0.216	0.0508	0.854	0.136251	0.783	0.084	0.0196
1.270	0.211	0.0500	0.853	0.130835	0.786	0.081	0.0191
1.280	0.206	0.0492	0.852	0.125507	0.788	0.078	0.0186
1.290	0.200	0.0483	0.850	0.120268	0.790	0.075	0.0181
1.300	0.195	0.0475	0.848	0.115116	0.793	0.072	0.0177
1.310	0.189	0.0466	0.845	0.110053	0.795	0.070	0.0172
1.320	0.183	0.0457	0.841	0.105077	0.797	0.067	0.0167
1.330	0.177	0.0448	0.837	0.100188	0.799	0.064	0.0162
1.340	0.171	0.0439	0.832	0.095386	0.801	0.061	0.0157
1.350	0.165	0.0430	0.826	0.090671	0.804	0.059	0.0152
1.360	0.159	0.0421	0.819	0.086042	0.806	0.056	0.0148
1.370	0.153	0.0411	0.812	0.081498	0.808	0.053	0.0143
1.380	0.147	0.0401	0.803	0.077040	0.810	0.051	0.0138
1.390	0.140	0.0392	0.793	0.072666	0.812	0.048	0.0134
1.400	0.134	0.0382	0.782	0.068377	0.814	0.045	0.0129
1.410	0.128	0.0372	0.770	0.064172	0.816	0.043	0.0124
1.420	0.121	0.0362	0.757	0.060049	0.818	0.040	0.0120
1.430	0.115	0.0352	0.742	0.056009	0.820	0.038	0.0115
1.440	0.108	0.0341	0.725	0.052051	0.821	0.035	0.0111
1.450	0.101	0.0331	0.706	0.048175	0.823	0.033	0.0107
1.460	0.095	0.0321	0.686	0.044379	0.825	0.030	0.0102
1.470	0.088	0.0310	0.663	0.040663	0.827	0.028	0.0098
1.480	0.081	0.0300	0.638	0.037027	0.829	0.025	0.0094
1.490	0.074	0.0289	0.610	0.033469	0.830	0.023	0.0090
1.500	0.067	0.0278	0.578	0.029990	0.832	0.021	0.0086
1.510	0.061	0.0268	0.544	0.026588	0.834	0.018	0.0082
1.520	0.054	0.0257	0.506	0.023262	0.835	0.016	0.0078
1.530	0.047	0.0246	0.463	0.020013	0.837	0.014	0.0074
1.540	0.040	0.0236	0.415	0.016839	0.839	0.012	0.0070
1.550	0.033	0.0225	0.362	0.013740	0.840	0.010	0.0066
1.560	0.026	0.0214	0.302	0.010716	0.842	0.008	0.0062
1.570	0.019	0.0203	0.235	0.007764	0.843	0.006	0.0059
1.580	0.012	0.0192	0.159	0.004885	0.845	0.003	0.0055
1.590	0.005	0.0182	0.073	0.002078	0.846	0.001	0.0051
1.600	−0.002	0.0171	−0.025	−0.000657	0.848	−0.000	0.0048

TYPE SDRIV.DAT

DATA FILE: SDRIV
OWPP1 PROGRAM RELEASED: 21 AUG 84
STATOR ON PROP DRIVE

DIA (INCHES)	0.7R CHORD (INCHES)	HUB COR	VELINC	WATER TEMP (DEGREE F)	BAROMETER (MMHG)	ROOM TEMP (DEGREE F)
12.0000	4.0000	-0.0010	0.0000	78.0000	763.7399	72.00

TUNNEL VEL (FT/SEC)	STAT PRESS (MMHG)	RPM	T (LBS)	Q (INCH-LBS)	J CORR	WTEMP (F)	IMP RPM
10.646	816.967	11.110	1.758	-168.275	57.421	78.0	163.
12.526	807.520	11.185	0.144	-197.119	67.105	78.0	192.
14.084	798.810	11.245	0.628	-270.555	75.053	78.0	216.
14.724	794.617	11.125	-9.305	-299.110	79.111	78.0	225.
15.645	788.474	11.268	-9.876	-344.558	82.993	78.0	240.
16.797	781.141	11.148	-14.154	-403.653	89.914	78.0	257.
17.753	773.918	11.174	-14.985	-460.064	94.809	78.0	272.
18.975	764.231	11.208	-13.054	-511.330	101.239	78.0	291.
20.146	754.531	11.185	-18.050	-511.330	107.480	78.0	308.
22.036	737.121	11.317	-20.463	-511.330	116.391	78.0	337.
23.522	722.786	11.185	-32.639	-511.330	125.488	78.0	360.
24.922	707.778	11.185	-40.152	-511.330	132.903	78.0	382.
26.482	690.598	11.159	-45.717	-511.330	141.555	78.0	408.
26.486	677.465	11.275	-52.907	-511.330	139.996	78.0	425.
0.000	0.000	0.000	0.000	0.000	0.000	0.0	0.

.TYPE SDRIV2.DAT

DATA FILE: SDRIV2
OWPP1 PROGRAM RELEASED: 21 AUG 84
STATOR ON PROP DRIVE

DIA (INCHES)	0.7R CHORD (INCHES)	HUB COR	VELINC	WATER TEMP (DEGREE F)	BAROMETER (MMHG)	ROOM TEMP (DEGREE F)
12.0000	4.0000	-0.0010	0.0000	78.0000	763.7399	72.00

TUNNEL VEL (FT/SEC)	STAT PRESS (MMHG)	RPM	T (LBS)	Q (INCH-LBS)	J CORR	WTEMP (F)	IMP RPM
9.190	823.126	20.711	-5.598	-99.914	26.468	78.0	140.
11.815	811.432	20.854	-6.059	-186.451	33.866	78.0	180.
14.096	798.772	20.568	-11.522	-353.424	40.896	78.0	215.
15.597	789.057	20.688	-12.371	-365.801	44.986	78.0	238.
16.086	785.912	20.797	-14.302	-395.899	46.155	78.0	247.
17.165	778.191	20.628	-16.546	-456.741	49.655	78.0	263.
17.431	775.918	20.861	-22.144	-505.871	49.799	78.0	267.
18.487	767.688	20.756	-22.352	-505.871	53.128	78.0	283.
19.053	763.578	20.707	-24.043	-505.871	54.882	78.0	292.
20.269	753.370	20.696	-26.063	-505.871	58.418	78.0	310.
21.573	740.629	20.617	-34.421	-505.871	62.361	78.0	331.
23.044	727.675	20.621	-38.585	-505.871	66.601	78.0	353.
24.436	713.388	20.598	-44.813	-505.871	70.703	78.0	374.
0.000	0.000	0.000	0.000	0.000	0.000	0.0	0.

Appendix D
SSF-1 OUTPUT

```
         9
         1
        10
0.2721268       6.5282192E-03
0.3467805       7.4240533E-03
0.4214342       8.5248984E-03
0.4960878       9.7106444E-03
0.5707415       1.0921160E-02
0.6453952       1.1968476E-02
0.7200489       1.2695494E-02
0.7947026       1.2842632E-02
0.8693563       1.1967322E-02
0.9440100       9.1451388E-03
         2
        10
0.2721268       6.5279077E-03
0.3467805       7.4237674E-03
0.4214342       8.5246628E-03
0.4960878       9.7104106E-03
0.5707415       1.0920931E-02
0.6453952       1.1968298E-02
0.7200489       1.2695328E-02
0.7947026       1.2842465E-02
0.8693563       1.1967234E-02
0.9440100       9.1450736E-03
         3
        10
0.2721268       6.5283305E-03
0.3467805       7.4241101E-03
0.4214342       8.5249254E-03
0.4960878       9.7106565E-03
0.5707415       1.0921146E-02
0.6453952       1.1968455E-02
0.7200489       1.2695441E-02
0.7947026       1.2842576E-02
0.8693563       1.1967274E-02
0.9440100       9.1451416E-03
         4
        10
0.2721268       6.5283347E-03
0.3467805       7.4241445E-03
0.4214342       8.5249711E-03
0.4960878       9.7106891E-03
0.5707415       1.0921150E-02
0.6453952       1.1968406E-02
0.7200489       1.2695372E-02
0.7947026       1.2842479E-02
0.8693563       1.1967160E-02
0.9440100       9.1450494E-03
         5
        10
0.2721268       6.5277959E-03
0.3467805       7.4237054E-03
0.4214342       8.5246330E-03
```

```
0.4960878       9.7104581E-03
0.5707415       1.0920944E-02
0.6453952       1.1968271E-02
0.7200489       1.2695287E-02
0.7947026       1.2842474E-02
0.8693563       1.1967143E-02
0.9440100       9.1450447E-03
         6
        10
0.2721268       6.5284274E-03
0.3467805       7.4242610E-03
0.4214342       8.5250763E-03
0.4960878       9.7108483E-03
0.5707415       1.0921264E-02
0.6453952       1.1968572E-02
0.7200489       1.2695491E-02
0.7947026       1.2842577E-02
0.8693563       1.1967214E-02
0.9440100       9.1450708E-03
         7
        10
0.2721268       6.5280492E-03
0.3467805       7.4239429E-03
0.4214342       8.5247774E-03
0.4960878       9.7105466E-03
0.5707415       1.0921123E-02
0.6453952       1.1968487E-02
0.7200489       1.2695504E-02
0.7947026       1.2842617E-02
0.8693563       1.1967341E-02
0.9440100       9.1451593E-03
         8
        10
0.2721268       6.5281759E-03
0.3467805       7.4240509E-03
0.4214342       8.5248798E-03
0.4960878       9.7106276E-03
0.5707415       1.0921170E-02
0.6453952       1.1968526E-02
0.7200489       1.2695467E-02
0.7947026       1.2842628E-02
0.8693563       1.1967396E-02
0.9440100       9.1451928E-03
         9
        10
0.2721268       6.5280753E-03
0.3467805       7.4239294E-03
0.4214342       8.5247550E-03
0.4960878       9.7104870E-03
0.5707415       1.0921003E-02
0.6453952       1.1968384E-02
0.7200489       1.2695354E-02
0.7947026       1.2842589E-02
0.8693563       1.1967331E-02
```

0.9440100 9.1451807E-03

```
         9
         1
        10
0.2721268       6.8057715E-03
0.3467805       7.7518704E-03
0.4214342       8.9047551E-03
0.4960878       1.0137256E-02
0.5707415       1.1397047E-02
0.6453952       1.2477698E-02
0.7200489       1.3219172E-02
0.7947026       1.3355246E-02
0.8693563       1.2429432E-02
0.9440100       9.4883088E-03
         2
        10
0.2721268       6.8054935E-03
0.3467805       7.7516348E-03
0.4214342       8.9045241E-03
0.4960878       1.0137106E-02
0.5707415       1.1396856E-02
0.6453952       1.2477528E-02
0.7200489       1.3219036E-02
0.7947026       1.3355091E-02
0.8693563       1.2429317E-02
0.9440100       9.4882343E-03
         3
        10
0.2721268       6.8058684E-03
0.3467805       7.7519389E-03
0.4214342       8.9047849E-03
0.4960878       1.0137322E-02
0.5707415       1.1397101E-02
0.6453952       1.2477739E-02
0.7200489       1.3219163E-02
0.7947026       1.3355196E-02
0.8693563       1.2429361E-02
0.9440100       9.4882483E-03
         4
        10
0.2721268       6.8059522E-03
0.3467805       7.7520222E-03
0.4214342       8.9048911E-03
0.4960878       1.0137381E-02
0.5707415       1.1397103E-02
0.6453952       1.2477729E-02
0.7200489       1.3219153E-02
0.7947026       1.3355233E-02
0.8693563       1.2429395E-02
0.9440100       9.4882753E-03
         5
        10
0.2721268       6.8053808E-03
0.3467805       7.7515701E-03
0.4214342       8.9045139E-03
```

```
0.4960878       1.0137077E-02
0.5707415       1.1396892E-02
0.6453952       1.2477550E-02
0.7200489       1.3218986E-02
0.7947026       1.3355214E-02
0.8693563       1.2429360E-02
0.9440100       9.4882417E-03
         6
        10
0.2721268       6.8060267E-03
0.3467805       7.7521116E-03
0.4214342       8.9050084E-03
0.4960878       1.0137454E-02
0.5707415       1.1397218E-02
0.6453952       1.2477805E-02
0.7200489       1.3219222E-02
0.7947026       1.3355361E-02
0.8693563       1.2429475E-02
0.9440100       9.4883163E-03
         7
        10
0.2721268       6.8055149E-03
0.3467805       7.7516418E-03
0.4214342       8.9045623E-03
0.4960878       1.0137115E-02
0.5707415       1.1396971E-02
0.6453952       1.2477520E-02
0.7200489       1.3219085E-02
0.7947026       1.3355271E-02
0.8693563       1.2429461E-02
0.9440100       9.4882902E-03
         8
        10
0.2721268       6.8057543E-03
0.3467805       7.7518644E-03
0.4214342       8.9047179E-03
0.4960878       1.0137257E-02
0.5707415       1.1397040E-02
0.6453952       1.2477699E-02
0.7200489       1.3219153E-02
0.7947026       1.3355284E-02
0.8693563       1.2429445E-02
0.9440100       9.4882622E-03
         9
        10
0.2721268       6.8056579E-03
0.3467805       7.7517154E-03
0.4214342       8.9045856E-03
0.4960878       1.0137147E-02
0.5707415       1.1396919E-02
0.6453952       1.2477526E-02
0.7200489       1.3219087E-02
0.7947026       1.3355230E-02
0.8693563       1.2429453E-02
```

0.9440100 9.4882594E-03

```
         9
         1
        10
0.2721268       2.1254944E-02
0.3467805       2.2306718E-02
0.4214342       2.3508435E-02
0.4960878       2.4673378E-02
0.5707415       2.5571367E-02
0.6453952       2.6092848E-02
0.7200489       2.5987294E-02
0.7947026       2.4913538E-02
0.8693563       2.2193337E-02
0.9440100       1.6340559E-02
         2
        10
0.2721268       1.4494461E-02
0.3467805       1.5579796E-02
0.4214342       1.6644796E-02
0.4960878       1.7661966E-02
0.5707415       1.8708309E-02
0.6453952       1.9461619E-02
0.7200489       1.9752463E-02
0.7947026       1.9268097E-02
0.8693563       1.7429676E-02
0.9440100       1.3011266E-02
         3
        10
0.2721268       7.1340008E-03
0.3467805       7.8472961E-03
0.4214342       8.6224740E-03
0.4960878       9.4599314E-03
0.5707415       1.0271830E-02
0.6453952       1.1026465E-02
0.7200489       1.1544276E-02
0.7947026       1.1592996E-02
0.8693563       1.0760130E-02
0.9440100       8.1952643E-03
         4
        10
0.2721268      -3.0031153E-03
0.3467805      -2.5477826E-03
0.4214342      -1.9478098E-03
0.4960878      -1.1732639E-03
0.5707415      -2.9981980E-04
0.6453952       6.1695668E-04
0.7200489       1.5498905E-03
0.7947026       2.3588939E-03
0.8693563       2.8145500E-03
0.9440100       2.5096431E-03
         5
        10
0.2721268      -6.4823111E-03
0.3467805      -6.2765968E-03
0.4214342      -5.9051877E-03
```

```
0.4960878      -5.3566471E-03
0.5707415      -4.6464400E-03
0.6453952      -3.7866826E-03
0.7200489      -2.8073313E-03
0.7947026      -1.7704009E-03
0.8693563      -8.1045198E-04
0.9440100      -1.2219616E-04
         6
        10
0.2721268      -6.6159652E-03
0.3467805      -6.4162891E-03
0.4214342      -6.0180314E-03
0.4960878      -5.4584788E-03
0.5707415      -4.7375606E-03
0.6453952      -3.8623733E-03
0.7200489      -2.8687352E-03
0.7947026      -1.8174873E-03
0.8693563      -8.3982229E-04
0.9440100      -1.3146240E-04
         7
        10
0.2721268      -3.2303645E-03
0.3467805      -2.7348336E-03
0.4214342      -2.0251325E-03
0.4960878      -1.1864583E-03
0.5707415      -2.4804013E-04
0.6453952       7.2806596E-04
0.7200489       1.6778724E-03
0.7947026       2.4943650E-03
0.8693563       2.9531142E-03
0.9440100       2.6312040E-03
         8
        10
0.2721268       7.4081020E-03
0.3467805       8.2689878E-03
0.4214342       9.3080457E-03
0.4960878       1.0330791E-02
0.5707415       1.1264992E-02
0.6453952       1.2036547E-02
0.7200489       1.2526325E-02
0.7947026       1.2506584E-02
0.8693563       1.1547311E-02
0.9440100       8.7634185E-03
         9
        10
0.2721268       1.4685245E-02
0.3467805       1.5924480E-02
0.4214342       1.7347924E-02
0.4960878       1.8667376E-02
0.5707415       1.9770281E-02
0.6453952       2.0535162E-02
0.7200489       2.0786664E-02
0.7947026       2.0210361E-02
0.8693563       1.8227799E-02
```

0.9440100 1.3581386E-02

```
         9
         1
        10
0.2721268       1.9875202E-02
0.3467805       2.0656846E-02
0.4214342       2.1690205E-02
0.4960878       2.2797354E-02
0.5707415       2.3730611E-02
0.6453952       2.4350051E-02
0.7200489       2.4389703E-02
0.7947026       2.3497380E-02
0.8693563       2.1018183E-02
0.9440100       1.5534872E-02
         2
        10
0.2721268       1.3088644E-02
0.3467805       1.3948503E-02
0.4214342       1.4902722E-02
0.4960878       1.5909884E-02
0.5707415       1.7011948E-02
0.6453952       1.7871080E-02
0.7200489       1.8302249E-02
0.7947026       1.7985575E-02
0.8693563       1.6365061E-02
0.9440100       1.2279435E-02
         3
        10
0.2721268       4.1945255E-03
0.3467805       4.8928699E-03
0.4214342       5.7990816E-03
0.4960878       6.8431869E-03
0.5707415       7.9052355E-03
0.6453952       8.9263981E-03
0.7200489       9.7207064E-03
0.7947026       1.0053061E-02
0.8693563       9.5336335E-03
0.9440100       7.3815342E-03
         4
        10
0.2721268      -1.2915328E-03
0.3467805      -7.9251331E-04
0.4214342      -4.5745492E-05
0.4960878       8.6903863E-04
0.5707415       1.8618968E-03
0.6453952       2.8686346E-03
0.7200489       3.8032951E-03
0.7947026       4.5000687E-03
0.8693563       4.6909275E-03
0.9440100       3.8805353E-03
         5
        10
0.2721268      -1.7706522E-03
0.3467805      -1.4365921E-03
0.4214342      -8.8215299E-04
```

```
0.4960878      -1.7654711E-04
0.5707415       6.3022098E-04
0.6453952       1.4854361E-03
0.7200489       2.3195073E-03
0.7947026       3.0033782E-03
0.8693563       3.3130967E-03
0.9440100       2.8404784E-03
         6
        10
0.2721268      -1.7734164E-03
0.3467805      -1.4226027E-03
0.4214342      -8.5162441E-04
0.4960878      -1.3878947E-04
0.5707415       6.7552505E-04
0.6453952       1.5352308E-03
0.7200489       2.3704024E-03
0.7947026       3.0530924E-03
0.8693563       3.3601136E-03
0.9440100       2.8779253E-03
         7
        10
0.2721268      -1.3077059E-03
0.3467805      -7.3799171E-04
0.4214342       7.6039985E-05
0.4960878       1.0359877E-03
0.5707415       2.0736367E-03
0.6453952       3.1033370E-03
0.7200489       4.0375972E-03
0.7947026       4.7232090E-03
0.8693563       4.8937667E-03
0.9440100       4.0337434E-03
         8
        10
0.2721268       4.2983606E-03
0.3467805       5.1368671E-03
0.4214342       6.2507344E-03
0.4960878       7.4355807E-03
0.5707415       8.6008143E-03
0.6453952       9.6402075E-03
0.7200489       1.0420025E-02
0.7947026       1.0707621E-02
0.8693563       1.0100877E-02
0.9440100       7.7932784E-03
         9
        10
0.2721268       1.3188139E-02
0.3467805       1.4216806E-02
0.4214342       1.5506248E-02
0.4960878       1.6786363E-02
0.5707415       1.7933266E-02
0.6453952       1.8799637E-02
0.7200489       1.9193945E-02
0.7947026       1.8795036E-02
0.8693563       1.7049093E-02
```

0.9440100 1.2767860E-02

Appendix E
VELOCITY MEASUREMENTS

1
TANG,BL9,R/R.45
25
296.000 -0.210
298.000 -0.206
300.000 -0.185
302.000 -0.206
304.000 -0.224
306.000 -0.223
308.000 -0.224
310.000 -0.222
312.000 -0.222
314.000 -0.221
316.000 -0.218
318.000 -0.218
320.000 -0.219
322.000 -0.218
324.000 -0.215
326.000 -0.218
328.000 -0.223
330.000 -0.223
332.000 -0.226
334.000 -0.229
336.000 -0.232
338.000 -0.235
340.000 -0.240
342.000 -0.244
344.000 -0.234

1
TANG,BL8,R/R.45
25
256.000 -0.159
258.000 -0.161
260.000 -0.162
262.000 -0.161
264.000 -0.158
266.000 -0.141
268.000 -0.164
270.000 -0.164
272.000 -0.164
274.000 -0.165
276.000 -0.161
278.000 -0.165
280.000 -0.163
282.000 -0.165
284.000 -0.164
286.000 -0.164
288.000 -0.168
290.000 -0.170
292.000 -0.171
294.000 -0.173
296.000 -0.176
298.000 -0.178

```
300.000  -0.180
302.000  -0.184
304.000  -0.186

1
 TANG,BL7,R/R.45
25
216.000  -0.115
218.000  -0.118
220.000  -0.118
222.000  -0.119
224.000  -0.115
226.000  -0.117
228.000  -0.119
230.000  -0.103
232.000  -0.122
234.000  -0.123
236.000  -0.122
238.000  -0.124
240.000  -0.126
242.000  -0.128
244.000  -0.125
246.000  -0.128
248.000  -0.133
250.000  -0.134
252.000  -0.134
254.000  -0.135
256.000  -0.139
258.000  -0.140
260.000  -0.142
262.000  -0.145
264.000  -0.148

1
 TANG,R/R.45,NONA  BLADE 6
25
176.000  -0.092
178.000  -0.095
180.000  -0.094
182.000  -0.095
184.000  -0.093
186.000  -0.094
188.000  -0.097
190.000  -0.094
192.000  -0.087
194.000  -0.103
196.000  -0.103
198.000  -0.106
200.000  -0.108
202.000  -0.112
204.000  -0.108
206.000  -0.111
208.000  -0.115
210.000  -0.117
```

```
212.000  -0.119
214.000  -0.122
216.000  -0.125
218.000  -0.129
220.000  -0.129
222.000  -0.134
224.000  -0.135

1
 TANG,BL5,R/R.45
27
186.000  -0.089
184.000  -0.089
182.000  -0.094
180.000  -0.094
178.000  -0.095
176.000  -0.095
174.000  -0.094
172.000  -0.096
170.000  -0.086
168.000  -0.100
166.000  -0.104
164.000  -0.102
162.000  -0.106
160.000  -0.107
158.000  -0.114
156.000  -0.112
154.000  -0.116
152.000  -0.121
150.000  -0.124
148.000  -0.125
146.000  -0.128
144.000  -0.133
142.000  -0.137
140.000  -0.140
138.000  -0.145
136.000  -0.148
134.000  -0.154
1
 TANG,BL4,R/R.45
27
146.000  -0.107
144.000  -0.106
142.000  -0.111
140.00  -0.109
138.00  -0.111
136.00  -0.110
134.00  -0.112
132.00  -0.115
130.00  -0.113
128.00  -0.126
126.00  -0.128
124.00  -0.127
122.00  -0.131
```

```
120.00  -0.135
118.00  -0.140
116.00  -0.143
114.00  -0.136
112.00  -0.144
110.00  -0.148
108.00  -0.149
106.00  -0.155
104.00  -0.162
102.00  -0.167
100.00  -0.172
98.000  -0.177
96.000  -0.166
94.000  -0.143
1
 TANG,BL3,R/R.45
27
106.00  -0.140
104.00  -0.139
102.00  -0.146
100.0   -0.148
98.000  -0.148
96.000  -0.147
94.000  -0.147
92.000  -0.167
90.000  -0.165
88.000  -0.171
86.000  -0.174
84.000  -0.175
82.000  -0.181
80.000  -0.185
78.000  -0.193
76.000  -0.194
74.000  -0.200
72.000  -0.209
68.000  -0.216
66.000  -0.220
64.000  -0.227
62.000  -0.234
60.000  -0.229
58.000  -0.201
56.000  -0.199
54.000  -0.202
52.000  -0.211
1
 TANG,BL2,R/R.45
23
60.000 -0.171
58.000 -0.202
56.000 -0.218
54.000 -0.222
52.000 -0.225
50.000 -0.226
48.000 -0.232
```

```
46.000 -0.234
44.000 -0.234
42.000 -0.239
40.000 -0.243
38.000 -0.249
36.000 -0.248
34.000 -0.263
32.000 -0.266
30.000 -0.266
28.000 -0.254
26.000 -0.239
24.000 -0.247
22.000 -0.245
20.000 -0.249
18.000 -0.252
16.000 -0.258
1
 TANG,R/R.45,NONA , BLADE  0
27
26.000  -0.234
24.000  -0.261
22.000  -0.264
20.000  -0.261
18.000  -0.261
16.000  -0.257
14.000  -0.256
12.000  -0.265
10.000  -0.253
8.000   -0.252
6.000   -0.252
4.000   -0.254
2.000   -0.258
0.000   -0.254
358.0   -0.257
356.0   -0.258
354.0   -0.264
352.0   -0.272
350.0   -0.277
348.0   -0.279
346.0   -0.278
344.0   -0.245
342.0   -0.233
340.0   -0.232
338.0   -0.236
336.0   -0.239
334.0   -0.243
```

```
1
 TANG,BL9,R/R.6
25
296.000  -0.203
298.000  -0.209
300.000  -0.215
302.000  -0.213
304.000  -0.190
306.000  -0.214
308.000  -0.225
310.000  -0.219
312.000  -0.217
314.000  -0.214
316.000  -0.210
318.000  -0.206
320.000  -0.203
322.000  -0.200
324.000  -0.197
326.000  -0.197
328.000  -0.198
330.000  -0.198
332.000  -0.200
334.000  -0.201
336.000  -0.203
338.000  -0.204
340.000  -0.206
242.000  -0.209
244.000  -0.208

1
 TANG,BL8,R/R.6
25
256.000  -0.145
258.000  -0.146
260.000  -0.146
262.000  -0.148
264.000  -0.148
266.000  -0.151
268.000  -0.147
270.000  -0.143
272.000  -0.159
274.000  -0.156
276.000  -0.155
278.000  -0.150
280.000  -0.152
282.000  -0.150
284.000  -0.147
286.000  -0.150
288.000  -0.150
290.000  -0.149
292.000  -0.151
294.000  -0.151
296.000  -0.153
298.000  -0.154
```

```
300.000  -0.156
302.000  -0.157
304.000  -0.156
1
 TANG,BL7,R/R.6
25
216.000  -0.105
218.000  -0.106
220.000  -0.106
222.000  -0.106
224.000  -0.106
226.000  -0.107
228.000  -0.108
230.000  -0.109
232.000  -0.103
234.000  -0.116
236.000  -0.115
238.000  -0.114
240.000  -0.115
242.000  -0.117
244.000  -0.115
246.000  -0.118
248.000  -0.118
250.000  -0.118
252.000  -0.121
254.000  -0.122
256.000  -0.123
258.000  -0.124
260.000  -0.127
262.000  -0.129
264.000  -0.128
1
 TANG,BL6,R/R.6
25
176.000 -0.086
178.000 -0.086
180.000 -0.088
182.000 -0.090
184.000 -0.088
186.000 -0.091
188.000 -0.091
190.000 -0.092
192.000 -0.093
194.000 -0.094
196.000 -0.098
198.000 -0.097
200.000 -0.098
202.000 -0.102
204.000 -0.098
206.000 -0.103
208.000 -0.106
210.000 -0.103
212.000 -0.107
214.000 -0.108
```

```
216.000 -0.111
218.000 -0.113
220.000 -0.116
222.000 -0.117
224.000 -0.119
1
 TANG,BL5,R/R.6
27
186.000  -0.086
184.000  -0.085
182.000  -0.087
180.000  -0.090
178.000  -0.090
176.000  -0.087
174.000  -0.091
172.000  -0.091
170.000  -0.090
168.000  -0.083
166.000  -0.099
164.000  -0.100
162.000  -0.098
160.000  -0.102
158.000  -0.104
156.000  -0.101
154.000  -0.106
152.000  -0.110
150.000  -0.108
148.000  -0.111
146.000  -0.115
144.000  -0.117
142.000  -0.121
140.000  -0.124
138.000  -0.127
136.000  -0.128
134.000  -0.133
1
 TANG,BL4,R/R.6
27
146.000  -0.100
144.000  -0.097
142.000  -0.101
140.000  -0.101
138.000  -0.102
136.000  -0.103
134.000  -0.107
132.000  -0.108
130.000  -0.106
128.000  -0.115
126.000  -0.117
124.000  -0.118
122.000  -0.117
120.000  -0.119
118.000  -0.122
116.000  -0.120
```

```
114.000  -0.125
112.000  -0.128
110.000  -0.128
108.000  -0.134
106.000  -0.137
104.000  -0.140
102.000  -0.145
100.000  -0.149
98.000   -0.154
96.000   -0.155
94.000   -0.161
1
 TANG,BL3,R/R.6
27
106.00   -0.137
104.00   -0.135
102.00   -0.140
100.00   -0.142
98.000   -0.146
96.000   -0.147
94.000   -0.152
92.000   -0.151
90.000   -0.165
88.000   -0.165
86.000   -0.166
84.000   -0.166
82.000   -0.166
80.000   -0.170
78.000   -0.174
76.000   -0.169
74.000   -0.178
72.000   -0.182
70.000   -0.183
68.000   -0.191
66.000   -0.198
64.000   -0.201
62.000   -0.209
58.000   -0.217
56.000   -0.221
54.000   -0.197
52.000   -0.196
1
 TANG,BL2,R/R.6
27
66.000   -0.192
64.000   -0.195
62.000   -0.201
60.000   -0.209
58.000   -0.212
56.000   -0.198
54.000   -0.226
52.000   -0.222
50.000   -0.219
48.000   -0.220
```

```
46.000  -0.218
44.000  -0.217
42.000  -0.214
40.000  -0.215
38.000  -0.215
36.000  -0.211
34.000  -0.217
32.000  -0.219
30.000  -0.219
28.000  -0.223
26.000  -0.226
24.000  -0.231
22.000  -0.228
20.000  -0.220
18.000  -0.217
16.000  -0.229
14.000  -0.247
1
 TANG,R/R.6,NONA , BLADE 0
27
26.000  -0.207
24.000  -0.191
22.000  -0.189
20.000  -0.219
18.000  -0.257
16.000  -0.275
14.000  -0.291
12.000  -0.280
10.000  -0.272
8.000   -0.264
6.000   -0.256
4.000   -0.259
2.000   -0.245
0.000   -0.249
358.0   -0.233
356.0   -0.227
354.0   -0.231
352.0   -0.236
350.0   -0.237
348.0   -0.246
346.0   -0.252
344.0   -0.260
342.0   -0.264
340.0   -0.244
338.0   -0.242
336.0   -0.239
334.0   -0.242
```

```
1
 TANG,BL9,R/R.75
25
296.000  -0.164
298.000  -0.168
300.000  -0.178
302.000  -0.186
304.000  -0.195
306.000  -0.190
308.000  -0.185
310.000  -0.216
312.000  -0.214
314.000  -0.211
316.000  -0.208
318.000  -0.201
320.000  -0.193
322.000  -0.183
324.000  -0.175
326.000  -0.172
328.000  -0.167
330.000  -0.162
332.000  -0.161
334.000  -0.161
336.000  -0.159
338.000  -0.159
340.000  -0.161
342.000  -0.164
344.000  -0.171
1
 TANG,BL8,R/R.75
25
256.000  -0.112
258.000  -0.116
260.000  -0.122
262.000  -0.128
264.000  -0.363
266.000  -0.142
268.000  -0.149
270.000  -0.145
272.000  -0.165
274.000  -0.160
276.000  -0.157
278.000  -0.152
280.000  -0.147
282.000  -0.142
284.000  -0.136
286.000  -0.136
288.000  -0.132
290.000  -0.130
292.000  -0.128
294.000  -0.128
296.000  -0.126
298.000  -0.128
300.000  -0.128
```

```
302.000  -0.132
304.000  -0.135

1
 TANG,BL7,R/R.75
25
216.000  -0.083
218.000  -0.087
220.000  -0.092
222.000  -0.095
224.000  -0.097
226.000  -0.102
228.000  -0.105
230.000  -0.111
232.000  -0.110
234.000  -0.121
236.000  -0.119
238.000  -0.117
240.000  -0.113
242.000  -0.111
244.000  -0.109
246.000  -0.107
248.000  -0.106
250.000  -0.107
252.000  -0.108
254.000  -0.107
256.000  -0.106
258.000  -0.108
260.000  -0.109
262.000  -0.110
264.000  -0.114
1
 TANG,BL6,R/R.75
25
176.000  -0.076
178.000  -0.075
180.000  -0.080
182.000  -0.081
184.000  -0.085
186.000  -0.089
188.000  -0.090
190.000  -0.094
192.000  -0.094
194.000  -0.088
196.000  -0.103
198.000  -0.101
200.000  -0.099
202.000  -0.098
204.000  -0.094
206.000  -0.095
208.000  -0.096
210.000  -0.097
212.000  -0.097
214.000  -0.097
```

```
216.000  -0.097
218.000  -0.100
220.000  -0.100
222.000  -0.102
224.000  -0.107

1
 TANG,BL5,R/R.75
27
186.000  -0.073
184.000  -0.076
182.000  -0.081
180.000  -0.084
178.000  -0.085
176.000  -0.088
174.000  -0.092
172.000  -0.094
170.000  -0.098
168.000  -0.091
166.000  -0.106
164.000  -0.106
162.000  -0.102
160.000  -0.100
158.000  -0.097
156.000  -0.096
154.000  -0.097
152.000  -0.097
150.000  -0.098
148.000  -0.100
146.000  -0.101
144.000  -0.102
142.000  -0.105
140.000  -0.106
138.000  -0.110
136.000  -0.115
134.000  -0.120
1
 TANG,BL4,R/R.75
27
146.000  -0.086
144.000  -0.088
142.000  -0.093
140.000  -0.096
138.000  -0.099
136.000  -0.102
134.000  -0.107
132.000  -0.111
130.000  -0.113
128.000  -0.112
126.000  -0.120
124.000  -0.120
122.000  -0.117
120.000  -0.115
118.000  -0.112
```

```
116.000  -0.109
114.000  -0.110
112.000  -0.111
110.000  -0.114
108.000  -0.114
106.000  -0.115
104.000  -0.117
102.000  -0.121
100.000  -0.122
98.000   -0.129
96.000   -0.136
94.000   -0.147
1
 TANG,BL3,R/R.75
27
106.00   -0.116
104.00   -0.121
102.00   -0.126
100.00   -0.132
98.000   -0.137
96.000   -0.143
94.000   -0.149
92.000   -0.154
90.000   -0.150
88.000   -0.163
86.000   -0.159
84.000   -0.159
82.000   -0.156
80.000   -0.152
78.000   -0.147
76.000   -0.143
74.000   -0.143
72.000   -0.142
70.000   -0.143
68.000   -0.144
66.000   -0.144
64.000   -0.145
62.000   -0.150
60.000   -0.152
58.000   -0.159
56.000   -0.167
54.000   -0.165
1
 TANG,BL2,R/R.75
27
66.000   -0.157
64.000   -0.164
62.000   -0.173
60.000   -0.184
58.000   -0.192
56.000   -0.203
54.000   -0.197
52.000   -0.216
50.000   -0.218
```

```
48.000  -0.215
46.000  -0.211
44.000  -0.209
42.000  -0.205
40.000  -0.195
38.000  -0.190
36.000  -0.182
34.000  -0.181
32.000  -0.178
30.000  -0.178
28.000  -0.177
26.000  -0.178
24.000  -0.183
22.000  -0.187
20.000  -0.191
18.000  -0.199
16.000  -0.234
14.000  -0.291
1
 TANG,R/R.75,BL0
27
26.000  -0.187
24.000  -0.201
22.000  -0.201
20.000  -0.217
18.000  -0.231
16.000  -0.286
14.000  -0.317
12.000  -0.320
10.000  -0.320
8.000   -0.321
6.000   -0.311
4.000   -0.271
2.000   -0.245
0.000   -0.218
358.0   -0.201
356.0   -0.190
354.0   -0.183
352.0   -0.185
350.0   -0.182
348.0   -0.184
346.0   -0.184
344.0   -0.184
342.0   -0.187
340.0   -0.190
338.0   -0.191
336.0   -0.211
334.0   -0.239
```

```
1
 AXIAL,BL0,R/R.45
27
26.000 0.964
24.000 0.985
22.000 0.996
20.000 1.004
18.000 0.982
16.000 0.988
14.000 0.997
12.000 0.995
10.000 0.988
8.000  0.988
6.000  0.982
4.000  0.981
2.000  0.983
0.000   0.980
358.0   0.985
356.0   0.984
354.0   0.988
352.0   0.992
350.0   0.999
348.0   1.005
346.0   0.997
344.0   0.910
342.0   0.961
340.0   1.060
338.0   1.076
336.0   1.094
334.0   1.111


1
 AXIAL,BL2,R/R.45
27
66.000  1.073
64.000  1.058
62.000  1.018
60.000  0.924
58.000  0.982
56.000  1.004
54.000  0.995
52.000  0.990
50.000  0.985
48.000  0.980
46.000  0.975
44.000  0.969
42.000  0.969
40.000  0.968
38.000  0.971
36.000  0.973
34.000  0.973
32.000  0.976
30.000  0.985
```

```
28.000  0.988
26.000  0.943
24.000  0.892
22.000  0.954
20.000  1.006
18.000  1.027
16.000  1.054
14.000  1.080

1
 AXIAL,BL3,R/R.45
27
106.000 1.079
104.000 1.063
102.00  1.043
100.00  1.032
98.000  1.017
96.000  0.995
94.000  0.898
92.000  0.984
90.000  0.984
88.000  0.981
86.000  0.972
84.000  0.968
82.000  0.966
80.000  0.963
78.000  0.966
76.000  0.970
74.000  0.967
72.000  0.973
70.000  0.978
68.000  0.985
66.000  0.996
64.000  1.003
62.000  0.984
60.000  0.920
58.000  1.024
56.000  1.060
54.000  1.075
1
 AXIAL,BL4,R/R.45
27
146.000   1.091
144.000   1.075
142.000   1.057
140.000   1.045
138.000   1.029
136.000   1.016
134.000   1.008
132.000   0.970
130.000   0.929
128.000   0.990
126.000   0.982
124.000   0.978
```

```
122.000   0.977
120.000  0.973
118.000  0.975
116.000  0.977
114.000  0.976
112.000  0.980
110.000  0.988
108.000  0.993
106.000  1.001
104.000  1.011
102.000  1.022
100.000  1.032
98.0000  1.048
96.0000  1.014
94.0000  1.017
1
 AXIAL,BL5,R/R.45
27
186.000  1.097
184.000  1.081
182.000  1.061
180.000  1.050
178.000  1.034
176.000  1.022
174.000  1.011
172.000  1.004
170.000  0.924
168.000  0.957
166.000  0.984
164.000  0.982
162.000  0.978
160.000  0.979
158.000  0.981
156.000  0.982
154.000  0.983
152.000  0.986
150.000  0.990
148.000  0.996
146.000  1.006
144.000  1.013
142.000  1.028
140.000  1.038
138.000  1.052
136.000  1.070
134.000  1.084
1
 AXIAL,BL6,R/R.45        V_AXIAL
25
   224.0000        17.77489
   222.0000        17.73600
   220.0000        17.75497
   218.0000        17.67719
   216.0000        17.67245
   214.0000        17.66202
```

```
   212.0000        17.68004
   210.0000        17.39170
   208.0000        15.84469
   206.0000        17.60511
   204.0000        17.65063
   202.0000        17.71134
   200.0000        17.61459
   198.0000        17.63356
   196.0000        17.66676
   194.0000        17.58139
   192.0000        17.54346
   190.0000        17.58993
   188.0000        17.60321
   186.0000        17.62123
   184.0000        17.58803
   182.0000        17.57475
   180.0000        17.56337
   178.0000        17.58898
   176.0000        17.56812
1
 AXIAL,BL7,R/R.45
25
   264.0000        17.85931
   262.0000        17.81093
   260.0000        17.86405
   258.0000        17.78817
   256.0000        17.79291
   254.0000        17.78532
   252.0000        17.78437
   250.0000        16.07044
   248.0000        17.50457
   246.0000        17.86120
   244.0000        17.78912
   242.0000        17.87828
   240.0000        17.80334
   238.0000        17.83275
   236.0000        17.87448
   234.0000        17.80050
   232.0000        17.74738
   230.0000        17.75212
   228.0000        17.74169
   226.0000        17.77868
   224.0000        17.73505
   222.0000        17.77394
   220.0000        17.73790
   218.0000        17.72557
   216.0000        17.74264
1
 AXIAL,BL8,R/R.45
25
   304.0000        17.71893
   302.0000        17.64115
   300.0000        17.71988
   298.0000        17.67245
```

```
   296.0000        17.62218
   294.0000        15.71664
   292.0000        17.12801
   290.0000        17.83370
   288.0000        17.85172
   286.0000        17.81662
   284.0000        17.79291
   282.0000        17.83180
   280.0000        17.85267
   278.0000        17.88966
   276.0000        17.91622
   274.0000        17.85172
   272.0000        17.81188
   270.0000        17.84887
   268.0000        17.82516
   266.0000        17.85361
   264.0000        17.82137
   262.0000        17.83275
   260.0000        17.85267
   258.0000        17.82706
   256.0000        17.86405
1
 AXIAL,BL9,R/R.45
25
   344.0000        17.48085
   342.0000        17.03127
   340.0000        15.39131
   338.0000        16.50959
   336.0000        17.55863
   334.0000        17.62597
   332.0000        17.66012
   330.0000        17.64874
   328.0000        17.68478
   326.0000        17.66866
   324.0000        17.67340
   322.0000        17.70091
   320.0000        17.69332
   318.0000        17.72462
   316.0000        17.72936
   314.0000        17.72177
   312.0000        17.73410
   310.0000        17.72557
   308.0000        17.71419
   306.0000        17.70944
   304.0000        17.74738
   302.0000        17.76161
   300.0000        17.74833
   298.0000        17.73790
   296.0000        17.43817
```

1
AXIAL,BL0,R/R.6
27
26.000 1.086
24.000 1.061
22.000 1.008
20.000 0.924
18.000 0.873
16.000 0.862
14.000 0.872
12.000 0.909
10.000 0.935
8.000 0.955
6.000 0.964
4.000 0.977
2.000 0.981
358.0 0.984
356.0 0.989
354.0 0.989
352.0 0.993
350.0 0.995
348.0 1.002
346.0 1.009
344.0 1.017
342.0 1.026
340.0 1.033
338.0 0.931
336.0 0.980
340.0 1.084
338.0 1.104

1
AXIAL,BL2,R/R.6
27
66.000 1.079
64.000 1.058
62.000 1.043
60.000 1.028
58.000 1.008
56.000 0.873
54.000 0.980
52.000 0.991
50.000 0.985
48.000 0.982
46.000 0.978
44.000 0.972
42.000 0.973
40.000 0.973
38.000 0.973
36.000 0.975
34.000 0.980
32.000 0.983
30.000 0.989
28.000 0.996

```
26.000  1.006
24.000  1.016
22.000  1.020
20.000  1.016
18.000  0.960
16.000  0.906
14.000  0.915
1
 AXIAL,BL3,R/R.6
27
106.000  1.082
104.000  1.064
102.000  1.047
100.000  1.034
98.000  1.023
96.000  1.008
94.000  0.999
92.000  0.932
90.000  0.968
88.000  0.983
86.000  0.978
84.000  0.969
82.000  0.969
80.000  0.969
78.000  0.969
76.000  0.970
74.000  0.974
72.000  0.976
70.000  0.980
68.000  0.988
66.000  0.995
64.000  1.004
62.000  1.012
60.000  1.024
58.000  1.017
56.000  0.921
54.000  1.064
1
 AXIAL,BL4,R/R.45
27
146.000   1.100
144.000   1.078
142.000   1.062
140.000  1.048
138.000  1.035
136.000  1.022
134.000  1.012
132.000  1.005
130.000  0.975
128.000  0.965
126.000  0.988
124.000  0.981
122.000  0.982
120.000  0.982
```

```
118.000  0.980
116.000  0.981
114.000  0.985
112.000  0.985
110.000  0.991
108.000  0.998
106.000  1.006
104.000  1.014
102.000  1.023
100.000  1.038
98.000   1.050
96.000   1.066
94.000   1.079
1
 AXIAL,BL5,R/R.6
27
186.000  1.105
184.000  1.088
182.000  1.070
180.000  1.056
178.000  1.042
176.000  1.030
174.000  1.019
172.000  1.010
170.000  1.004
168.000  0.899
166.000  0.994
164.000  0.988
162.000  0.989
160.000  0.988
158.000  0.989
156.000  0.989
154.000  0.991
152.000  0.993
150.000  0.999
148.000  1.005
146.000  1.015
144.000  1.021
142.000  1.032
140.000  1.044
138.000  1.059
136.000  1.071
134.000  1.088
1
 AXIAL,BL6,R/R.6
25
   224.0000        17.82326
   222.0000        17.80903
   220.0000        17.82706
   218.0000        17.81852
   216.0000        17.78248
   214.0000        17.79101
   212.0000        17.79101
   210.0000        17.78058
```

```
   208.0000        17.65917
   206.0000        16.93073
   204.0000        17.75782
   202.0000        17.79671
   200.0000        17.79671
   198.0000        17.73600
   196.0000        17.75592
   194.0000        17.71703
   192.0000        17.69522
   190.0000        17.68194
   188.0000        17.69237
   186.0000        17.68004
   184.0000        17.66771
   182.0000        17.65253
   180.0000        17.68668
   178.0000        17.65822
   176.0000        17.61744
1
 AXIAL,BL7,R/R.6
25
   264.0000        17.86784
   262.0000        17.87922
   260.0000        17.90483
   258.0000        17.90673
   256.0000        17.88112
   254.0000        17.86215
   252.0000        17.86500
   250.0000        17.88112
   248.0000        16.59590
   246.0000        17.88871
   244.0000        17.87353
   242.0000        17.91811
   240.0000        17.91622
   238.0000        17.90483
   236.0000        17.89820
   234.0000        17.87069
   232.0000        17.79860
   230.0000        17.84223
   228.0000        17.83749
   226.0000        17.85456
   224.0000        17.81188
   222.0000        17.82326
   220.0000        17.84223
   218.0000        17.80714
   216.0000        17.79481
1
 AXIAL,BL8,R/R.6
25
   304.0000        17.77679
   302.0000        17.74359
   300.0000        17.76161
   298.0000        17.77394
   296.0000        17.76825
   294.0000        17.77868
```

```
   292.0000        17.61744
   290.0000        16.13968
   288.0000        17.95605
   286.0000        17.86784
   284.0000        17.82611
   282.0000        17.87164
   280.0000        17.91242
   278.0000        17.90009
   276.0000        17.87828
   274.0000        17.90768
   272.0000        17.90863
   270.0000        17.91052
   268.0000        17.92286
   266.0000        17.91242
   264.0000        17.93044
   262.0000        17.84413
   260.0000        17.90958
   258.0000        17.83464
   256.0000        17.82421
1
 AXIAL,BL9,R/R.6
25
   344.0000        17.45714
   342.0000        17.48939
   340.0000        17.47232
   338.0000        17.39075
   336.0000        15.09348
   334.0000        16.65566
   332.0000        17.58709
   330.0000        17.63546
   328.0000        17.71419
   326.0000        17.72557
   324.0000        17.68288
   322.0000        17.72746
   320.0000        17.72841
   318.0000        17.74169
   316.0000        17.78627
   314.0000        17.79291
   312.0000        17.80714
   310.0000        17.79386
   308.0000        17.79386
   306.0000        17.80239
   304.0000        17.82516
   302.0000        17.83085
   300.0000        17.81947
   298.0000        17.79860
   296.0000        17.79101
```

```
1
 AXIAL,BL0,R/R.75
27
26.000  1.080
24.000  1.063
22.000  1.049
20.000  1.006
18.000  0.923
16.000  0.817
14.000  0.759
12.000  0.772
10.000  0.828
8.000   0.868
6.000   0.924
4.000   0.953
2.000   0.972
0.000    0.979
358.0    0.984
356.0    0.984
354.0    0.993
352.0    0.997
350.0    1.002
348.0    1.013
346.0    1.017
344.0    1.030
342.0    1.038
340.0    1.054
338.0    1.062
336.0    0.936
334.0    1.098
1
 AXIAL,BL2,R/R.75
27
66.000  1.079
64.000  1.060
62.000  1.046
60.000  1.033
58.000  1.017
56.000  1.005
54.000  0.924
52.000  0.942
50.000  0.980
48.000  0.977
46.000  0.970
44.000  0.972
42.000  0.970
40.000  0.973
38.000  0.976
36.000  0.975
34.000  0.978
32.000  0.985
30.000  0.989
28.000  0.996
26.000  1.003
```

```
24.000  1.013
22.000  1.021
20.000  1.030
18.000  1.037
16.000  0.987
14.000  0.890

1
 AXIAL,BL3,R/R.75
27
106.000 1.083
104.000 1.064
102.000 1.051
100.000 1.036
98.000  1.021
96.000  1.009
94.000  0.999
92.000  0.987
90.000  0.888
88.000  0.975
86.000  0.967
84.000  0.967
82.000  0.965
80.000  0.967
78.000  0.971
76.000  0.967
74.000  0.972
72.000  0.978
70.000  0.980
68.000  0.987
66.000  0.996
64.000  1.004
62.000  1.012
60.000  1.027
58.000  1.037
56.000  1.053
54.000  1.030
1
 axial,BL4,R/R.75
27
146.000   1.099
144.000   1.079
142.000   1.064
140.000  1.050
138.000  1.033
136.000  1.023
134.000  1.013
132.000  1.003
130.000  0.992
128.000  0.914
126.000  0.977
124.000  0.981
122.000  0.978
120.000  0.979
```

```
118.000  0.981
116.000  0.978
114.000  0.982
112.000  0.986
110.000  0.989
108.000  0.997
106.000  1.005
104.000  1.014
102.000  1.020
100.000  1.036
98.000   1.047
96.000   1.060
94.000   1.076
1
 AXIAL,BL5,R/R.75
27
186.000  1.109
184.000  1.085
182.000  1.071
180.000  1.056
178.000  1.042
176.000  1.033
174.000  1.020
172.000  1.011
170.000  1.002
168.000  0.923
166.000  0.991
164.000  0.989
162.000  0.987
160.000  0.987
158.000  0.988
156.000  0.988
154.000  0.992
152.000  0.994
150.000  0.999
148.000  1.007
146.000  1.013
144.000  1.023
142.000  1.033
140.000  1.042
138.000  1.058
136.000  1.072
134.000  1.087
1
 AXIAL,BL6,R/R.75          V_AXIAL
  25
   224.0000        17.80050
   222.0000        17.80809
   220.0000        17.79386
   218.0000        17.75592
   216.0000        17.79101
   214.0000        17.76920
   212.0000        17.79481
   210.0000        17.71134
```

```
   208.0000        17.70755
   206.0000        15.84374
   204.0000        17.72841
   202.0000        17.70470
   200.0000        17.73410
   198.0000        17.73505
   196.0000        17.68478
   194.0000        17.68004
   192.0000        17.71608
   190.0000        17.64115
   188.0000        17.65538
   186.0000        17.67530
   184.0000        17.67719
   182.0000        17.61364
   180.0000        17.62977
   178.0000        17.60131
   176.0000        17.60795
1
 AXIAL,BL7,R/R.75
25
   264.0000        17.88492
   262.0000        17.91622
   260.0000        17.92380
   258.0000        17.88776
   256.0000        17.88492
   254.0000        17.88586
   252.0000        17.84603
   250.0000        17.83844
   248.0000        17.55294
   246.0000        17.36703
   244.0000        17.82990
   242.0000        17.82706
   240.0000        17.86595
   238.0000        17.88017
   236.0000        17.81568
   234.0000        17.82611
   232.0000        17.83464
   230.0000        17.78912
   228.0000        17.80619
   226.0000        17.82232
   224.0000        17.80145
   222.0000        17.76635
   220.0000        17.77489
   218.0000        17.75687
   216.0000        17.75876
 AXIAL,BL8,R/R.75
25
   304.0000        17.79007
   302.0000        17.84508
   300.0000        17.85741
   298.0000        17.81188
   296.0000        17.84508
   294.0000        17.87448
   292.0000        17.84034
```

290.0000	16.73249
288.0000	17.58424
286.0000	17.71229
284.0000	17.83749
282.0000	17.81378
280.0000	17.82611
278.0000	17.87069
276.0000	17.83844
274.0000	17.84982
272.0000	17.86215
270.0000	17.89156
268.0000	17.91906
266.0000	17.92286
264.0000	17.93234
262.0000	17.86215
260.0000	17.81757
258.0000	17.81283
256.0000	17.82042

1
AXIAL,BL9,R/R.75
25

344.0000	17.53397
342.0000	17.58614
340.0000	17.61459
338.0000	17.59562
336.0000	17.64305
334.0000	17.18587
332.0000	15.44348
330.0000	17.55768
328.0000	17.62882
326.0000	17.65158
324.0000	17.65253
322.0000	17.66297
320.0000	17.71893
318.0000	17.71324
316.0000	17.72367
314.0000	17.75592
312.0000	17.77489
310.0000	17.76540
308.0000	17.78437
306.0000	17.81283
304.0000	17.82895
302.0000	17.79291
300.0000	17.78058
298.0000	17.80429
296.0000	17.78153